

Explicit a posteriori error representation for variational problems and application to TV-minimization

Sören Bartels^{*1} and Alex Kaltenbach^{†2}

¹Department of Applied Mathematics, University of Freiburg, Hermann–Herder–Straße 10, 79104 Freiburg

²Institute of Mathematics, Technical University of Berlin, Straße des 17. Juni 136, 10623 Berlin

July 11, 2023

Abstract

In this paper, we propose a general approach for explicit a posteriori error representation for convex minimization problems using basic convex duality relations. Exploiting discrete orthogonality relations in the space of element-wise constant vector fields as well as a discrete integration-by-parts formula between the Crouzeix–Raviart and the Raviart–Thomas element, all convex duality relations are transferred to a discrete level, making the explicit a posteriori error representation –initially based on continuous arguments only– practicable from a numerical point of view. In addition, we provide a generalized Marini formula for the primal solution that determines a discrete primal solution in terms of a given discrete dual solution. We benchmark all these concepts via the Rudin–Osher–Fatemi model. This leads to an adaptive algorithm that yields a (quasi-optimal) linear convergence rate.

Keywords: Explicit a posteriori error representation; convex duality; Crouzeix–Raviart element; Raviart–Thomas element; Rudin–Osher–Fatemi model.

AMS MSC (2020): 35Q68; 49M25; 49M29; 65N30; 65N50

1. INTRODUCTION

The numerical analysis of the approximation of variational problems is challenging when these are non-differentiable, degenerate, or involve constraints. In particular, following established concepts for linear elliptic partial differential equations often leads to sub-optimal results only. The framework of convex duality provides an attractive concept to reveal hidden information and structures to obtain quasi-optimal error representation formulas under meaningful regularity conditions. Similar to [44, 43], we first exploit this idea to derive explicit computable a posteriori error estimates for a *natural* error measure. Then, this general result is transferred to a non-differentiable model problem with discontinuous solutions. As a whole, our results, similar to [44, 43], show that the question of developing asymptotically exact a posteriori error estimators is rather a question of identifying optimal error quantities. However, different from [44, 43], we also propose a general approach for making our results practicable from a numerical point of view.

Given a domain $\Omega \subseteq \mathbb{R}^d$, $d \in \mathbb{N}$, a convex energy density $\phi: \mathbb{R} \rightarrow \mathbb{R} \cup \{+\infty\}$, a (Lebesgue) measurable energy density $\psi: \Omega \times \mathbb{R} \rightarrow \mathbb{R} \cup \{+\infty\}$ that is convex with respect to the second argument, and a Banach space X consisting of functions defined in Ω , we denote by the minimization of the energy functional $I: X \rightarrow \mathbb{R} \cup \{+\infty\}$, for every $v \in X$ defined by

$$I(v) := \int_{\Omega} \phi(\nabla v) \, dx + \int_{\Omega} \psi(\cdot, v) \, dx, \quad (1.1)$$

the *primal problem*.

^{*}Email: bartels@mathematik.uni-freiburg.de

[†]Email: kaltenbach@math.tu-berlin.de

Its (Fenchel) *dual problem* consists in the maximization of the functional $D: Y \rightarrow \mathbb{R} \cup \{-\infty\}$, where Y is a Banach space consisting of vector fields defined in Ω , for every $y \in Y$ is defined by

$$D(y) := - \int_{\Omega} \phi^*(y) \, dx - \int_{\Omega} \psi^*(\cdot, \operatorname{div} y) \, dx. \quad (1.2)$$

Here, $\phi^*: \mathbb{R}^d \rightarrow \mathbb{R} \cup \{+\infty\}$ and $\psi^*: \Omega \times \mathbb{R} \rightarrow \mathbb{R} \cup \{+\infty\}$ (with respect to the second argument) denote the (Fenchel) conjugates of $\phi: \mathbb{R} \rightarrow \mathbb{R} \cup \{+\infty\}$ and $\psi: \Omega \times \mathbb{R} \rightarrow \mathbb{R} \cup \{+\infty\}$, respectively. Under rather general conditions, cf. [49, 31], we have the well-posedness of the primal problem and the dual problem, i.e., the existence of a minimizer $u \in X$ of (1.1), i.e., a *primal solution*, and of a maximizer $z \in Y$ of (1.2), i.e., a *dual solution*, and the *strong duality relation*

$$\min_{v \in X} I(v) = I(u) = D(z) = \max_{y \in Y} D(y). \quad (1.3)$$

Since $u \in X$ and $z \in Y$ are optimal for (1.1) and (1.2), respectively, it holds $0 \in \partial I(u)$ and $0 \in \partial D(z)$. In particular, for every $v \in X$ and $y \in Y$, the quantities

$$\rho_I^2(v, u) := I(v) - I(u), \quad (1.4)$$

$$\rho_{-D}^2(y, z) := D(z) - D(y), \quad (1.5)$$

are non-negative. They define distances, if (1.1) and (1.2), respectively, are strictly convex, and are called coercivity functionals or optimal convexity measures.

For accessible and admissible approximations $v \in X$ and $y \in Y$ of the solutions $u \in X$ and $z \in Y$, given the definitions (1.4) and (1.5), the strong duality relation (1.3) implies the error identity

$$\rho_I^2(v, u) + \rho_{-D}^2(y, z) = I(v) - D(z) =: \eta^2(v, y). \quad (1.6)$$

Hence, the fully computable error estimator $\eta^2: X \times Y \rightarrow \mathbb{R} \cup \{+\infty\}$, cf. (1.6), exactly represents the sum of the primal and dual approximation errors, i.e., of (1.4) and (1.5).

The error representation (1.6) can be seen as a generalization of the Prager–Synge result, cf. [41, 19, 18], which states that for the Poisson problem, i.e., $\phi := \frac{1}{2}|\cdot|^2 \in C^1(\mathbb{R}^d)$, $\psi := ((t, x)^\top \mapsto -f(x)t): \Omega \times \mathbb{R} \rightarrow \mathbb{R} \cup \{+\infty\}$, where $f \in L^2(\Omega)$, $X := W_D^{1,2}(\Omega)$, and $Y := W_N^2(\operatorname{div}; \Omega)$, for every $v \in W_D^{1,2}(\Omega)$ and $y \in W_N^2(\operatorname{div}; \Omega)$ with $-\operatorname{div} y = f$ a.e. in Ω , we have that

$$\frac{1}{2} \|\nabla v - \nabla u\|_{L^2(\Omega; \mathbb{R}^d)}^2 + \frac{1}{2} \|y - z\|_{L^2(\Omega; \mathbb{R}^d)}^2 = \frac{1}{2} \|\nabla v - y\|_{L^2(\Omega; \mathbb{R}^d)}^2. \quad (1.7)$$

The equation (1.7) has been used by various authors to define error estimators; for a comprehensive list of references, we refer the reader to [17]. Often, local procedures are devised to construct an admissible vector field $y \in W_N^2(\operatorname{div}; \Omega)$ with $-\operatorname{div} y = f$ a.e. in Ω from a given function $v \in W_D^{1,2}(\Omega)$. While this leads to efficient procedures to obtain accurate error estimators, the arguments cannot be expected to transfer to non-linear problems. Another alternative to computing approximations for the primal and dual problems consists in using finite element methods for which reconstruction formulas are available, e.g., using the discontinuous Crouzeix–Raviart finite element method and the Marini formula in the case of the Poisson problem, cf. [37].

It has recently been found (cf. [25, 4]) that the discontinuous Crouzeix–Raviart finite element method leads to quasi-optimal a priori error estimates for non-linear and non-differentiable problems, while continuous finite element methods provide only a sub-optimal convergence behavior. In the derivation of those results, a general discrete convex duality theory with Raviart–Thomas vector fields has emerged that also leads to reconstruction formulas in rather general settings. As a consequence, given an approximation $v \in X$ or $y \in Y$, respectively, the missing one can be obtained via a simple post-processing procedure. Then, the pair leads to the error representation formula (1.6). It should also be noted that neither $v \in X$ nor $y \in Y$ needs to be optimal in a subspace of X or Y . By introducing appropriate residuals, any pair of admissible approximations of $u \in X$ and $z \in Y$ can be used. This is particularly important for non-linear problems, i.e., non-quadratic functionals, where an exact solution of discrete problems is neither possible nor rational.

A difficulty in the application of the explicit a posteriori error representation formula (1.6) arises from the condition that $v \in X$ and $y \in Y$ need to be admissible for the functionals (1.1) and (1.2).

In the case of the Poisson problem, this arises, e.g., via element-wise constant approximations of $f \in L^2(\Omega)$ that are the images of Raviart–Thomas vector fields under the divergence operator. While data terms can be controlled by introducing appropriate data oscillation terms, structural peculiarities of the energy densities $\phi: \mathbb{R}^d \rightarrow \mathbb{R} \cup \{+\infty\}$ and $\psi: \Omega \times \mathbb{R} \rightarrow \mathbb{R} \cup \{+\infty\}$ and their (Fenchel) conjugates $\phi^*: \mathbb{R}^d \rightarrow \mathbb{R} \cup \{+\infty\}$ and $\psi^*: \Omega \times \mathbb{R} \rightarrow \mathbb{R} \cup \{+\infty\}$ are often more challenging. We illustrate this by analyzing a non-differentiable problem which leads to a new error analysis and an adaptive refinement procedure for the computationally challenging minimization problem.

With $\phi = |\cdot| \in C^0(\mathbb{R}^d)$ and $\psi = ((x, t)^\top \mapsto \frac{\alpha}{2}(t - g(x))^2): \Omega \times \mathbb{R} \rightarrow \mathbb{R}$ for a given function $g \in L^2(\Omega)$, i.e., the *noisy image*, and a given parameter $\alpha > 0$, i.e., the *fidelity parameter*, the Rudin–Osher–Fatemi (ROF) model, cf. [45], seeks a minimizing function $u \in BV(\Omega) \cap L^2(\Omega)$, i.e., the *de-noised image*, where $BV(\Omega)$ denotes the space of functions with bounded variation, for the functional $I: BV(\Omega) \cap L^2(\Omega) \rightarrow \mathbb{R}$, for every $v \in BV(\Omega) \cap L^2(\Omega)$ defined by

$$I(v) := |Dv|(\Omega) + \frac{\alpha}{2} \|v - g\|_{L^2(\Omega)}^2, \quad (1.8)$$

where $|D(\cdot)|(\Omega): BV(\Omega) \rightarrow [0, +\infty]$ denotes the total variation functional. The (Fenchel) (pre-)dual problem to the minimization of the functional (1.8) consists in the maximization of the functional $D: W_N^2(\operatorname{div}; \Omega) \cap L^\infty(\Omega; \mathbb{R}^d) \rightarrow \mathbb{R} \cup \{-\infty\}$, for every $y \in W_N^2(\operatorname{div}; \Omega) \cap L^\infty(\Omega; \mathbb{R}^d)$ defined by

$$D(y) := -I_{K_1(0)}(y) - \frac{1}{2\alpha} \|\operatorname{div} y + \alpha g\|_{L^2(\Omega)}^2 + \frac{\alpha}{2} \|g\|_{L^2(\Omega)}^2, \quad (1.9)$$

where $I_{K_1(0)}(y) := 0$ if $|y| \leq 1$ a.e. in Ω and $I_{K_1(0)}(y) := +\infty$ else. The primal solution $u \in BV(\Omega) \cap L^2(\Omega)$, i.e., the unique minimizer of (1.8), and a dual solution $z \in W_N^2(\operatorname{div}; \Omega) \cap L^\infty(\Omega; \mathbb{R}^d)$, i.e., a (possibly non-unique) maximizer of (1.9), are (formally) related via, cf. [24, p. 284],

$$z \in \begin{cases} \left\{ \frac{\nabla u}{|\nabla u|} \right\} & \text{if } |\nabla u| > 0 \\ K_1(0) & \text{if } |\nabla u| = 0 \end{cases} \quad \text{a.e. in } \Omega, \quad (1.10)$$

$$\operatorname{div} z = \alpha (u - g) \quad \text{a.e. in } \Omega.$$

The relations (1.10) determine $z \in W_N^2(\operatorname{div}; \Omega) \cap L^\infty(\Omega; \mathbb{R}^d)$ via $u \in BV(\Omega) \cap L^2(\Omega)$ and vice versa. A Crouzeix–Raviart finite element approximation of (1.1) is given by the minimization of the regularized, discrete functional $I_{h,\varepsilon}^{cr}: \mathcal{S}^{1,cr}(\mathcal{T}_h) \rightarrow \mathbb{R}$, $h, \varepsilon > 0$, for every $v_h \in \mathcal{S}^{1,cr}(\mathcal{T}_h)$ defined by

$$I_{h,\varepsilon}^{cr}(v_h) := \|f_\varepsilon(|\nabla_h v_h|)\|_{L^1(\Omega)} + \frac{\alpha}{2} \|\Pi_h(v_h - g)\|_{L^2(\Omega)}^2.$$

Here, ∇_h is the element-wise application of the gradient operator and $f_\varepsilon \in C^1(\mathbb{R})$ is a regularization of the modulus $|\cdot|$, and Π_h denotes the (local) L^2 -projection onto element-wise constant functions. A quasi-optimal dual Raviart–Thomas vector field $z_{h,\varepsilon}^{rt} \in \mathcal{RT}_N^0(\mathcal{T}_h)$ can be associated with a minimizing function $u_{h,\varepsilon}^{cr} \in \mathcal{S}^{1,cr}(\mathcal{T}_h)$ of $I_{h,\varepsilon}^{cr}: \mathcal{S}^{1,cr}(\mathcal{T}_h) \rightarrow \mathbb{R}$ via the reconstruction formula

$$z_{h,\varepsilon}^{rt} = \frac{f'_\varepsilon(|\nabla_h u_{h,\varepsilon}^{cr}|)}{|\nabla_h u_{h,\varepsilon}^{cr}|} \nabla_h u_{h,\varepsilon}^{cr} + \alpha \frac{\Pi_h(u_{h,\varepsilon}^{cr} - g)}{d} (\operatorname{id}_{\mathbb{R}^d} - \Pi_h \operatorname{id}_{\mathbb{R}^d}) \quad \text{in } \mathcal{RT}_N^0(\mathcal{T}_h). \quad (1.11)$$

For canonical choices of $f_\varepsilon \in C^1(\mathbb{R})$, e.g., $f_\varepsilon = |\cdot|_\varepsilon = ((\cdot)^2 + \varepsilon^2)^{1/2}$, it holds $|\Pi_h z_{h,\varepsilon}^{rt}| \leq 1$ a.e. in Ω , but not $|z_{h,\varepsilon}^{rt}| \leq 1$ a.e. in Ω . Thus, we employ $f_\varepsilon = (1 - \varepsilon) |\cdot|_\varepsilon$, so that $|f'_\varepsilon(t)| \leq 1 - \varepsilon$ for all $t \in \mathbb{R}$. The choice $\varepsilon \sim h^2$ in (1.11) and an additional projection step onto $K_1(0)$ lead to an accurate approximation $\bar{z}_{h,\varepsilon}^{rt} \in \mathcal{RT}_N^0(\mathcal{T}_h)$ of $z \in W_N^2(\operatorname{div}; \Omega) \cap L^\infty(\Omega; \mathbb{R}^d)$, which satisfies $|\bar{z}_{h,\varepsilon}^{rt}| \leq 1$ a.e. in Ω and, thus, represents an admissible test function that leads to the definition of an error estimator. The resulting adaptive mesh-refinement procedure leads to significantly improved experimental convergence rates compared to recent related contributions, cf. [12, 8, 10]. More precisely, we report quasi-optimal linear convergence rates which have been obtained only for meshes with quadratic grading towards a sufficiently simple jump set of a piece-wise regular g in [10].

This article is organized as follows: In Section 2, we introduce the employed notation and the relevant finite element spaces. In Section 3, we propose a general approach for explicit a posteriori error representation for convex minimization problems based on (discrete) convex duality relations. In Section 4, we transfer the concepts of Section 3 to the Rudin–Osher–Fatemi model and propose a regularization scheme. In Section 5, we review our theoretical findings via numerical experiments.

2. PRELIMINARIES

2.1 Convex analysis

For a (real) Banach space X , which is equipped with the norm $\|\cdot\|_X: X \rightarrow \mathbb{R}_{\geq 0}$, we denote its corresponding (continuous) dual space by X^* equipped with the dual norm $\|\cdot\|_{X^*}: X^* \rightarrow \mathbb{R}_{\geq 0}$, defined by $\|x^*\|_{X^*} := \sup_{\|x\|_X \leq 1} \langle x^*, x \rangle_X$ for every $x^* \in X^*$, where $\langle \cdot, \cdot \rangle_X: X^* \times X \rightarrow \mathbb{R}$, defined by $\langle x^*, x \rangle_X := x^*(x)$ for every $x^* \in X^*$ and $x \in X$, denotes the duality pairing. A functional $F: X \rightarrow \mathbb{R} \cup \{+\infty\}$ is called *sub-differentiable* in $x \in X$, if $F(x) < \infty$ and if there exists $x^* \in X^*$, called *sub-gradient*, such that for every $y \in X$, it holds

$$\langle x^*, y - x \rangle_X \leq F(y) - F(x). \quad (2.1)$$

The *sub-differential* $\partial F: X \rightarrow 2^{X^*}$ of a functional $F: X \rightarrow \mathbb{R} \cup \{+\infty\}$ for every $x \in X$ is defined by $(\partial F)(x) := \{x^* \in X^* \mid (2.1) \text{ holds for } x^*\}$ if $F(x) < \infty$ and $(\partial F)(x) := \emptyset$ else.

For a given functional $F: X \rightarrow \mathbb{R} \cup \{\pm\infty\}$, we denote its corresponding (*Fenchel*) *conjugate* by $F^*: X^* \rightarrow \mathbb{R} \cup \{\pm\infty\}$, which for every $x^* \in X^*$ is defined by

$$F^*(x^*) := \sup_{x \in X} \langle x^*, x \rangle_X - F(x). \quad (2.2)$$

If $F: X \rightarrow \mathbb{R} \cup \{+\infty\}$ is a proper, convex, and lower semi-continuous functional, then also its (Fenchel) conjugate $F^*: X^* \rightarrow \mathbb{R} \cup \{+\infty\}$ is a proper, convex, and lower semi-continuous functional, cf. [31, p. 17]. Furthermore, for every $x^* \in X^*$ and $x \in X$ such that $F^*(x^*) + F(x)$ is well-defined, i.e., the critical case $\infty - \infty$ does not occur, the *Fenchel–Young inequality*

$$\langle x^*, x \rangle_X \leq F^*(x^*) + F(x) \quad (2.3)$$

applies. In particular, for every $x^* \in X^*$ and $x \in X$, it holds the *Fenchel–Young identity*

$$x^* \in (\partial F)(x) \iff \langle x^*, x \rangle_X = F^*(x^*) + F(x). \quad (2.4)$$

The following convexity measures for functionals play an important role in the derivation of an explicit a posteriori error representation for convex minimization problems in Section 3; for further information, please refer to [21, 39, 40, 12].

Definition 2.1 (Brégman distance and symmetric Brégman distance). *Let X be a (real) Banach space and $F: X \rightarrow \mathbb{R} \cup \{+\infty\}$ proper, i.e., $D(F) := \{x \in X \mid F(x) < \infty\} \neq \emptyset$.*

(i) *The Brégman distance $\sigma_F^2: D(F) \times X \rightarrow [0, +\infty]$ for every $x \in D(F)$ and $y \in X$ is defined by*

$$\sigma_F^2(y, x) := F(y) - F(x) - \sup_{x^* \in (\partial F)(x)} \langle x^*, y - x \rangle_X,$$

where we use the convention $\sup(\emptyset) := -\infty$.

(ii) *The Brégman distance $\sigma_F^2: D(F)^2 \rightarrow [0, +\infty]$ for every $x, y \in D(F)$ is defined by*

$$\sigma_{F,s}^2(y, x) := \sigma_F^2(y, x) + \sigma_F^2(x, y) = \inf_{x^* \in (\partial F)(x); y^* \in (\partial F)(y)} \langle x^* - y^*, x - y \rangle_X,$$

where we use the convention $\inf(\emptyset) := +\infty$.

Definition 2.2 (Optimal convexity measure at a minimizer). *Let X be a (real) Banach space and $F: X \rightarrow \mathbb{R} \cup \{+\infty\}$ proper. Moreover, let $x \in X$ be minimal for $F: X \rightarrow \mathbb{R} \cup \{+\infty\}$. Then, the optimal convexity measure $\rho_F^2: X^2 \rightarrow [0, +\infty]$ at $x \in X$ for every $y \in X$ is defined by*

$$\rho_F^2(y, x) := F(y) - F(x) \geq 0.$$

Remark 2.3. *Let X be a (real) Banach space and $F: X \rightarrow \mathbb{R} \cup \{+\infty\}$ proper. Moreover, let $x \in X$ be minimal for $F: X \rightarrow \mathbb{R} \cup \{+\infty\}$. Then, due to $0 \in (\partial F)(x)$, for every $y \in X$, it holds*

$$\sigma_F^2(y, x) \leq \rho_F^2(y, x).$$

2.2 Function spaces

Throughout the article, we denote by $\Omega \subseteq \mathbb{R}^d$, $d \in \mathbb{N}$, a bounded polyhedral Lipschitz domain, whose (topological) boundary is disjointly divided into a closed Dirichlet part Γ_D and an open Neumann part Γ_N , i.e., $\partial\Omega = \Gamma_D \cup \Gamma_N$ and $\emptyset = \Gamma_D \cap \Gamma_N$.

For $p \in [1, \infty]$ and $l \in \mathbb{N}$, we employ the standard notations¹

$$W_D^{1,p}(\Omega; \mathbb{R}^l) := \{v \in L^p(\Omega; \mathbb{R}^l) \mid \nabla v \in L^p(\Omega; \mathbb{R}^{l \times d}), \text{tr } v = 0 \text{ in } L^p(\Gamma_D; \mathbb{R}^l)\},$$

$$W_N^p(\text{div}; \Omega) := \{y \in L^p(\Omega; \mathbb{R}^d) \mid \text{div } y \in L^p(\Omega), \text{tr}_n y = 0 \text{ in } W^{-\frac{1}{p}, p}(\Gamma_N)\},$$

$W^{1,p}(\Omega; \mathbb{R}^l) := W_D^{1,p}(\Omega; \mathbb{R}^l)$ if $\Gamma_D = \emptyset$, and $W^p(\text{div}; \Omega) := W_N^p(\text{div}; \Omega)$ if $\Gamma_N = \emptyset$, where we denote by $\text{tr}: W^{1,p}(\Omega; \mathbb{R}^l) \rightarrow L^p(\partial\Omega; \mathbb{R}^l)$ and by $\text{tr}_n(\cdot): W^p(\text{div}; \Omega) \rightarrow W^{-\frac{1}{p}, p}(\partial\Omega)$, the trace and normal trace operator, respectively. In particular, we always omit $\text{tr}(\cdot)$ and $\text{tr}_n(\cdot)$. In addition, we employ the abbreviations $L^p(\Omega) := L^p(\Omega; \mathbb{R}^1)$, $W^{1,p}(\Omega) := W^{1,p}(\Omega; \mathbb{R}^1)$, and $W_D^{1,p}(\Omega) := W_D^{1,p}(\Omega; \mathbb{R}^1)$. For (Lebesgue) measurable functions $u, v: \Omega \rightarrow \mathbb{R}$ and a (Lebesgue) measurable set $M \subseteq \Omega$, we write

$$(u, v)_M := \int_M u v \, dx,$$

whenever the right-hand side is well-defined. Analogously, for (Lebesgue) measurable vector fields $z, y: \Omega \rightarrow \mathbb{R}^d$ and a (Lebesgue) measurable set $M \subseteq \Omega$, we write $(z, y)_M := \int_M z \cdot y \, dx$. Moreover, let $|\text{D}(\cdot)|(\Omega): L^1_{\text{loc}}(\Omega) \rightarrow \mathbb{R} \cup \{+\infty\}$, for every $v \in L^1_{\text{loc}}(\Omega)$ defined by²

$$|\text{D}v|(\Omega) := \sup \left\{ - (v, \text{div } \phi)_\Omega \mid \phi \in C_c^\infty(\Omega; \mathbb{R}^d); \|\phi\|_{L^\infty(\Omega; \mathbb{R}^d)} \leq 1 \right\},$$

denote the *total variation* functional. Then, the *space of functions with bounded variation* is defined by

$$BV(\Omega) := \{v \in L^1(\Omega) \mid |\text{D}v|(\Omega) < \infty\}.$$

2.3 Triangulations

Throughout the entire paper, we denote by $\{\mathcal{T}_h\}_{h>0}$, a family of regular, i.e., uniformly shape regular and conforming, triangulations of $\Omega \subseteq \mathbb{R}^d$, $d \in \mathbb{N}$, cf. [32]. Here, $h > 0$ refers to the *average mesh-size*, i.e., if we set $h_T := \text{diam}(T)$ for all $T \in \mathcal{T}_h$, then, we have that $h = \frac{1}{\text{card}(\mathcal{T}_h)} \sum_{T \in \mathcal{T}_h} h_T$. For every element $T \in \mathcal{T}_h$, we denote by $\rho_T > 0$, the supremum of diameters of inscribed balls. We assume that there exists a constant $\omega_0 > 0$, independent of $h > 0$, such that $\max_{T \in \mathcal{T}_h} h_T \rho_T^{-1} \leq \omega_0$. The smallest such constant is called the *chunkiness* of $\{\mathcal{T}_h\}_{h>0}$. The sets \mathcal{S}_h , \mathcal{S}_h^i , \mathcal{S}_h^∂ , and \mathcal{N}_h contain the sides, interior sides, boundary sides, and vertices, respectively, of the elements of \mathcal{T}_h . We have the following relation between the average mesh-size and the number of vertices:

$$h \sim \text{card}(\mathcal{N}_h)^{-1/d}.$$

For $k \in \mathbb{N} \cup \{0\}$ and $T \in \mathcal{T}_h$, let $\mathcal{P}_k(T)$ denote the set of polynomials of maximal degree k on T . Then, for $k \in \mathbb{N} \cup \{0\}$ and $l \in \mathbb{N}$, the sets of continuous and element-wise polynomial functions or vector fields, respectively, are defined by

$$\begin{aligned} \mathcal{L}^k(\mathcal{T}_h)^l &:= \{v_h \in L^\infty(\Omega; \mathbb{R}^l) \mid v_h|_T \in \mathcal{P}_k(T)^l \text{ for all } T \in \mathcal{T}_h\}, \\ \mathcal{S}^k(\mathcal{T}_h)^l &:= \mathcal{L}^k(\mathcal{T}_h)^l \cap C^0(\bar{\Omega}; \mathbb{R}^l). \end{aligned}$$

For every $T \in \mathcal{T}_h$ and $S \in \mathcal{S}_h$, let $x_T := \frac{1}{d+1} \sum_{z \in \mathcal{N}_h \cap T} z \in T$ and $x_S := \frac{1}{d} \sum_{z \in \mathcal{N}_h \cap S} z \in S$ denote the barycenters of T and S , respectively. The (local) L^2 -projection operator $\Pi_h: L^1(\Omega; \mathbb{R}^l) \rightarrow \mathcal{L}^0(\mathcal{T}_h)^l$ onto element-wise constant functions or vector fields, respectively, for every $v \in L^1(\Omega)$, is defined by $\Pi_h v|_T := \int_T v \, dx$ for all $T \in \mathcal{T}_h$. The element-wise gradient $\nabla_h: \mathcal{L}^1(\mathcal{T}_h)^l \rightarrow \mathcal{L}^0(\mathcal{T}_h)^{l \times d}$, for every $v_h \in \mathcal{L}^1(\mathcal{T}_h)^l$, is defined by $\nabla_h v_h|_T := \nabla(v_h|_T)$ for all $T \in \mathcal{T}_h$.

¹Here, $W^{-\frac{1}{p}, p}(\Gamma_N) := (W^{1-\frac{1}{p}, p'}(\Gamma_N))^*$ and $W^{-\frac{1}{p}, p}(\partial\Omega) := (W^{1-\frac{1}{p}, p'}(\partial\Omega))^*$.

²Here, $C_c^\infty(\Omega; \mathbb{R}^d)$ denotes the space of smooth and in Ω compactly supported vector fields.

2.3.1 Crouzeix–Raviart element

The Crouzeix–Raviart finite element space, cf. [26], consists of element-wise affine functions that are continuous at the barycenters of inner element sides, i.e.,³

$$\mathcal{S}^{1,cr}(\mathcal{T}_h) := \{v_h \in \mathcal{L}^1(\mathcal{T}_h) \mid \llbracket v_h \rrbracket_S(x_S) = 0 \text{ for all } S \in \mathcal{S}_h^i\}.$$

Note that $\mathcal{S}^{1,cr}(\mathcal{T}_h) \subseteq BV(\Omega)$. More precisely, for every $v_h \in \mathcal{S}^{1,cr}(\mathcal{T}_h)$, cf. [20, Theorem 1.63], we have that $Dv_h = \nabla_h v_h \otimes dx + \llbracket v_h \rrbracket \otimes ds|_{\mathcal{S}_h}$ with $\nabla_h v_h \otimes dx \perp \llbracket v_h \rrbracket \otimes ds|_{\mathcal{S}_h}$, so that, cf. [14],

$$|Dv_h|(\Omega) = \|\nabla_h v_h\|_{L^1(\Omega; \mathbb{R}^d)} + \|\llbracket v_h \rrbracket\|_{L^1(\mathcal{S}_h)}. \quad (2.5)$$

The Crouzeix–Raviart finite element space with homogeneous Dirichlet boundary condition on Γ_D is defined by

$$\mathcal{S}_D^{1,cr}(\mathcal{T}_h) := \{v_h \in \mathcal{S}^{1,cr}(\mathcal{T}_h) \mid v_h(x_S) = 0 \text{ for all } S \in \mathcal{S}_h \cap \Gamma_D\}.$$

A basis for $\mathcal{S}^{1,cr}(\mathcal{T}_h)$ is given by functions $\varphi_S \in \mathcal{S}^{1,cr}(\mathcal{T}_h)$, $S \in \mathcal{S}_h$, satisfying the Kronecker property $\varphi_S(x_{S'}) = \delta_{S,S'}$ for all $S, S' \in \mathcal{S}_h$. A basis for $\mathcal{S}_D^{1,cr}(\mathcal{T}_h)$ is given by $\varphi_S \in \mathcal{S}_D^{1,cr}(\mathcal{T}_h)$, $S \in \mathcal{S}_h \setminus \Gamma_D$.

2.3.2 Raviart–Thomas element

The Raviart–Thomas finite element space, cf. [42], consists of element-wise affine vector fields that have continuous constant normal components on inner element sides, i.e.,⁴

$$\begin{aligned} \mathcal{RT}^0(\mathcal{T}_h) := \{y_h \in \mathcal{L}^1(\mathcal{T}_h)^d \mid y_h|_T \cdot n_T = \text{const on } \partial T \text{ for all } T \in \mathcal{T}_h, \\ \llbracket y_h \cdot n \rrbracket_S = 0 \text{ on } S \text{ for all } S \in \mathcal{S}_h^i\}. \end{aligned}$$

Note that $\mathcal{RT}_N^0(\mathcal{T}_h) \subseteq W_N^\infty(\text{div}; \Omega)$. The Raviart–Thomas finite element space with homogeneous normal component boundary condition on Γ_N is defined by

$$\mathcal{RT}_N^0(\mathcal{T}_h) := \{y_h \in \mathcal{RT}^0(\mathcal{T}_h) \mid y_h \cdot n = 0 \text{ on } \Gamma_N\}.$$

A basis for $\mathcal{RT}^0(\mathcal{T}_h)$ is given by vector fields $\psi_S \in \mathcal{RT}^0(\mathcal{T}_h)$, $S \in \mathcal{S}_h$, satisfying Kronecker property $\psi_S|_{S'} \cdot n_{S'} = \delta_{S,S'}$ on S' for all $S' \in \mathcal{S}_h$, where n_S is the unit normal vector on S pointing from T_- to T_+ if $T_+ \cap T_- = S \in \mathcal{S}_h$. A basis for $\mathcal{RT}_N^0(\mathcal{T}_h)$ is given by $\psi_S \in \mathcal{RT}_N^0(\mathcal{T}_h)$, $S \in \mathcal{S}_h \setminus \Gamma_N$.

2.3.3 Discrete integration-by-parts formula

For every $v_h \in \mathcal{S}_D^{1,cr}(\mathcal{T}_h)$ and $y_h \in \mathcal{RT}_N^0(\mathcal{T}_h)$, it holds the *discrete integration-by-parts formula*

$$(\nabla_h v_h, \Pi_h y_h)_\Omega = -(\Pi_h v_h, \text{div } y_h)_\Omega. \quad (2.6)$$

In addition, cf. [11, Section 2.4], if a vector field $y_h \in \mathcal{L}^0(\mathcal{T}_h)^d$ satisfies for every $v_h \in \mathcal{S}_D^{1,cr}(\mathcal{T}_h)$

$$(y_h, \nabla_h v_h)_\Omega = 0,$$

then, choosing $v_h = \varphi_S \in \mathcal{S}_D^{1,cr}(\mathcal{T}_h)$ for all $S \in \mathcal{S}_h \setminus \Gamma_D$, one finds that $y_h \in \mathcal{RT}_N^0(\mathcal{T}_h)$. Similarly, if a function $v_h \in \mathcal{L}^0(\mathcal{T}_h)$ satisfies for every $y_h \in \mathcal{RT}_N^0(\mathcal{T}_h)$

$$(v_h, \text{div } y_h)_\Omega = 0,$$

then, choosing $y_h = \psi_S \in \mathcal{RT}_N^0(\mathcal{T}_h)$ for all $S \in \mathcal{S}_h \setminus \Gamma_N$, one finds that $v_h \in \mathcal{S}_D^{1,cr}(\mathcal{T}_h)$. In other words, we have the orthogonal (with respect to the inner product $(\cdot, \cdot)_\Omega$) decompositions

$$\mathcal{L}^0(\mathcal{T}_h)^d = \ker(\text{div}|_{\mathcal{RT}_N^0(\mathcal{T}_h)}) \oplus \nabla_h(\mathcal{S}_D^{1,cr}(\mathcal{T}_h)), \quad (2.7)$$

$$\mathcal{L}^0(\mathcal{T}_h) = \ker(\nabla_h|_{\mathcal{S}_D^{1,cr}(\mathcal{T}_h)}) \oplus \text{div}(\mathcal{RT}_N^0(\mathcal{T}_h)). \quad (2.8)$$

³Here, for every inner side $S \in \mathcal{S}_h^i$, $\llbracket v_h \rrbracket_S := v_h|_{T_+} - v_h|_{T_-}$ on S , where $T_+, T_- \in \mathcal{T}_h$ satisfy $\partial T_+ \cap \partial T_- = S$, and for every boundary side $S \in \mathcal{S}_h^\partial$, $\llbracket v_h \rrbracket_S := v_h|_T$ on S , where $T \in \mathcal{T}_h$ satisfies $S \subseteq \partial T$.

⁴Here, for every inner side $S \in \mathcal{S}_h^i$, $\llbracket y_h \cdot n \rrbracket_S := y_h|_{T_+} \cdot n_{T_+} + y_h|_{T_-} \cdot n_{T_-}$ on S , where $T_+, T_- \in \mathcal{T}_h$ satisfy $\partial T_+ \cap \partial T_- = S$ and for every $T \in \mathcal{T}_h$, $n_T : \partial T \rightarrow \mathbb{S}^{d-1}$ denotes the outward unit normal vector field to T , and for every boundary side $S \in \mathcal{S}_h^\partial$, $\llbracket y_h \cdot n \rrbracket_S := y_h|_T \cdot n$ on S , where $T \in \mathcal{T}_h$ satisfies $S \subseteq \partial T$ and $n : \partial \Omega \rightarrow \mathbb{S}^{d-1}$ denotes the outward unit normal vector field to Ω .

3. EXACT A POSTERIORI ERROR ESTIMATION FOR CONVEX MINIMIZATION PROBLEMS

3.1 Continuous convex minimization problem and continuous convex duality

Let $\phi: \mathbb{R}^d \rightarrow \mathbb{R} \cup \{+\infty\}$ be a proper, convex, and lower semi-continuous function and let $\psi: \Omega \times \mathbb{R} \rightarrow \mathbb{R} \cup \{+\infty\}$ be a (Lebesgue) measurable function such that for a.e. $x \in \Omega$, the function $\psi(x, \cdot): \Omega \times \mathbb{R} \rightarrow \mathbb{R} \cup \{+\infty\}$ is proper, convex, and lower semi-continuous. We examine the convex minimization problem that seeks for a function $u \in W_D^{1,p}(\Omega)$, $p \in (1, \infty)$, that is minimal for the functional $I: W_D^{1,p}(\Omega) \rightarrow \mathbb{R} \cup \{+\infty\}$, for every $v \in W_D^{1,p}(\Omega)$ defined by

$$I(v) := \int_{\Omega} \phi(\nabla v) \, dx + \int_{\Omega} \psi(\cdot, v) \, dx. \quad (3.1)$$

In what follows, we refer to the minimization of $I: W_D^{1,p}(\Omega) \rightarrow \mathbb{R} \cup \{+\infty\}$ as the *primal problem*. A (Fenchel) *dual problem* to the minimization of (3.1) consists in the maximization of the functional $D: L^{p'}(\Omega; \mathbb{R}^d) \rightarrow \mathbb{R} \cup \{-\infty\}$, for every $y \in L^{p'}(\Omega; \mathbb{R}^d)$ defined by

$$D(y) := - \int_{\Omega} \phi^*(y) \, dx - F^*(\text{Div } y), \quad (3.2)$$

where the distributional divergence $\text{Div}: L^{p'}(\Omega; \mathbb{R}^d) \rightarrow (W_D^{1,p}(\Omega))^*$ for every $y \in L^{p'}(\Omega; \mathbb{R}^d)$ and $v \in W_D^{1,p}(\Omega)$ is defined by $\langle \text{Div } y, v \rangle_{W_D^{1,p}(\Omega)} := -(y, \nabla v)_{\Omega}$ and $F^*: L^{p'}(\Omega) \rightarrow \mathbb{R} \cup \{\pm\infty\}$ denotes the Fenchel conjugate to $F: L^p(\Omega) \rightarrow \mathbb{R} \cup \{+\infty\}$, defined by $F(v) := \int_{\Omega} \psi(\cdot, v) \, dx$ for all $v \in L^p(\Omega)$. Note that for every $y \in W_N^{p'}(\text{div}; \Omega)$, we have that $\langle \text{Div } y, v \rangle_{W_D^{1,p}(\Omega)} = (\text{div } y, v)_{\Omega}$ for all $v \in W_D^{1,p}(\Omega)$ and, thus, the representation

$$D(y) = - \int_{\Omega} \phi^*(y) \, dx - \int_{\Omega} \psi^*(\cdot, \text{div } y) \, dx. \quad (3.3)$$

A *weak duality relation* applies, cf. [31, Proposition 1.1, p. 48], i.e.,

$$\inf_{v \in W_D^{1,p}(\Omega)} I(v) \geq \sup_{y \in L^{p'}(\Omega; \mathbb{R}^d)} D(y). \quad (3.4)$$

In what follows, we always assume that $\phi: \mathbb{R}^d \rightarrow \mathbb{R} \cup \{+\infty\}$ and $\psi: \Omega \times \mathbb{R} \rightarrow \mathbb{R} \cup \{+\infty\}$ are such that (3.1) admits at least one minimizer $u \in W_D^{1,p}(\Omega)$, called the *primal solution*, (3.2) at least one maximizer $z \in L^{p'}(\Omega; \mathbb{R}^d)$, called the *dual solution*, and that a *strong duality relation* applies, i.e.,

$$I(u) = D(z). \quad (3.5)$$

By the Fenchel–Young inequality (cf. (2.3)), (3.5) is equivalent to the *convex optimality relations*

$$z \cdot \nabla u = \phi^*(z) + \phi(\nabla u) \quad \text{a.e. in } \Omega, \quad (3.6)$$

$$\text{Div } z \in \partial F(u). \quad (3.7)$$

If $z \in W_N^{p'}(\text{div}; \Omega)$, then the convex optimality relation (3.7) is equivalent to

$$\text{div } z u = \psi^*(\cdot, \text{div } z) + \psi(\cdot, u) \quad \text{a.e. in } \Omega. \quad (3.8)$$

If $\phi \in C^1(\mathbb{R}^d)$, then, by the Fenchel–Young identity (cf. (2.4)), (3.6) is equivalent to

$$z = D\phi(\nabla u) \quad \text{in } L^{p'}(\Omega; \mathbb{R}^d). \quad (3.9)$$

Similarly, if $z \in W_N^{p'}(\text{div}; \Omega)$ and $\psi(x, \cdot) \in C^1(\mathbb{R})$ for a.e. $x \in \Omega$, then (3.8) is equivalent to

$$\text{div } z = D\psi(\cdot, u) \quad \text{in } L^{p'}(\Omega). \quad (3.10)$$

The convex duality relations (3.4)–(3.10) motivate introducing the *primal-dual error estimator* $\eta^2: W_D^{1,p}(\Omega) \times L^{p'}(\Omega; \mathbb{R}^d) \rightarrow [0, +\infty]$, for every $v \in W_D^{1,p}(\Omega)$ and $y \in L^{p'}(\Omega; \mathbb{R}^d)$ defined by

$$\eta^2(v, y) := I(v) - D(y). \quad (3.11)$$

Note that the sign of the estimator (3.11) is a consequence of the weak duality relation (3.4).

Together with the optimal convexity measures (cf. Definition 2.2) $\rho_I^2: W_D^{1,p}(\Omega)^2 \rightarrow [0, +\infty]$ of (3.1) at a primal solution $u \in W_D^{1,p}(\Omega)$ and $\rho_{-D}^2: L^{p'}(\Omega; \mathbb{R}^d) \rightarrow [0, +\infty]$ of the negative of (3.2) at a dual solution $z \in L^{p'}(\Omega; \mathbb{R}^d)$, we arrive at the following explicit a posteriori error representation.

Theorem 3.1 (Explicit (a posteriori) error representation). *The following statements apply:*

(i) For every $v \in W_D^{1,p}(\Omega)$ and $y \in L^{p'}(\Omega; \mathbb{R}^d)$, we have that

$$\rho_I^2(v, u) + \rho_{-D}^2(y, z) = \eta^2(v, y).$$

(ii) For every $v \in W_D^{1,p}(\Omega)$ and $y \in W_N^{p'}(\operatorname{div}; \Omega)$, we have that

$$\eta^2(v, y) = \int_{\Omega} \phi(\nabla v) - \nabla v \cdot y + \phi^*(y) \, dx + \int_{\Omega} \psi(\cdot, v) - v \operatorname{div} y + \psi^*(\cdot, \operatorname{div} y) \, dx. \quad (3.12)$$

Remark 3.2. (i) By the Fenchel–Young inequality (2.3), the integrands in the representation (3.12), are non-negative and, thus, suitable as local refinement indicators.

(ii) Appealing to Remark 2.3, from Theorem 3.1 (i), for every $v \in W_D^{1,p}(\Omega)$ and $y \in L^{p'}(\Omega; \mathbb{R}^d)$, it follows that $\sigma_I^2(v, u) + \sigma_{-D}^2(y, z) \leq \eta^2(v, y)$.

Proof (of Theorem 3.1). ad (i). Due to $I(u) = D(z)$, cf. (3.5), Definition 2.2, and (3.11), for every $v \in W_D^{1,p}(\Omega)$ and $y \in L^{p'}(\Omega; \mathbb{R}^d)$, we have that

$$\rho_I^2(v, u) + \rho_{-D}^2(y, z) = I(v) - I(u) + D(z) - D(y) = \eta^2(v, y).$$

ad (ii). Using (3.1), (3.3), and integration-by-parts, we conclude that (3.12) applies. \square

Remark 3.3 (Examples). (i) In the p -Dirichlet problem, cf. [29, 28], i.e., $\phi := \frac{1}{p} |\cdot|^p \in C^1(\mathbb{R})$, $p \in (1, \infty)$, and $\psi := ((t, x)^\top \mapsto -f(x)t): \Omega \times \mathbb{R} \rightarrow \mathbb{R}$, where $f \in L^{p'}(\Omega)$, cf. [46], we have that

$$\rho_I^2(v, u) \sim \|F(\nabla v) - F(\nabla u)\|_{L^2(\Omega; \mathbb{R}^d)}^2, \quad \rho_{-D}^2(y, z) \sim \|F^*(y) - F^*(z)\|_{L^2(\Omega; \mathbb{R}^d)}^2,$$

where $F, F^*: \mathbb{R}^d \rightarrow \mathbb{R}^d$ for every $a \in \mathbb{R}^d$ are defined by $F(a) := |a|^{\frac{p-2}{2}} a$ and $F^*(a) := |a|^{\frac{p'-2}{2}} a$.

(ii) In the obstacle problem, cf. [7], i.e., $\phi := \frac{1}{2} |\cdot|^2 \in C^1(\mathbb{R})$ and $\psi := ((t, x)^\top \mapsto -f(x)t + I_{\chi(x)}(t)): \Omega \times \mathbb{R} \rightarrow \mathbb{R} \cup \{+\infty\}$, where $f \in L^2(\Omega)$ and $\chi \in W^{1,2}(\Omega)$ with $\chi \leq 0$ on Γ_D , cf. [7], where $I_{\chi(x)}(t) := 0$ if $t \geq 0$ and $I_{\chi(x)}(t) := +\infty$ else, we have that

$$\rho_I^2(v, u) = \frac{1}{2} \|\nabla v - \nabla u\|_{L^2(\Omega; \mathbb{R}^d)}^2 + \langle -\Lambda, v - u \rangle_{W_D^{1,2}(\Omega)}, \quad \rho_{-D}^2(y, z) \geq \frac{1}{2} \|y - z\|_{L^2(\Omega; \mathbb{R}^d)}^2,$$

where $\Lambda \in (W_D^{1,2}(\Omega))^*$ is defined by $\langle \Lambda, v \rangle_{W_D^{1,2}(\Omega)} := (f, v)_\Omega - (\nabla u, \nabla v)_\Omega$ for all $v \in W_D^{1,2}(\Omega)$.

(iii) In an optimal design problem, cf. [22], i.e., $\phi := \zeta \circ |\cdot| \in C^1(\mathbb{R})$, where $\zeta(0) := 0$, $\zeta'(t) := \mu_2 t$ if $t \in [0, t_1]$, $\zeta'(t) := \mu_2 t_1$ if $t \in [t_1, t_2]$, and $\zeta'(t) := \mu_1 t$ if $t \in [t_2, +\infty)$ for some $0 < t_1 < t_2$ and $0 < \mu_1 < \mu_2$ with $t_1 \mu_2 = t_2 \mu_1$, and $\psi := ((t, x)^\top \mapsto -f(x)t): \Omega \times \mathbb{R} \rightarrow \mathbb{R}$, where $f \in L^2(\Omega)$, cf. [22, Lemma 3.4], we have that

$$\rho_I^2(v, u) \geq \frac{1}{2\mu} \|D\phi(\nabla v) - D\phi(\nabla u)\|_{L^2(\Omega; \mathbb{R}^d)}^2, \quad \rho_{-D}^2(y, z) \geq \frac{1}{2\mu} \|y - z\|_{L^2(\Omega; \mathbb{R}^d)}^2.$$

(iv) In the Rudin–Osher–Fatemi (ROF) problem, cf. [45], i.e., $\phi := |\cdot| \in C^0(\mathbb{R})$ and $\psi := ((t, x)^\top \mapsto \frac{\alpha}{2}(t - g(x))^2): \Omega \times \mathbb{R} \rightarrow \mathbb{R}$, where $g \in L^2(\Omega)$, cf. [3, Lemma 10.2], we have that

$$\rho_I^2(v, u) \geq \frac{\alpha}{2} \|v - u\|_{L^2(\Omega)}^2, \quad \rho_{-D}^2(y, z) \geq \frac{1}{2\alpha} \|\operatorname{div} y - \operatorname{div} z\|_{L^2(\Omega)}^2.$$

Since the dual problem to the minimization of the negative of (3.2), in turn, consists in the maximization of the negative of (3.1), the roles of the primal problem and the dual problem may be interchanged. An advantage of Theorem 3.1 consists in the fact that it yields reliable and efficient a posteriori error estimators for both the primal problem and the dual problem, i.e.,

Remark 3.4 (Reliability and efficiency). *Theorem 3.1 also shows that for each $y \in L^{p'}(\Omega; \mathbb{R}^d)$, the estimator $\eta_{I,y}^2 := (v \mapsto \eta^2(v, y)): W_D^{1,p}(\Omega) \rightarrow [0, +\infty]$ satisfies*

$$\rho_I^2(v, u) + \rho_{-D}^2(y, z) = \eta_{I,y}^2(v), \quad (3.13)$$

and for each $v \in W_D^{1,p}(\Omega)$, the estimator $\eta_{-D,v}^2 := (y \mapsto \eta^2(v, y)): L^{p'}(\Omega; \mathbb{R}^d) \rightarrow [0, +\infty]$ satisfies

$$\rho_I^2(v, u) + \rho_{-D}^2(y, z) = \eta_{-D,v}^2(y). \quad (3.14)$$

For the a posteriori error estimators (3.13) and (3.14) for being numerically practicable, it is necessary to have a computationally cheap way to obtain sufficiently accurate approximation of the dual solution (for (3.13)) and/or of the primal solution (for (3.14)), respectively. In Section 3.2, resorting to (discrete) convex duality relations between a non-conforming Crouzeix–Raviart approximation of the primal problem and a Raviart–Thomas approximation of the dual problem, we arrive at discrete reconstruction formulas, called *generalized Marini formula*, cf. [37, 4].

3.2 Discrete convex minimization problem and discrete convex duality

Let $\psi_h: \Omega \times \mathbb{R} \rightarrow \mathbb{R} \cup \{+\infty\}$ denote a suitable approximation⁵ of $\psi: \Omega \times \mathbb{R} \rightarrow \mathbb{R} \cup \{+\infty\}$ such that $\psi_h(\cdot, t) \in \mathcal{L}^0(\mathcal{T}_h)$ for all $t \in \mathbb{R}$ and for a.e. $x \in \Omega$, $\psi_h(x, \cdot): \Omega \times \mathbb{R} \rightarrow \mathbb{R} \cup \{+\infty\}$ is a proper, convex, and lower semi-continuous functional. Then, we examine the (discrete) convex minimization problem that seeks for a function $u_h^{cr} \in \mathcal{S}_D^{1,cr}(\mathcal{T}_h)$ that is minimal for the functional $I_h^{cr}: \mathcal{S}_D^{1,cr}(\mathcal{T}_h) \rightarrow \mathbb{R} \cup \{+\infty\}$, for every $v_h \in \mathcal{S}_D^{1,cr}(\mathcal{T}_h)$ defined by

$$I_h^{cr}(v_h) := \int_{\Omega} \phi(\nabla_h v_h) \, dx + \int_{\Omega} \psi_h(\cdot, \Pi_h v_h) \, dx. \quad (3.15)$$

In what follows, we refer the minimization of $I_h^{cr}: \mathcal{S}_D^{1,cr}(\mathcal{T}_h) \rightarrow \mathbb{R} \cup \{+\infty\}$ to as the *discrete primal problem*. In [4, 11], it is shown that the corresponding (Fenchel) dual problem to the minimization of (3.15) consists in the maximization of $D_h^{rt}: \mathcal{RT}_N^0(\mathcal{T}_h) \rightarrow \mathbb{R} \cup \{-\infty\}$, for every $y_h \in \mathcal{RT}_N^0(\mathcal{T}_h)$ defined by

$$D_h^{rt}(y_h) := - \int_{\Omega} \phi^*(\Pi_h y_h) \, dx - \int_{\Omega} \psi_h^*(\cdot, \operatorname{div} y_h) \, dx. \quad (3.16)$$

A *discrete weak duality relation*, cf. [4, Proposition 3.1], applies

$$\inf_{v_h \in \mathcal{S}_D^{1,cr}(\mathcal{T}_h)} I_h^{cr}(v_h) \geq \sup_{y_h \in \mathcal{RT}_N^0(\mathcal{T}_h)} D_h^{rt}(y_h). \quad (3.17)$$

We will always assume that $\phi: \mathbb{R}^d \rightarrow \mathbb{R} \cup \{+\infty\}$ and $\psi_h: \Omega \times \mathbb{R} \rightarrow \mathbb{R} \cup \{+\infty\}$ are such that (3.15) admits at least one minimizer $u_h^{cr} \in \mathcal{S}_D^{1,cr}(\mathcal{T}_h)$, called the *discrete primal solution*, (3.16) admits at least one maximizer $z_h^{rt} \in \mathcal{RT}_N^0(\mathcal{T}_h)$, called the *discrete dual solution*, and that a *discrete strong duality relation* applies, i.e.,

$$I_h^{cr}(u_h^{cr}) = D_h^{rt}(z_h^{rt}). \quad (3.18)$$

By the Fenchel–Young identity (cf. (2.4)), (3.18) is equivalent to the *discrete convex optimality relations*

$$\Pi_h z_h^{rt} \cdot \nabla_h u_h^{cr} = \phi^*(\Pi_h z_h^{rt}) + \phi(\nabla_h u_h^{cr}) \quad \text{a.e. in } \Omega, \quad (3.19)$$

$$\operatorname{div} z_h^{rt} \Pi_h u_h^{cr} = \psi_h^*(\cdot, \operatorname{div} z_h^{rt}) + \psi_h(\cdot, \Pi_h u_h^{cr}) \quad \text{a.e. in } \Omega. \quad (3.20)$$

If $\phi \in C^1(\mathbb{R}^d)$, then, by the Fenchel–Young identity (cf. (2.4)), (3.19) is equivalent to

$$\Pi_h z_h^{rt} = D\phi(\nabla_h u_h^{cr}) \quad \text{in } \mathcal{L}^0(\mathcal{T}_h)^d, \quad (3.21)$$

and if $\phi^* \in C^1(\mathbb{R}^d)$, then, by the Fenchel–Young identity (cf. (2.4)), (3.20) is equivalent to

$$\nabla_h u_h^{cr} = D\phi^*(\Pi_h z_h^{rt}) \quad \text{in } \mathcal{L}^0(\mathcal{T}_h)^d. \quad (3.22)$$

Similarly, if $\psi_h(x, \cdot) \in C^1(\mathbb{R})$ for a.e. $x \in \Omega$, then (3.20) is equivalent to

$$\operatorname{div} z_h^{rt} = D\psi_h(\cdot, \Pi_h u_h^{cr}) \quad \text{in } \mathcal{L}^0(\mathcal{T}_h), \quad (3.23)$$

and if $\psi_h^*(x, \cdot) \in C^1(\mathbb{R})$ for a.e. $x \in \Omega$, then (3.20) is equivalent to

$$\Pi_h u_h^{cr} = D\psi_h^*(\cdot, \operatorname{div} z_h^{rt}) \quad \text{in } \mathcal{L}^0(\mathcal{T}_h). \quad (3.24)$$

⁵We refrain from being too precise concerning what we mean with *approximation* to allow for more flexibility. Assumptions on both $\phi: \mathbb{R}^d \rightarrow \mathbb{R} \cup \{+\infty\}$ and $\psi_h: \Omega \times \mathbb{R} \rightarrow \mathbb{R} \cup \{+\infty\}$, $h > 0$, that imply, e.g., Γ -convergence results can be found in [4, Proposition 3.3].

The relations (3.21)–(3.24) motivate the following discrete reconstruction formulas for a discrete dual solution $z_h^{rt} \in \mathcal{RT}_N^0(\mathcal{T}_h)$ from a discrete primal solution $u_h^{cr} \in \mathcal{S}_D^{1,cr}(\mathcal{T}_h)$ and vice versa, called *generalized Marini formulas*, cf. [37, 4].

Proposition 3.5 (Generalized Marini formulas). *The following statements apply:*

(i) *If $\phi \in C^1(\mathbb{R}^d)$ and $\psi_h(x, \cdot) \in C^1(\mathbb{R})$ for a.e. $x \in \Omega$, then, given a minimizer $u_h^{cr} \in \mathcal{S}_D^{1,cr}(\mathcal{T}_h)$ of (3.15), a maximizer $z_h^{rt} \in \mathcal{RT}_N^0(\mathcal{T}_h)$ of (3.16) is given via*

$$z_h^{rt} = D\phi(\nabla_h u_h^{cr}) + \frac{D\psi_h(\cdot, \Pi_h u_h^{cr})}{d} (\text{id}_{\mathbb{R}^d} - \Pi_h \text{id}_{\mathbb{R}^d}) \quad \text{in } \mathcal{RT}_N^0(\mathcal{T}_h), \quad (3.25)$$

a discrete strong duality relation applies, i.e., (3.18).

(ii) *If $\phi^* \in C^1(\mathbb{R}^d)$ and $\psi_h^*(x, \cdot) \in C^1(\mathbb{R})$ for a.e. $x \in \Omega$, then, given a maximizer $z_h^{rt} \in \mathcal{RT}_N^0(\mathcal{T}_h)$ of (3.16), a minimizer $u_h^{cr} \in \mathcal{S}_D^{1,cr}(\mathcal{T}_h)$ of (3.15) is given via*

$$u_h^{cr} = D\psi_h^*(\cdot, \text{div } z_h^{rt}) + D\phi^*(\Pi_h z_h^{rt}) \cdot (\text{id}_{\mathbb{R}^d} - \Pi_h \text{id}_{\mathbb{R}^d}) \quad \text{in } \mathcal{S}_D^{1,cr}(\mathcal{T}_h), \quad (3.26)$$

a discrete strong duality relation applies, i.e., (3.18).

Remark 3.6. *It is possible to derive reconstructions formulas similar to (3.25) and (3.26) under weak conditions, e.g., resorting to a regularization argument (cf. Proposition 4.5) or given discrete Lagrange multipliers (cf. [7, Proposition 3.3]).*

Proof. ad (i). See [4, Proposition 3.1].

ad (ii). By definition, it holds $u_h^{cr} \in \mathcal{L}^1(\mathcal{T}_h)$ and the discrete convex optimality relation (3.24) is satisfied. Since $z_h^{rt} \in \mathcal{RT}_N^0(\mathcal{T}_h)$ is maximal for (3.16) as well as $\phi^* \in C^1(\mathbb{R}^d)$ and $\psi_h^*(x, \cdot) \in C^1(\mathbb{R})$ for a.e. $x \in \Omega$, for every $y_h \in \mathcal{RT}_N^0(\mathcal{T}_h)$, we have that

$$(D\phi^*(\Pi_h z_h^{rt}), \Pi_h y_h)_\Omega + (D\psi_h^*(\cdot, \text{div } z_h^{rt}), \text{div } y_h)_\Omega = 0. \quad (3.27)$$

In particular, (3.27) implies that $D\phi^*(\Pi_h z_h^{rt}) \in (\ker(\text{div}|_{\mathcal{RT}_N^0(\mathcal{T}_h)}))^\perp$. Appealing to [25, Lemma 2.4], it holds $(\ker(\text{div}|_{\mathcal{RT}_N^0(\mathcal{T}_h)}))^\perp = \nabla_h(\mathcal{S}_D^{1,cr}(\mathcal{T}_h))$. Therefore, there exists $v_h \in \mathcal{S}_D^{1,cr}(\mathcal{T}_h)$ such that

$$\nabla_h v_h = D\phi^*(\Pi_h z_h^{rt}) \quad \text{in } \mathcal{L}^0(\mathcal{T}_h)^d. \quad (3.28)$$

Hence, for every $y_h \in \mathcal{RT}_N^0(\mathcal{T}_h)$, resorting to the discrete integration-by-parts formula (2.6), (3.28), (3.27), and (3.24), we find that

$$(\Pi_h v_h - \Pi_h u_h^{cr}, \text{div } y_h)_\Omega = -(D\phi^*(\Pi_h z_h^{rt}), \Pi_h y_h)_\Omega - (D\psi_h^*(\cdot, \text{div } z_h^{rt}), \text{div } y_h)_\Omega = 0.$$

In other words, for every $y_h \in \mathcal{RT}_N^0(\mathcal{T}_h)$, we have that

$$(v_h - u_h^{cr}, \text{div } y_h)_\Omega = (\Pi_h v_h - \Pi_h u_h^{cr}, \text{div } y_h)_\Omega = 0. \quad (3.29)$$

On the other hand, we have that $\nabla_h(v_h - u_h^{cr}) = 0$ in $\mathcal{L}^0(\mathcal{T}_h)^d$, i.e., $v_h - u_h^{cr} \in \mathcal{L}^0(\mathcal{T}_h)$. Therefore, (3.29) in conjunction with (2.8) implies that $v_h - u_h^{cr} \in (\text{div}(\mathcal{RT}_N^0(\mathcal{T}_h)))^\perp = \ker(\nabla_h|_{\mathcal{S}_D^{1,cr}(\mathcal{T}_h)})$. As a result, due to $v_h \in \mathcal{S}_D^{1,cr}(\mathcal{T}_h)$, we conclude that $u_h^{cr} \in \mathcal{S}_D^{1,cr}(\mathcal{T}_h)$ with

$$\begin{aligned} \nabla_h u_h^{cr} &= D\phi^*(\Pi_h z_h^{rt}) && \text{in } \mathcal{L}^0(\mathcal{T}_h)^d, \\ \Pi_h u_h^{cr} &= D\psi_h^*(\cdot, \text{div } z_h^{rt}) && \text{in } \mathcal{L}^0(\mathcal{T}_h). \end{aligned} \quad (3.30)$$

By the Fenchel–Young identity, cf. (2.4), (3.30) is equivalent to

$$\begin{aligned} \Pi_h z_h^{rt} \cdot \nabla_h u_h^{cr} &= \phi^*(\Pi_h z_h^{rt}) + \phi(\nabla_h u_h^{cr}) && \text{a.e. in } \Omega, \\ \text{div } z_h^{rt} \Pi_h u_h^{cr} &= \psi_h^*(\cdot, \text{div } z_h^{rt}) + \psi_h(\cdot, \Pi_h u_h^{cr}) && \text{a.e. in } \Omega. \end{aligned} \quad (3.31)$$

Eventually, adding (3.31)₁ and (3.31)₂, subsequently, integration with respect to $x \in \Omega$, resorting to the discrete integration-by-parts formula (2.6), and using the definitions (3.15) and (3.16), we arrive at $I_h^{cr}(u_h^{cr}) = D_h^{rt}(z_h^{rt})$, which, appealing to the discrete weak duality relation (3.17), implies that $u_h^{cr} \in \mathcal{S}_D^{1,cr}(\mathcal{T}_h)$ is minimal for (3.15). \square

4. APPLICATION TO THE RUDIN–OSHER–FATEMI (ROF) MODEL

In this section, we transfer the concepts derived in Section 3 to the non-differentiable Rudin–Osher–Fatemi (ROF) model, cf. [45]. The approximation of the ROF model has been investigated by numerous authors: A priori error estimates has been derived in [9, 25, 4, 10, 6]. A posteriori error estimates and adaptivity results can be found in [12, 33, 8, 10, 16].

4.1 The continuous Rudin–Osher–Fatemi (ROF) model

Given a function $g \in L^2(\Omega)$, i.e., the *noisy image*, and a constant parameter $\alpha > 0$, the *fidelity parameter* the Rudin–Osher–Fatemi (ROF) model, cf. [45], consists in the minimization of the functional $I: BV(\Omega) \cap L^2(\Omega) \rightarrow \mathbb{R}$, for every $v \in BV(\Omega) \cap L^2(\Omega)$ defined by

$$I(v) := |Dv|(\Omega) + \frac{\alpha}{2} \|v - g\|_{L^2(\Omega)}^2. \quad (4.1)$$

In [3, Theorem 10.5 & Theorem 10.6], it has been established that there exists a unique minimizer $u \in BV(\Omega) \cap L^2(\Omega)$ of (4.1). Appealing to [34, Theorem 2.2] or [3, Section 10.1.3], the corresponding (Fenchel) dual problem to the minimization of (4.1) consists in the maximization of the functional $D: W_N^2(\operatorname{div}; \Omega) \cap L^\infty(\Omega; \mathbb{R}^d) \rightarrow \mathbb{R} \cup \{-\infty\}$, for every $y \in W_N^2(\operatorname{div}; \Omega) \cap L^\infty(\Omega; \mathbb{R}^d)$ defined by

$$D(y) := -I_{K_1(0)}(y) - \frac{1}{2\alpha} \|\operatorname{div} y + \alpha g\|_{L^2(\Omega)}^2 + \frac{\alpha}{2} \|g\|_{L^2(\Omega)}^2, \quad (4.2)$$

where $I_{K_1(0)}: L^\infty(\Omega; \mathbb{R}^d) \rightarrow \mathbb{R} \cup \{\infty\}$ is defined by $I_{K_1(0)}(y) := 0$ if $y \in L^\infty(\Omega; \mathbb{R}^d)$ with $|y| \leq 1$ a.e. in Ω and $I_{K_1(0)}(y) := \infty$ else. Apart from that, in [34, Theorem 2.2], it is shown that (4.2) admits a maximizer $z \in W_N^2(\operatorname{div}; \Omega) \cap L^\infty(\Omega; \mathbb{R}^d)$ and that a strong duality relation applies, i.e.,

$$I(u) = D(z). \quad (4.3)$$

Appealing to [3, Proposition 10.4], (4.3) is equivalent to the convex optimality relations

$$\operatorname{div} z = \alpha(u - g) \quad \text{in } L^2(\Omega), \quad (4.4)$$

$$-(u, \operatorname{div} z)_\Omega = |Du|(\Omega). \quad (4.5)$$

Next, if we introduce, by analogy with Section 3, the *primal-dual error estimator* $\eta^2: BV(\Omega) \times (W_N^2(\operatorname{div}; \Omega) \cap L^\infty(\Omega; \mathbb{R}^d)) \rightarrow [0, +\infty]$, for every $v \in BV(\Omega)$ and $y \in W_N^2(\operatorname{div}; \Omega) \cap L^\infty(\Omega; \mathbb{R}^d)$ defined by

$$\eta^2(v, y) := I(v) - D(y), \quad (4.6)$$

then the concepts of Section 3 can be transferred to the ROF model.

Theorem 4.1 (Explicit (a posteriori) error representation). *The following statements apply:*

(i) For every $v \in BV(\Omega)$ and $y \in W_N^2(\operatorname{div}; \Omega) \cap L^\infty(\Omega; \mathbb{R}^d)$, we have that

$$\rho_I^2(v, u) + \rho_{-D}^2(y, z) = \eta^2(v, y).$$

(ii) For every $v \in BV(\Omega)$ and $y \in W_N^2(\operatorname{div}; \Omega) \cap L^\infty(\Omega; \mathbb{R}^d)$, we have that

$$\eta^2(v, y) = |Dv|(\Omega) + (\operatorname{div} y, v)_\Omega + \frac{1}{2\alpha} \|\operatorname{div} y - \alpha(v - g)\|_{L^2(\Omega)}^2 + I_{K_1(0)}(y). \quad (4.7)$$

Proof. ad (i). Due to $I(u) = D(z)$, cf. (4.3), Definition 2.2, and (4.6), for every $v \in BV(\Omega)$ and $y \in W_N^2(\operatorname{div}; \Omega) \cap L^\infty(\Omega; \mathbb{R}^d)$, we have that

$$\rho_I^2(v, u) + \rho_{-D}^2(y, z) = I(v) - I(u) + D(z) - D(y) = \eta^2(v, y).$$

ad (ii). For every $v \in BV(\Omega)$ and $y \in W_N^2(\operatorname{div}; \Omega) \cap L^\infty(\Omega; \mathbb{R}^d)$, we have that

$$\begin{aligned} \eta^2(v, y) &= |Dv|(\Omega) + (\operatorname{div} y, v)_\Omega + \frac{1}{2\alpha} \|\alpha(v - g)\|_{L^2(\Omega)}^2 \\ &\quad - \frac{1}{2\alpha} 2(\operatorname{div} y, \alpha v)_\Omega + \frac{1}{2\alpha} \|\operatorname{div} y + \alpha g\|_{L^2(\Omega)}^2 - \frac{\alpha}{2} \|g\|_{L^2(\Omega)}^2 + I_{K_1(0)}(y) \\ &= |Dv|(\Omega) + (\operatorname{div} y, v)_\Omega + \frac{\alpha}{2} \|v - g\|_{L^2(\Omega)}^2 \\ &\quad - \frac{1}{2\alpha} \|\operatorname{div} y - \alpha(v - g)\|_{L^2(\Omega)}^2 - \frac{\alpha}{2} \|v - g\|_{L^2(\Omega)}^2 + I_{K_1(0)}(y), \end{aligned}$$

which yields the claimed representation. \square

Restricting the estimator (4.6) to subclasses of $BV(\Omega)$ and $W_N^2(\operatorname{div}; \Omega) \cap L^\infty(\Omega; \mathbb{R}^d)$, respectively, for which an appropriate integration-by-parts formula apply, e.g., (2.6), it is possible to derive alternative representations of the estimator (4.6), whose integrands are point-wise non-negative and, thus, suitable as local refinement indicators.

Remark 4.2 (Alternative representations of (4.6) and local refinement indicators).

(i) For every $v \in W^{1,1}(\Omega)$ and $y \in W_N^2(\operatorname{div}; \Omega) \cap L^\infty(\Omega; \mathbb{R}^d)$, by integration-by-parts, it holds

$$\eta^2(v, y) = \|\nabla v\|_{L^1(\Omega; \mathbb{R}^d)} - (\nabla v, y)_\Omega + \frac{1}{2\alpha} \|\operatorname{div} y + \alpha(v - g)\|_{L^2(\Omega)}^2 + I_{K_1(0)}(y) \geq 0.$$

(ii) For every $T \in \mathcal{T}_h$, we define the local refinement indicator $\eta_T^2: W^{1,1}(\Omega) \times W_N^2(\operatorname{div}; \Omega) \cap L^\infty(\Omega; \mathbb{R}^d) \rightarrow [0, +\infty]$ for every $v \in W^{1,1}(\Omega)$ and $y \in W_N^2(\operatorname{div}; \Omega) \cap L^\infty(\Omega; \mathbb{R}^d)$ by

$$\eta_{T,W}^2(v, y) := \|\nabla v\|_{L^1(T; \mathbb{R}^d)} - (\nabla v, y)_T + \frac{1}{2\alpha} \|\operatorname{div} y + \alpha(v - g)\|_{L^2(T)}^2 + I_{K_1(0)}(y) \geq 0.$$

(iii) For every $v_h \in \mathcal{S}^{1,cr}(\Omega)$ and $y_h \in \mathcal{RT}_N^0(\mathcal{T}_h)$, by the representation of the total variation of Crouzeix–Raviart functions (2.5) and the discrete integration-by-parts formula (2.6), it holds

$$\begin{aligned} \eta^2(v_h, y_h) &= \|\nabla_h v_h\|_{L^1(\Omega; \mathbb{R}^d)} + \|[[v_h]]\|_{L^1(\mathcal{S}_h)} - (\nabla_h v_h, \Pi_h y_h)_\Omega \\ &\quad + \frac{1}{2\alpha} \|\operatorname{div} y_h + \alpha(v_h - g)\|_{L^2(\Omega)}^2 + I_{K_1(0)}(y_h) \geq 0. \end{aligned}$$

(iv) For every $T \in \mathcal{T}_h$, we define the discrete local refinement indicator $\eta_{T,CR}^2: \mathcal{S}^{1,cr}(\mathcal{T}_h) \times \mathcal{RT}_N^0(\mathcal{T}_h) \rightarrow [0, +\infty]$ for every $v_h \in \mathcal{S}^{1,cr}(\mathcal{T}_h)$ and $y_h \in \mathcal{RT}_N^0(\mathcal{T}_h)$ by

$$\begin{aligned} \eta_{T,CR}^2(v_h, y_h) &:= \|\nabla v_h\|_{L^1(T; \mathbb{R}^d)} + \sum_{S \in \mathcal{S}_h; S \subseteq T} \|[[v_h]]\|_{L^1(S)} - (\nabla_h v_h, \Pi_h y_h)_T \\ &\quad + \frac{1}{2\alpha} \|\operatorname{div} y_h + \alpha(v_h - g)\|_{L^2(T)}^2 + I_{K_1(0)}(y_h) \geq 0. \end{aligned}$$

We emphasize that the primal-dual error estimator (4.6) and the representations (4.7) or in Remark 4.2 (i) & (ii) are well-known, cf. [12, 8, 10]. However, the combination of (4.6) with the representation of the total variation of Crouzeix–Raviart functions (2.5) and the discrete integration-by-parts formula (2.6) in Remark 4.2 (iii) & (iv), to the best of the authors' knowledge, is new and leads to significantly improved experimental convergence rates of the corresponding adaptive mesh-refinement procedure compared to the contributions [12, 8, 10], cf. Section 5.

4.2 The discretized Rudin–Osher–Fatemi (ROF) model

Given $g \in L^2(\Omega)$ and $\alpha > 0$, with $g_h := \Pi_h g \in \mathcal{L}^0(\mathcal{T}_h)$, the discretized ROF model, proposed in [25], consists in the minimization of $I_h^{cr}: \mathcal{S}^{1,cr}(\mathcal{T}_h) \rightarrow \mathbb{R}$, for every $v_h \in \mathcal{S}^{1,cr}(\mathcal{T}_h)$ defined by

$$I_h^{cr}(v_h) := \|\nabla_h v_h\|_{L^1(\Omega; \mathbb{R}^d)} + \frac{\alpha}{2} \|\Pi_h v_h - \alpha g_h\|_{L^2(\Omega)}^2. \quad (4.8)$$

Note that the functional (4.8) defines a non-conforming approximation of the functional (4.1), as, e.g., jump terms of across inner element sides are not included. This, however, turned out to be essential in the derivation of optimal a priori error estimate in [25, 4]. Since the functional (4.8) is proper, strictly convex, weakly coercive, and lower semi-continuous, the direct method in the calculus of variations, cf. [27], yields the existence of a unique minimizer $u_h^{cr} \in \mathcal{S}^{1,cr}(\mathcal{T}_h)$, called the *discrete primal solution*. Appealing to [25, 4], the corresponding (Fenchel) dual problem to the minimization of (4.8) consists in the maximization of the functional $D_h^{rt}: \mathcal{RT}_N^0(\mathcal{T}_h) \rightarrow \mathbb{R} \cup \{-\infty\}$, for every $y_h \in \mathcal{RT}_N^0(\mathcal{T}_h)$ defined by

$$D_h^{rt}(y_h) := -I_{K_1(0)}(\Pi_h y_h) - \frac{1}{2\alpha} \|\operatorname{div} y_h + \alpha g_h\|_{L^2(\Omega)}^2 + \frac{\alpha}{2} \|g_h\|_{L^2(\Omega)}^2. \quad (4.9)$$

Appealing to Theorem 4.8 (below), there exists a maximizer $z_h^{rt} \in \mathcal{RT}_N^0(\mathcal{T}_h)$ of (4.9), which satisfies $|\Pi_h z_h^{rt}| \leq 1$ a.e. in Ω , a discrete strong duality relation applies, i.e.,

$$I_h^{cr}(u_h^{cr}) = D_h^{rt}(z_h^{rt}), \quad (4.10)$$

and the discrete convex optimality relations

$$\operatorname{div} z_h^{rt} = \alpha (\Pi_h u_h^{cr} - g_h) \quad \text{in } \mathcal{L}^0(\mathcal{T}_h), \quad (4.11)$$

$$\Pi_h z_h^{rt} \cdot \nabla_h u_h^{cr} = |\nabla_h u_h^{cr}| \quad \text{in } \mathcal{L}^0(\mathcal{T}_h). \quad (4.12)$$

4.3 The regularized, discretized Rudin–Osher–Fatemi model

To approximate a discrete minimizer $u_h^{cr} \in \mathcal{S}^{1,cr}(\mathcal{T}_h)$ of (4.8), it is common to approximate the modulus function by strictly convex regularizations. In this connection, for every $\varepsilon \in (0, 1)$, we define a special regularization $f_\varepsilon: \mathbb{R} \rightarrow \mathbb{R}_{\geq 0}$ of the modulus function, for every $t \in \mathbb{R}$, via

$$f_\varepsilon(t) := (1 - \varepsilon) |t|_\varepsilon, \quad |t|_\varepsilon := (t^2 + \varepsilon^2)^{\frac{1}{2}}, \quad (4.13)$$

where $|\cdot|_\varepsilon: \mathbb{R} \rightarrow \mathbb{R}_{\geq 0}$ is commonly referred to as the *standard regularization*.

Let us collect the most important properties of the regularization (4.13).

Lemma 4.3. *For every $\varepsilon \in (0, 1)$, the following statements apply:*

- (i) $f_\varepsilon \in C^1(\mathbb{R})$ with $f'_\varepsilon(0) = 0$.
- (ii) For every $t \in \mathbb{R}$, it holds $-\varepsilon |t| - \varepsilon^2 \leq f_\varepsilon(t) - |t| \leq \varepsilon(1 - |t|)$.
- (iii) For every $t \in \mathbb{R}$, it holds $|f'_\varepsilon(t)| \leq 1 - \varepsilon$.
- (iv) For every $s \in \mathbb{R}$, it holds

$$f_\varepsilon^*(s) := \begin{cases} -\varepsilon((1 - \varepsilon)^2 - |s|^2)^{\frac{1}{2}} & \text{if } |s| \leq 1 - \varepsilon \\ +\infty & \text{if } |s| > 1 - \varepsilon \end{cases}.$$

Remark 4.4. *The main reason to consider the regularization $f_\varepsilon: \mathbb{R} \rightarrow \mathbb{R}_{\geq 0}$ instead of the standard regularization $|\cdot|_\varepsilon: \mathbb{R} \rightarrow \mathbb{R}_{\geq 0}$ consists in the property (iii) in Lemma 4.3. This additional slope reduction enables us later to construct a sufficiently accurate, admissible approximation of the dual solution using an additional projection step, cf. Remark 4.6 (below) and Section 5 (below).*

Proof. ad (i). The claimed regularity $f_\varepsilon \in C^1(\mathbb{R})$ is evident. Since for every $t \in \mathbb{R}$, it holds

$$f'_\varepsilon(t) = (1 - \varepsilon) \frac{t}{(t^2 + \varepsilon^2)^{\frac{1}{2}}}, \quad (4.14)$$

we have that $f'_\varepsilon(0) = 0$.

ad (ii). For every $t \in \mathbb{R}$, due to $0 \leq |t|_\varepsilon - |t| \leq \varepsilon$, we have that

$$-\varepsilon |t| - \varepsilon^2 \leq -\varepsilon |t|_\varepsilon \leq f_\varepsilon(t) - |t| = \varepsilon - \varepsilon |t|_\varepsilon \leq \varepsilon(1 - |t|).$$

ad (iii). Immediate consequence of the representation (4.14).

ad (iv). Due to [15, Proposition 13.20 (i)], for every $s \in \mathbb{R}$ and $\varepsilon \in (0, 1)$, we have that

$$f_\varepsilon^*(s) = ((1 - \varepsilon) |\cdot|_\varepsilon)^*(s) = (1 - \varepsilon) (|\cdot|_\varepsilon)^*\left(\frac{s}{1 - \varepsilon}\right).$$

Since for every $s \in \mathbb{R}$ and $\varepsilon \in (0, 1)$, it holds

$$(|\cdot|_\varepsilon)^*(s) = \begin{cases} -\varepsilon(1 - |s|^2)^{\frac{1}{2}} & \text{if } |s| \leq 1 \\ +\infty & \text{if } |s| > 1 \end{cases},$$

we conclude that the claimed representation of the Fenchel conjugate applies. \square

Given $g \in L^2(\Omega)$, $\alpha > 0$, and an element-wise constant regularization parameter $\varepsilon_h \in \mathcal{L}^0(\mathcal{T}_h)$ with $0 < \varepsilon_h < 1$ a.e. in Ω , for $g_h := \Pi_h g \in \mathcal{L}^0(\mathcal{T}_h)$, the regularized, discrete ROF model consists in the minimization of the functional $I_{h,\varepsilon_h}^{cr}: \mathcal{S}^{1,cr}(\mathcal{T}_h) \rightarrow \mathbb{R}$, for every $v_h \in \mathcal{S}^{1,cr}(\mathcal{T}_h)$ defined by

$$I_{h,\varepsilon_h}^{cr}(v_h) := \|f_{\varepsilon_h}(|\nabla_h v_h|)\|_{L^1(\Omega)} + \frac{\alpha}{2} \|\Pi_h v_h - g_h\|_{L^2(\Omega)}^2. \quad (4.15)$$

Since the functional (4.15) is proper, strictly convex, weakly coercive, and lower semi-continuous, the direct method in the calculus of variations, cf. [27], yields the existence of a unique minimizer $u_{h,\varepsilon_h}^{cr} \in \mathcal{S}^{1,cr}(\mathcal{T}_h)$, called the *regularized, discrete primal solution*. Appealing to $(f_{\varepsilon_h} \circ |\cdot|)^* = f_{\varepsilon_h}^* \circ |\cdot|$, cf. [15, Example 13.7], the corresponding (Fenchel) dual problem to the minimization of (4.8) consists in the maximization of functional $D_{h,\varepsilon_h}^{rt}: \mathcal{RT}_N^0(\mathcal{T}_h) \rightarrow \mathbb{R} \cup \{-\infty\}$, for every $y_h \in \mathcal{RT}_N^0(\mathcal{T}_h)$ defined by

$$D_{h,\varepsilon_h}^{rt}(y_h) := - \int_{\Omega} f_{\varepsilon_h}^*(|\Pi_h y_h|) \, dx - \frac{1}{2\alpha} \|\operatorname{div} y_h + \alpha g_h\|_{L^2(\Omega)}^2 + \frac{\alpha}{2} \|g_h\|_{L^2(\Omega)}^2. \quad (4.16)$$

The following proposition clarifies the well-posedness of the dual regularized, discretized ROF model, i.e., the existence of a maximizer of (4.16). It also yields a discrete reconstruction formula for a maximizer of (4.16) from a minimizer of (4.15) and proves discrete strong duality.

Proposition 4.5. *The following statements apply:*

(i) *A discrete weak duality relation applies, i.e.,*

$$\inf_{v_h \in \mathcal{S}_D^{1,cr}(\mathcal{T}_h)} I_{h,\varepsilon_h}^{cr}(v_h) \geq \sup_{y_h \in \mathcal{RT}_N^0(\mathcal{T}_h)} D_{h,\varepsilon_h}^{rt}(y_h). \quad (4.17)$$

(ii) *The discrete flux $z_h^{rt} \in \mathcal{L}^1(\mathcal{T}_h)$, defined via the generalized Marini formula*

$$z_{h,\varepsilon_h}^{rt} := \frac{f'_{\varepsilon_h}(|\nabla_h u_{h,\varepsilon_h}^{cr}|)}{|\nabla_h u_{h,\varepsilon_h}^{cr}|} \nabla_h u_{h,\varepsilon_h}^{cr} + \alpha \frac{\Pi_h u_{h,\varepsilon_h}^{cr} - g_h}{d} (\text{id}_{\mathbb{R}^d} - \Pi_h \text{id}_{\mathbb{R}^d}), \quad (4.18)$$

satisfies $z_{h,\varepsilon_h}^{rt} \in \mathcal{RT}_N^0(\mathcal{T}_h)$ and the discrete convex optimality relations

$$\text{div } z_{h,\varepsilon_h}^{rt} = \alpha (\Pi_h u_{h,\varepsilon_h}^{cr} - g_h) \quad \text{in } \mathcal{L}^0(\mathcal{T}_h), \quad (4.19)$$

$$\Pi_h z_{h,\varepsilon_h}^{rt} = \frac{f'_{\varepsilon_h}(|\nabla_h u_{h,\varepsilon_h}^{cr}|)}{|\nabla_h u_{h,\varepsilon_h}^{cr}|} \nabla_h u_{h,\varepsilon_h}^{cr} \quad \text{in } \mathcal{L}^0(\mathcal{T}_h)^d. \quad (4.20)$$

(iii) *The discrete flux $z_h^{rt} \in \mathcal{RT}_N^0(\mathcal{T}_h)$ is a maximizer of (4.16) and discrete strong duality applies, i.e.,*

$$I_{h,\varepsilon_h}^{cr}(u_{h,\varepsilon_h}^{cr}) = D_{h,\varepsilon_h}^{rt}(z_h^{rt}).$$

Note that, by the Fenchel–Young identity, cf. [31, Proposition 5.1, p. 21], (4.20) is equivalent to

$$\Pi_h z_{h,\varepsilon_h}^{rt} \cdot \nabla_h u_{h,\varepsilon_h}^{cr} = f_{\varepsilon_h}^*(|\Pi_h z_{h,\varepsilon_h}^{rt}|) + f_{\varepsilon_h}(|\nabla_h u_{h,\varepsilon_h}^{cr}|) \quad \text{in } \mathcal{L}^0(\mathcal{T}_h). \quad (4.21)$$

Remark 4.6. *Appealing to Lemma 4.3 (iii), we have that $|\Pi_h z_{h,\varepsilon_h}^{rt}| \leq 1 - \varepsilon_h$ a.e. in Ω . Therefore, if $\|\Pi_h u_{h,\varepsilon_h}^{cr} - g_h\|_{L^\infty(\Omega)} \leq c_0$ for some $c_0 > 0$, which can be expected by discrete maximum principles, then, choosing $\varepsilon_h := \frac{\alpha c_0}{d} h$, yields that $\|z_{h,\varepsilon_h}^{rt}\|_{L^\infty(\Omega; \mathbb{R}^d)} \leq 1$. However, choices like $\varepsilon_h \sim h$ let us expect convergence rates not better than $\mathcal{O}(h^{1/2})$, cf. Proposition 4.7 (i) (below). In order to allow for the convergence rate $\mathcal{O}(h)$, one needs to choose $\varepsilon_h \sim h^2$. But, in this case, we cannot guarantee that $\|z_{h,\varepsilon_h}^{rt}\|_{L^\infty(\Omega; \mathbb{R}^d)} \leq 1$, so that we instead consider the scaled vector field $\bar{z}_{h,\varepsilon_h}^{rt} := z_{h,\varepsilon_h}^{rt} (\max\{1, \|z_{h,\varepsilon_h}^{rt}\|_{L^\infty(\Omega; \mathbb{R}^d)}\})^{-1} \in \mathcal{RT}_N^0(\mathcal{T}_h)$, which is still a sufficiently accurate approximation of the dual solution, as indicated by the numerical experiments, cf. Section 5.*

Proof. ad (i). Using element-wise that $f_{\varepsilon_h} = f_{\varepsilon_h}^{**}$, the definition of the convex conjugate, cf. (2.2), and the discrete integration-by-parts formula (2.6), we find that

$$\begin{aligned} \inf_{v_h \in \mathcal{S}_D^{1,cr}(\mathcal{T}_h)} I_{h,\varepsilon_h}^{cr}(v_h) &= \inf_{v_h \in \mathcal{S}_D^{1,cr}(\mathcal{T}_h)} \|f_{\varepsilon_h}^{**}(|\nabla_h v_h|)\|_{L^1(\Omega)} + \frac{\alpha}{2} \|\Pi_h v_h - g_h\|_{L^2(\Omega)}^2 \\ &= \inf_{v_h \in \mathcal{S}_D^{1,cr}(\mathcal{T}_h)} \sup_{\bar{y}_h \in \mathcal{L}^0(\mathcal{T}_h)^d} - \int_{\Omega} f_{\varepsilon_h}^*(|\bar{y}_h|) \, dx + (\bar{y}_h, \nabla_h v_h)_{\Omega} + \frac{\alpha}{2} \|\Pi_h v_h - g_h\|_{L^2(\Omega)}^2 \\ &\geq \inf_{v_h \in \mathcal{S}_D^{1,cr}(\mathcal{T}_h)} \sup_{y_h \in \mathcal{RT}_N^0(\mathcal{T}_h)} - \int_{\Omega} f_{\varepsilon_h}^*(|\Pi_h y_h|) \, dx - (\text{div } y_h, \Pi_h v_h)_{\Omega} + \frac{\alpha}{2} \|\Pi_h v_h - g_h\|_{L^2(\Omega)}^2 \\ &\geq \sup_{y_h \in \mathcal{RT}_N^0(\mathcal{T}_h)} - \int_{\Omega} f_{\varepsilon_h}^*(|\Pi_h y_h|) \, dx - \sup_{\bar{v}_h \in \mathcal{L}^0(\mathcal{T}_h)} (\text{div } y_h, \bar{v}_h)_{\Omega} - \frac{\alpha}{2} \|\bar{v}_h - g_h\|_{L^2(\Omega)}^2 \\ &= \sup_{y_h \in \mathcal{RT}_N^0(\mathcal{T}_h)} - \int_{\Omega} f_{\varepsilon_h}^*(|\Pi_h y_h|) \, dx - \frac{1}{2\alpha} \|\text{div } y_h + \alpha g_h\|_{L^2(\Omega)}^2 + \frac{\alpha}{2} \|g_h\|_{L^2(\Omega)}^2 \\ &= \sup_{y_h \in \mathcal{RT}_N^0(\mathcal{T}_h)} D_{h,\varepsilon_h}^{rt}(y_h), \end{aligned}$$

which is the claimed discrete weak duality relation.

ad (ii). By Lemma 4.3, the minimality of $u_{h,\varepsilon_h}^{cr} \in \mathcal{S}^{1,cr}(\mathcal{T}_h)$ for (4.15), for every $v_h \in \mathcal{S}^{1,cr}(\mathcal{T}_h)$, yields that

$$\left(f'_{\varepsilon_h} (|\nabla_h u_{h,\varepsilon_h}^{cr}|) \frac{\nabla_h u_{h,\varepsilon_h}^{cr}}{|\nabla_h u_{h,\varepsilon_h}^{cr}|}, \nabla_h v_h \right)_{\Omega} + \alpha (\Pi_h u_{h,\varepsilon_h}^{cr} - g_h, \Pi_h v_h)_{\Omega} = 0. \quad (4.22)$$

By definition, the discrete flux $z_{h,\varepsilon_h}^{rt} \in \mathcal{L}^1(\mathcal{T}_h)^d$, defined by (4.18), satisfies the discrete convex optimality condition (4.20) and $\operatorname{div}(z_{h,\varepsilon_h}^{rt}|_T) = \alpha (\Pi_h u_{h,\varepsilon_h}^{cr} - g_h)|_T$ in T for all $T \in \mathcal{T}_h$. Choosing $v_h = 1 \in \mathcal{S}^{1,cr}(\mathcal{T}_h)$ in (4.22), we find that $\int_{\Omega} \alpha (\Pi_h u_{h,\varepsilon_h}^{cr} - g_h) dx = 0$. Hence, since for $\Gamma_D = \emptyset$ the divergence operator $\operatorname{div}: \mathcal{RT}_N^0(\mathcal{T}_h) \rightarrow \mathcal{L}^0(\mathcal{T}_h)/\mathbb{R}$ is surjective, there exists $y_h \in \mathcal{RT}_N^0(\mathcal{T}_h)$ such that $\operatorname{div} y_h = \alpha (\Pi_h u_{h,\varepsilon_h}^{cr} - g_h)$ in $\mathcal{L}^0(\mathcal{T}_h)$. Then, we have that $\operatorname{div}((z_{h,\varepsilon_h}^{rt} - y_h)|_T) = 0$ in T for all $T \in \mathcal{T}_h$, i.e., $z_{h,\varepsilon_h}^{rt} - y_h \in \mathcal{L}^0(\mathcal{T}_h)^d$. In addition, for every $v_h \in \mathcal{S}^{1,cr}(\mathcal{T}_h)$, it holds

$$\begin{aligned} (\Pi_h y_h, \nabla_h v_h)_{\Omega} &= -(\operatorname{div} y_h, \Pi_h v_h)_{\Omega} \\ &= -\alpha (\Pi_h u_{h,\varepsilon_h}^{cr} - g_h, \Pi_h v_h)_{\Omega} \\ &= \left(f'_{\varepsilon_h} (|\nabla_h u_{h,\varepsilon_h}^{cr}|) \frac{\nabla_h u_{h,\varepsilon_h}^{cr}}{|\nabla_h u_{h,\varepsilon_h}^{cr}|}, \nabla_h v_h \right)_{\Omega} \\ &= (\Pi_h z_{h,\varepsilon_h}^{rt}, \nabla_h v_h)_{\Omega}. \end{aligned}$$

In other words, for every $v_h \in \mathcal{S}^{1,cr}(\mathcal{T}_h)$, it holds

$$(y_h - z_{h,\varepsilon_h}^{rt}, \nabla_h v_h)_{\Omega} = (\Pi_h y_h - \Pi_h z_{h,\varepsilon_h}^{rt}, \nabla_h v_h)_{\Omega} = 0,$$

i.e., $y_h - z_{h,\varepsilon_h}^{rt} \in \nabla_h(\mathcal{S}_D^{1,cr}(\mathcal{T}_h))^{\perp}$. By the decomposition (2.7), we have that $\nabla_h(\mathcal{S}_D^{1,cr}(\mathcal{T}_h))^{\perp} = \ker(\operatorname{div}|_{\mathcal{RT}_N^0(\mathcal{T}_h)}) \subseteq \mathcal{RT}_N^0(\mathcal{T}_h)$. As a result, it holds $y_h - z_{h,\varepsilon_h}^{rt} \in \mathcal{RT}_N^0(\mathcal{T}_h)$. Due to $y_h \in \mathcal{RT}_N^0(\mathcal{T}_h)$, we conclude that $z_{h,\varepsilon_h}^{rt} \in \mathcal{RT}_N^0(\mathcal{T}_h)$. In particular, now from $\operatorname{div}(z_{h,\varepsilon_h}^{rt}|_T) = \alpha (\Pi_h u_{h,\varepsilon_h}^{cr} - g_h)|_T$ in T for all $T \in \mathcal{T}_h$, it follows the discrete optimality condition (4.19).

ad (iii). Using (4.21), (4.19), and the discrete integration-by-parts formula (2.6), we find that

$$\begin{aligned} I_{h,\varepsilon_h}^{cr}(u_{h,\varepsilon_h}^{cr}) &= \|f_{\varepsilon_h}(|\nabla_h u_{h,\varepsilon_h}^{cr}|)\|_{L^1(\Omega)} + \frac{\alpha}{2} \|\Pi_h u_{h,\varepsilon_h}^{cr} - g_h\|_{L^2(\Omega)}^2 \\ &= - \int_{\Omega} f_{\varepsilon_h}^* (|\Pi_h z_{h,\varepsilon_h}^{rt}|) dx + (\Pi_h z_{h,\varepsilon_h}^{rt}, \nabla_h u_{h,\varepsilon_h}^{cr})_{\Omega} + \frac{1}{2\alpha} \|\operatorname{div} z_{h,\varepsilon_h}^{rt}\|_{L^2(\Omega)}^2 \\ &= - \int_{\Omega} f_{\varepsilon_h}^* (|\Pi_h z_{h,\varepsilon_h}^{rt}|) dx - (\operatorname{div} z_{h,\varepsilon_h}^{rt}, \Pi_h u_{h,\varepsilon_h}^{cr})_{\Omega} + \frac{1}{2\alpha} \|\operatorname{div} z_{h,\varepsilon_h}^{rt}\|_{L^2(\Omega)}^2 \\ &= - \int_{\Omega} f_{\varepsilon_h}^* (|\Pi_h z_{h,\varepsilon_h}^{rt}|) dx - \frac{1}{\alpha} (\operatorname{div} z_{h,\varepsilon_h}^{rt}, \operatorname{div} z_{h,\varepsilon_h}^{rt} + \alpha g_h)_{\Omega} + \frac{1}{2\alpha} \|\operatorname{div} z_{h,\varepsilon_h}^{rt}\|_{L^2(\Omega)}^2 \\ &= - \int_{\Omega} f_{\varepsilon_h}^* (|\Pi_h z_{h,\varepsilon_h}^{rt}|) dx - \frac{1}{2\alpha} \|\operatorname{div} z_{h,\varepsilon_h}^{rt} + \alpha g_h\|_{L^2(\Omega)}^2 \\ &= D_{h,\varepsilon_h}^{rt}(z_{h,\varepsilon_h}^{rt}), \end{aligned}$$

which is the claimed discrete strong duality relation and, thus, appealing to the discrete weak duality relation (4.17), proves the maximality of $z_{h,\varepsilon_h}^{rt} \in \mathcal{RT}_N^0(\mathcal{T}_h)$ for (4.16). \square

The following proposition describes the approximative behavior the regularized, discretized ROF problem towards the (unregularized) discretized ROF problem, given uniform convergence (to zero) of the element-wise constant regularization parameter $\varepsilon_h \in \mathcal{L}^0(\mathcal{T}_h)$. In what follows, in the convergence $\|\varepsilon_h\|_{L^\infty(\Omega)} \rightarrow 0$, the average mesh-size $h > 0$ is always fixed.

Proposition 4.7. *If $\|\varepsilon_h\|_{L^\infty(\Omega)} < 1$, then the following statements apply:*

- (i) It holds $\frac{\alpha}{2} \|\Pi_h u_{h,\varepsilon_h}^{cr} - \Pi_h u_h^{cr}\|_{L^2(\Omega)}^2 \leq \frac{\|\varepsilon_h\|_{L^\infty(\Omega)}}{1 - \|\varepsilon_h\|_{L^\infty(\Omega)}} \left(\frac{\alpha}{2} \|g\|_{L^2(\Omega)}^2 + 2|\Omega| \right)$.
- (ii) $\operatorname{div} z_{h,\varepsilon_h}^{rt} \rightarrow \alpha (\Pi_h u_h^{cr} - g_h)$ in $\mathcal{L}^0(\mathcal{T}_h)$ ($\|\varepsilon_h\|_{L^\infty(\Omega)} \rightarrow 0$).
- (iii) $f_{\varepsilon_h}^* (|\Pi_h z_{h,\varepsilon_h}^{rt}|) \rightarrow 0$ in $\mathcal{L}^0(\mathcal{T}_h)$ ($\|\varepsilon_h\|_{L^\infty(\Omega)} \rightarrow 0$).
- (iv) $f_{\varepsilon_h} (|\nabla_h u_{h,\varepsilon_h}^{cr}|) \rightarrow \nabla_h u_h^{cr}$ in $\mathcal{L}^0(\mathcal{T}_h)$ ($\|\varepsilon_h\|_{L^\infty(\Omega)} \rightarrow 0$).

Proof. *ad (i).* Using both the strong convexity of $I_h^{cr} : \mathcal{S}^{1,cr}(\mathcal{T}_h) \rightarrow \mathbb{R} \cup \{+\infty\}$ and Lemma 4.3 (ii), we obtain

$$\begin{aligned}
\frac{\alpha}{2} \|\Pi_h u_{h,\varepsilon_h}^{cr} - \Pi_h u_h^{cr}\|_{L^2(\Omega)}^2 &\leq I_h^{cr}(u_{h,\varepsilon_h}^{cr}) - I_h^{cr}(u_h^{cr}) \\
&\leq \frac{1}{1-\|\varepsilon_h\|_{L^\infty(\Omega)}} I_{h,\varepsilon_h}^{cr}(u_{h,\varepsilon_h}^{cr}) + \frac{\|\varepsilon_h\|_{L^\infty(\Omega)}^2}{1-\|\varepsilon_h\|_{L^\infty(\Omega)}} |\Omega| - I_h^{cr}(u_h^{cr}) \\
&\leq \frac{1}{1-\|\varepsilon_h\|_{L^\infty(\Omega)}} I_{h,\varepsilon_h}^{cr}(u_h^{cr}) + \frac{\|\varepsilon_h\|_{L^\infty(\Omega)}^2}{1-\|\varepsilon_h\|_{L^\infty(\Omega)}} |\Omega| - I_h^{cr}(u_h^{cr}) \\
&\leq \frac{1}{1-\|\varepsilon_h\|_{L^\infty(\Omega)}} (I_h^{cr}(u_h^{cr}) + 2\|\varepsilon_h\|_{L^\infty(\Omega)} |\Omega|) - I_h^{cr}(u_h^{cr}) \\
&= \frac{\|\varepsilon_h\|_{L^\infty(\Omega)}}{1-\|\varepsilon_h\|_{L^\infty(\Omega)}} (I_h^{cr}(u_h^{cr}) + 2|\Omega|).
\end{aligned} \tag{4.23}$$

Since, by the minimality of $u_h^{cr} \in \mathcal{S}^{1,cr}(\mathcal{T}_h)$ for (4.8) and the L^2 -stability of $\Pi_h : L^2(\Omega) \rightarrow \mathcal{L}^0(\mathcal{T}_h)$, it holds

$$I_h^{cr}(u_h^{cr}) \leq I_h^{cr}(0) = \frac{\alpha}{2} \|g_h\|_{L^2(\Omega)}^2 \leq \frac{\alpha}{2} \|g\|_{L^2(\Omega)}^2, \tag{4.24}$$

from (4.25) we conclude the claimed error estimate.

ad (ii). From claim (i), it follows that

$$\Pi_h u_{h,\varepsilon_h}^{cr} \rightarrow \Pi_h u_h^{cr} \quad \text{in } \mathcal{L}^0(\mathcal{T}_h) \quad (\|\varepsilon_h\|_{L^\infty(\Omega)} \rightarrow 0). \tag{4.25}$$

Thus, using (4.25), from $\operatorname{div} z_{h,\varepsilon_h}^{rt} = \alpha(\Pi_h u_{h,\varepsilon_h}^{cr} - g_h)$ in $\mathcal{L}^0(\mathcal{T}_h)$, cf. (4.19), we conclude that

$$\operatorname{div} z_{h,\varepsilon_h}^{rt} \rightarrow \alpha(\Pi_h u_h^{cr} - g_h) \quad \text{in } \mathcal{L}^0(\mathcal{T}_h) \quad (\|\varepsilon_h\|_{L^\infty(\Omega)} \rightarrow 0).$$

ad (iii). Due to $\Pi_h z_{h,\varepsilon_h}^{rt} = \frac{f'_{\varepsilon_h}(|\nabla_h u_{h,\varepsilon_h}^{cr}|)}{|\nabla_h u_{h,\varepsilon_h}^{cr}|} \nabla_h u_{h,\varepsilon_h}^{cr}$ and Lemma 4.3 (iii), we have that

$$|\Pi_h z_{h,\varepsilon_h}^{rt}| = |f'_{\varepsilon_h}(|\nabla_h u_{h,\varepsilon_h}^{cr}|)| \leq 1 - \varepsilon_h \quad \text{a.e. in } \Omega. \tag{4.26}$$

Therefore, using Lemma 4.3 (iv) together with (4.26), we conclude that

$$\left. \begin{aligned} |f_{\varepsilon_h}^*(|\Pi_h z_{h,\varepsilon_h}^{rt}|)| &= \varepsilon_h ((1 - \varepsilon_h)^2 - |\Pi_h z_{h,\varepsilon_h}^{rt}|^2)^{\frac{1}{2}} \\ &\leq \varepsilon_h (1 - \varepsilon_h) \leq \varepsilon_h \end{aligned} \right\} \quad \text{a.e. in } \Omega,$$

which implies that $f_{\varepsilon_h}^*(|\Pi_h z_{h,\varepsilon_h}^{rt}|) \rightarrow 0$ in $\mathcal{L}^0(\mathcal{T}_h)$ ($\|\varepsilon_h\|_{L^\infty(\Omega)} \rightarrow 0$).

ad (iv). Due to (4.24), $(u_{h,\varepsilon_h}^{cr})_{\|\varepsilon_h\|_{L^\infty(\Omega)} \rightarrow 0} \subseteq \mathcal{S}^{1,cr}(\mathcal{T}_h)$ is bounded. The finite-dimensionality of $\mathcal{S}^{1,cr}(\mathcal{T}_h)$ and the Bolzano–Weierstraß theorem yield a subsequence $(u_{h,\varepsilon'_h}^{cr})_{\|\varepsilon'_h\|_{L^\infty(\Omega)} \rightarrow 0} \subseteq \mathcal{S}^{1,cr}(\mathcal{T}_h)$ and a function $\tilde{u}_h^{cr} \in \mathcal{S}^{1,cr}(\mathcal{T}_h)$ such that

$$u_{h,\varepsilon'_h}^{cr} \rightarrow \tilde{u}_h^{cr} \quad \text{in } \mathcal{S}^{1,cr}(\mathcal{T}_h) \quad (\|\varepsilon'_h\|_{L^\infty(\Omega)} \rightarrow 0). \tag{4.27}$$

From (4.27) it is readily derived that

$$f_{\varepsilon'_h}(|\nabla_h u_{h,\varepsilon'_h}^{cr}|) \rightarrow \nabla_h \tilde{u}_h^{cr} \quad \text{in } \mathcal{L}^0(\mathcal{T}_h) \quad (\|\varepsilon'_h\|_{L^\infty(\Omega)} \rightarrow 0).$$

Consequently, for every $v_h \in \mathcal{S}^{1,cr}(\mathcal{T}_h)$, we find that

$$\begin{aligned} I_h^{cr}(\tilde{u}_h^{cr}) &= \lim_{\|\varepsilon'_h\|_{L^\infty(\Omega)} \rightarrow 0} I_{h,\varepsilon'_h}^{cr}(u_{h,\varepsilon'_h}^{cr}) \\ &\leq \lim_{\|\varepsilon'_h\|_{L^\infty(\Omega)} \rightarrow 0} I_{h,\varepsilon'_h}^{cr}(v_h) \\ &= I_h^{cr}(v_h). \end{aligned}$$

Thus, due to the uniqueness of $u_h^{cr} \in \mathcal{S}^{1,cr}(\mathcal{T}_h)$ as a minimizer of (4.8), we get $\tilde{u}_h^{cr} = u_h^{cr}$ in $\mathcal{S}^{1,cr}(\mathcal{T}_h)$. Since this argumentation remains valid for each subsequence of $(u_{h,\varepsilon_h}^{cr})_{\|\varepsilon_h\|_{L^\infty(\Omega)} \rightarrow 0} \subseteq \mathcal{S}^{1,cr}(\mathcal{T}_h)$, the standard subsequence principle implies that $f_{\varepsilon_h}(|\nabla_h u_{h,\varepsilon_h}^{cr}|) \rightarrow \nabla_h u_h^{cr}$ in $\mathcal{L}^0(\mathcal{T}_h)$ ($\|\varepsilon_h\|_{L^\infty(\Omega)} \rightarrow 0$). \square

The approximation properties of the regularized, discrete ROF model (4.15) (and (4.16)) towards the (unregularized) discrete ROF model (4.8) (and (4.16)) enable us to transfer the discrete convex duality relations established in Proposition 4.5, which apply mainly due to the differentiability of the regularized, discrete ROF model, to the non-differentiable discrete ROF model. To the best of the authors' knowledge, the following discrete convex duality relations for the (unregularized) discrete ROF model (4.8) seem to be new.

Theorem 4.8. *There exists a vector field $z_h^{rt} \in \mathcal{RT}_N^0(\mathcal{T}_h)$ with $|\Pi_h z_h^{rt}| \leq 1$ a.e. in Ω and the following properties:*

(i) *For a not relabeled subsequence, it holds*

$$z_{h,\varepsilon_h}^{rt} \rightarrow z_h^{rt} \quad \text{in } \mathcal{RT}_N^0(\mathcal{T}_h) \quad (\|\varepsilon_h\|_{L^\infty(\Omega)} \rightarrow 0).$$

(ii) *There hold the following discrete convex optimality relations:*

$$\begin{aligned} \operatorname{div} z_h^{rt} &= \alpha (\Pi_h u_h^{cr} - g_h) && \text{in } \mathcal{L}^0(\mathcal{T}_h), \\ \Pi_h z_h^{rt} \cdot \nabla_h u_h^{cr} &= |\nabla_h u_h^{cr}| && \text{in } \mathcal{L}^0(\mathcal{T}_h). \end{aligned}$$

(iii) *The discrete flux $z_h^{rt} \in \mathcal{RT}_N^0(\mathcal{T}_h)$ is maximal for $D_h^{rt}: \mathcal{RT}_N^0(\mathcal{T}_h) \rightarrow \mathbb{R}$ and discrete strong duality applies, i.e.,*

$$I_h^{cr}(u_h^{cr}) = D_h^{rt}(z_h^{rt}).$$

Proof. *ad (i).* Due to Proposition 4.7 (ii) and (4.26), the sequence $(z_{h,\varepsilon_h}^{rt})_{\|\varepsilon_h\|_{L^\infty(\Omega)} \rightarrow 0} \subseteq \mathcal{RT}_N^0(\mathcal{T}_h)$ is bounded. Thus, by the finite-dimensionality of $\mathcal{RT}_N^0(\mathcal{T}_h)$, the Bolzano–Weierstraß theorem yields a not relabeled subsequence and a vector field $z_h^{rt} \in \mathcal{RT}_N^0(\mathcal{T}_h)$ such that

$$z_{h,\varepsilon_h}^{rt} \rightarrow z_h^{rt} \quad \text{in } \mathcal{RT}_N^0(\mathcal{T}_h) \quad (\|\varepsilon_h\|_{L^\infty(\Omega)} \rightarrow 0). \quad (4.28)$$

Due to the continuity of $\Pi_h: L^1(\Omega) \rightarrow \mathcal{L}^0(\mathcal{T}_h)$ and $\mathcal{RT}_N^0(\mathcal{T}_h) \hookrightarrow L^1(\Omega)$, from (4.28), we obtain

$$\Pi_h z_{h,\varepsilon_h}^{rt} \rightarrow \Pi_h z_h^{rt} \quad \text{in } \mathcal{L}^0(\mathcal{T}_h) \quad (\|\varepsilon_h\|_{L^\infty(\Omega)} \rightarrow 0). \quad (4.29)$$

From $|\Pi_h z_{h,\varepsilon_h}^{rt}| \leq 1 - \varepsilon_h$ a.e. in Ω , cf. (4.26), and (4.29), we obtain $|\Pi_h z_h^{rt}| \leq 1$ a.e. in Ω , i.e.,

$$I_{K_1(0)}(\Pi_h z_h^{rt}) = 0. \quad (4.30)$$

ad (ii). Using Proposition 4.7, (4.19), and (4.21), we find that

$$\left. \begin{aligned} \operatorname{div} z_h^{rt} &= \lim_{\|\varepsilon_h\|_{L^\infty(\Omega)} \rightarrow 0} \operatorname{div} z_{h,\varepsilon_h}^{rt} \\ &= \lim_{\|\varepsilon_h\|_{L^\infty(\Omega)} \rightarrow 0} \alpha (\Pi_h u_{h,\varepsilon_h}^{cr} - g_h) \\ &= \alpha (\Pi_h u_h^{cr} - g_h) \end{aligned} \right\} \quad \text{a.e. in } \Omega,$$

as well as

$$\left. \begin{aligned} \Pi_h z_h^{rt} \cdot \nabla_h u_h^{cr} &= \lim_{\|\varepsilon_h\|_{L^\infty(\Omega)} \rightarrow 0} \Pi_h z_{h,\varepsilon_h}^{rt} \cdot \nabla_h u_{h,\varepsilon_h}^{cr} \\ &= \lim_{\|\varepsilon_h\|_{L^\infty(\Omega)} \rightarrow 0} f_{\varepsilon_h}^*(|\Pi_h z_{h,\varepsilon_h}^{rt}|) + f_{\varepsilon_h}(|\nabla_h u_{h,\varepsilon_h}^{cr}|) \\ &= |\nabla_h u_h^{cr}| \end{aligned} \right\} \quad \text{a.e. in } \Omega,$$

i.e., the claimed discrete convex optimality conditions.

ad (iii). Using Proposition 4.7 and (4.30), we find that

$$\begin{aligned} I_h^{cr}(u_h^{cr}) &= \lim_{\|\varepsilon_h\|_{L^\infty(\Omega)} \rightarrow 0} I_{h,\varepsilon_h}^{cr}(u_{h,\varepsilon_h}^{cr}) \\ &= \lim_{\|\varepsilon_h\|_{L^\infty(\Omega)} \rightarrow 0} D_{h,\varepsilon_h}^{rt}(z_{h,\varepsilon_h}^{rt}) \\ &= D_h^{rt}(z_h^{rt}), \end{aligned}$$

i.e., the claimed discrete strong duality relation. \square

5. NUMERICAL EXPERIMENTS

In this section, we review the theoretical findings of Section 4 via numerical experiments. To compare approximations to an exact solution, we impose Dirichlet boundary conditions on $\Gamma_D = \partial\Omega$, though an existence theory is difficult to establish, in general. However, the concepts derived in Section 4 carry over verbatimly with $\Gamma_N = \emptyset$ provided that the existence of a minimizer is given. All experiments were conducted deploying the finite element software package **FEniCS** (version 2019.1.0), cf. [36]. All graphics were generated using the **Matplotlib** library (version 3.5.1), cf. [35], and the **Vedo** library (version 2023.4.4), cf. [38].

5.1 Implementation details regarding the optimization procedure

All computations are based on the regularized, discrete ROF problem (4.15). This is motivated by the fact that appealing to Proposition 4.7 (i), in order to bound the error $\|u - \Pi_h u_h^{cr}\|_{L^2(\Omega)}$, it suffices to determine the error $\|u - \Pi_h u_{h,\varepsilon_h}^{cr}\|_{L^2(\Omega)}$. The iterative minimization of (4.15) is realized using a semi-implicit discretized L^2 -gradient flow from [5] (see also [4, Section 5]) modified with a residual stopping criterion guaranteeing the necessary accuracy in the optimization procedure.

Algorithm 5.1 (Semi-implicit discretized L^2 -gradient flow). *Let $g_h, \varepsilon_h \in \mathcal{L}^0(\mathcal{T}_h)$ be such that $\varepsilon_h > 0$ a.e. in Ω and $\|\varepsilon_h\|_{L^\infty(\Omega)} < 1$, and choose $\tau, \varepsilon_{stop}^h > 0$. Moreover, let $u_h^0 \in \mathcal{S}_D^{1,cr}(\mathcal{T}_h)$. Then, for every $k \in \mathbb{N}$:*

(i) *Compute the iterate $u_h^k \in \mathcal{S}_D^{1,cr}(\mathcal{T}_h)$ such that for every $v_h \in \mathcal{S}_D^{1,cr}(\mathcal{T}_h)$, it holds*

$$(d_\tau u_h^k, v_h)_\Omega + \left(\frac{f'_{\varepsilon_h}(|\nabla_h u_h^{k-1}|)}{|\nabla_h u_h^{k-1}|} \nabla_h u_h^k, \nabla_h v_h \right)_\Omega + \alpha (\Pi_h u_h^k - g_h, \Pi_h v_h)_\Omega = 0, \quad (5.1)$$

where $d_\tau u_h^k := \frac{1}{\tau}(u_h^k - u_h^{k-1})$ denotes the backward difference quotient.

(ii) *Compute the residual $r_h^k \in \mathcal{S}_D^{1,cr}(\mathcal{T}_h)$ such that for every $v_h \in \mathcal{S}_D^{1,cr}(\mathcal{T}_h)$, it holds*

$$(r_h^k, v_h)_\Omega = \left(\frac{f'_{\varepsilon_h}(|\nabla_h u_h^k|)}{|\nabla_h u_h^k|} \nabla_h u_h^k, \nabla_h v_h \right)_\Omega + \alpha (\Pi_h u_h^k - g_h, \Pi_h v_h)_\Omega. \quad (5.2)$$

Stop if $\|r_h^k\|_{L^2(\Omega)} \leq \varepsilon_{stop}^h$; otherwise, increase $k \rightarrow k+1$ and continue with step (i).

Appealing to [4, Remark 5.5], the iterates $u_h^k \in \mathcal{S}_D^{1,cr}(\mathcal{T}_h)$, $k \in \mathbb{N}$, the residuals $r_h^k \in \mathcal{S}_D^{1,cr}(\mathcal{T}_h)$, $k \in \mathbb{N}$, generated by Algorithm 5.1, and the minimizer $u_{h,\varepsilon_h}^{cr} \in \mathcal{S}_D^{1,cr}(\mathcal{T}_h)$ of (4.15) satisfy

$$\|u_{h,\varepsilon_h}^{cr} - u_h^k\|_{L^2(\Omega)} \leq 2 \|r_h^k\|_{L^2(\Omega)}. \quad (5.3)$$

In consequence, if we choose as a stopping criterion that $\|r_h^{k^*}\|_{L^2(\Omega)} \leq \varepsilon_{stop}^h := c_{stop} h$ for $k^* \in \mathbb{N}$, where $c_{stop} > 0$ does not depend on $h > 0$, then, owing to Proposition 4.7 (i) and (5.3), we have that

$$\|\Pi_h(u_h^{cr} - u_h^{k^*})\|_{L^2(\Omega)}^2 \leq \frac{\|\varepsilon_h\|_{L^\infty(\Omega)}}{1 - \|\varepsilon_h\|_{L^\infty(\Omega)}} (2 \|g\|_{L^2(\Omega)}^2 + \frac{8}{\alpha} |\Omega|) + 8 c_{stop}^2 h^2.$$

If $\|\varepsilon_h\|_{L^\infty(\Omega)} \leq c_{reg} h^2$, where $c_{reg} \in (0, 1)$, then, we arrive at $\|\Pi_h(u_h^{cr} - u_h^{k^*})\|_{L^2(\Omega)} = \mathcal{O}(h)$. Thus, to bound the error $\|u - \Pi_h u_h^{cr}\|_{L^2(\Omega)}$ experimentally, it is sufficient to compute $\|u - \Pi_h u_h^{k^*}\|_{L^2(\Omega)}$.

The following proposition proves the well-posedness, stability, and convergence of Algorithm 5.1.

Proposition 5.2. *Let the assumptions of Algorithm 5.1 be satisfied and let $\varepsilon_h \in \mathcal{L}^0(\mathcal{T}_h)$ such that $\varepsilon_h > 0$ a.e. in Ω and $\|\varepsilon_h\|_{L^\infty(\Omega)} < 1$. Then, the following statements apply:*

- (i) *Algorithm 5.1 is well-posed, i.e., for every $k \in \mathbb{N}$, given the most-recent iterate $u_h^{k-1} \in \mathcal{S}_D^{1,cr}(\mathcal{T}_h)$, there exists a unique iterate $u_h^k \in \mathcal{S}_D^{1,cr}(\mathcal{T}_h)$ solving (5.1).*
- (ii) *Algorithm 5.1 is unconditionally strongly stable, i.e., for every $L \in \mathbb{N}$, it holds*

$$I_{h,\varepsilon_h}^{cr}(u_h^L) + \tau \sum_{k=1}^L \|d_\tau u_h^k\|_{L^2(\Omega)}^2 \leq I_{h,\varepsilon_h}^{cr}(u_h^0).$$

- (iii) *Algorithm 5.1 terminates after a finite number of steps, i.e., there exists $k^* \in \mathbb{N}$ such that $\|r_h^{k^*}\|_{L^2(\Omega)} \leq \varepsilon_{stop}^h$.*

The proof of Proposition 5.2 (ii) is essentially based on the following inequality.

Lemma 5.3. *For every $\varepsilon \in (0, 1)$ and $a, b \in \mathbb{R}^d$, it holds*

$$\frac{f'_\varepsilon(|a|)}{|a|} b \cdot (b - a) \geq f_\varepsilon(|b|) - f_\varepsilon(|a|) + \frac{1}{2} \frac{f'_\varepsilon(|a|)}{|a|} |b - a|^2.$$

Proof. Follows from [4, Appendix A.2], since $f_\varepsilon \in C^1(\mathbb{R}_{\geq 0})$ and $(t \mapsto f'_\varepsilon(t)/t) \in C^0(\mathbb{R}_{\geq 0})$ is positive and non-decreasing for all $\varepsilon \in (0, 1)$. \square

Proof (of Proposition 5.2). *ad (i).* Since $\frac{f'_\varepsilon(t)}{t} \geq 0$ for all $\varepsilon \in (0, 1)$ and $t \geq 0$, the well-posedness of Algorithm 5.1 is a direct consequence of the Lax–Milgram lemma.

ad (ii). Let $L \in \mathbb{N}$ be arbitrary. Then, for every $k \in \{1, \dots, L\}$, choosing $v_h = d_\tau u_h^k \in \mathcal{S}_D^{1,cr}(\mathcal{T}_h)$ in (5.1), we find that

$$\|d_\tau u_h^k\|_{L^2(\Omega)}^2 + \left(\frac{f'_{h,\varepsilon_h}(|\nabla_h u_h^{k-1}|)}{|\nabla_h u_h^{k-1}|} \nabla_h u_h^k, \nabla_h d_\tau u_h^k \right)_\Omega + \alpha (\Pi_h u_h^k - g_h, \Pi_h d_\tau u_h^k)_\Omega. \quad (5.4)$$

Appealing to Lemma 5.3 with $a = \nabla_h u_h^{k-1}|_T \in \mathbb{R}^d$ and $b = \nabla_h u_h^k|_T \in \mathbb{R}^d$ applied for all $T \in \mathcal{T}_h$, for every $k \in \{1, \dots, L\}$, we have that

$$\frac{f'_{h,\varepsilon_h}(|\nabla_h u_h^{k-1}|)}{|\nabla_h u_h^{k-1}|} \nabla_h u_h^k \cdot \nabla_h d_\tau u_h^k \geq d_\tau f_{h,\varepsilon_h}(|\nabla_h u_h^k|) \quad \text{a.e. in } \Omega. \quad (5.5)$$

In addition, since $d_\tau g_h = 0$, for every $k \in \{1, \dots, L\}$, we have that

$$(\Pi_h u_h^k - g_h) \Pi_h d_\tau u_h^k = (\Pi_h u_h^k - g_h) d_\tau (\Pi_h u_h^k - g_h) = \frac{d_\tau}{2} |\Pi_h u_h^k - g_h|^2. \quad (5.6)$$

Using (5.5) and (5.6) in (5.4), for every $k \in \{1, \dots, L\}$, we arrive at

$$\|d_\tau u_h^k\|_{L^2(\Omega)}^2 + d_\tau I_{h,\varepsilon_h}^{cr}(u_h^k) \leq 0. \quad (5.7)$$

Summation of (5.7) with respect to $k \in \{1, \dots, L\}$, using $\sum_{k=1}^L d_\tau I_{h,\varepsilon_h}^{cr}(u_h^k) = I_{h,\varepsilon_h}^{cr}(u_h^L) - I_{h,\varepsilon_h}^{cr}(u_h^0)$, yields the claimed stability estimate.

ad (iii). Due to (i), we have that $\|d_\tau u_h^k\|_{L^2(\Omega)}^2 \rightarrow 0$ ($k \rightarrow \infty$), i.e., by the finite-dimensionality of $\mathcal{S}_D^{1,cr}(\mathcal{T}_h)$ and the equivalence of norms, it holds

$$u_h^k - u_h^{k-1} \rightarrow 0 \quad \text{in } \mathcal{S}_D^{1,cr}(\mathcal{T}_h) \quad (k \rightarrow \infty). \quad (5.8)$$

In addition, due to (i), we have that $I_{h,\varepsilon_h}^{cr}(u_h^k) \leq I_{h,\varepsilon_h}^{cr}(u_h^0)$, which, using Lemma 4.3, implies that $(u_h^k)_{k \in \mathbb{N}} \subseteq \mathcal{S}_D^{1,cr}(\mathcal{T}_h)$ is bounded. Due to the finite-dimensionality of $\mathcal{S}_D^{1,cr}(\mathcal{T}_h)$, the Bolzano–Weierstraß theorem yields a subsequence $(u_h^{k_l})_{l \in \mathbb{N}} \subseteq \mathcal{S}_D^{1,cr}(\mathcal{T}_h)$ and a function $\tilde{u}_h \in \mathcal{S}_D^{1,cr}(\mathcal{T}_h)$ such that

$$u_h^{k_l} \rightarrow \tilde{u}_h \quad \text{in } \mathcal{S}_D^{1,cr}(\mathcal{T}_h) \quad (l \rightarrow \infty). \quad (5.9)$$

Due to (5.8), from (5.9), we deduce that

$$u_h^{k_l-1} \rightarrow \tilde{u}_h \quad \text{in } \mathcal{S}_D^{1,cr}(\mathcal{T}_h) \quad (l \rightarrow \infty). \quad (5.10)$$

As a result, using (5.8)–(5.10), by passing for $l \rightarrow \infty$ in (5.1), for every $v_h \in \mathcal{S}_D^{1,cr}(\mathcal{T}_h)$, we obtain

$$\left(\frac{f'_{h,\varepsilon_h}(|\nabla_h \tilde{u}_h|)}{|\nabla_h \tilde{u}_h|} \nabla_h \tilde{u}_h, \nabla_h v_h \right)_\Omega + \alpha (\Pi_h \tilde{u}_h - g_h, \Pi_h v_h)_\Omega = 0, \quad (5.11)$$

and, by uniqueness, $\tilde{u}_h = u_{h,\varepsilon_h}^{cr}$. Hence, using (5.8) and (5.11), for every $v_h \in \mathcal{S}_D^{1,cr}(\mathcal{T}_h)$, we obtain

$$\begin{aligned} (r_h^{k_l}, v_h)_\Omega &= \left(\frac{f'_{h,\varepsilon_h}(|\nabla_h u_h^{k_l}|)}{|\nabla_h u_h^{k_l}|} \nabla_h u_h^{k_l}, \nabla_h v_h \right)_\Omega + \alpha (\Pi_h u_h^{k_l} - g_h, \Pi_h v_h)_\Omega \\ &\rightarrow \left(\frac{f'_{h,\varepsilon_h}(|\nabla_h u_{h,\varepsilon_h}^{cr}|)}{|\nabla_h u_{h,\varepsilon_h}^{cr}|} \nabla_h u_{h,\varepsilon_h}^{cr}, \nabla_h v_h \right)_\Omega + \alpha (\Pi_h u_{h,\varepsilon_h}^{cr} - g_h, \Pi_h v_h)_\Omega = 0 \quad (l \rightarrow \infty), \end{aligned}$$

i.e., $r_h^{k_l} \rightarrow 0$ in $\mathcal{S}_D^{1,cr}(\mathcal{T}_h)$ ($l \rightarrow \infty$), and, thus, by the finite-dimensionality of $\mathcal{S}_D^{1,cr}(\mathcal{T}_h)$, $r_h^{k_l} \rightarrow 0$ in $\mathcal{S}_D^{1,cr}(\mathcal{T}_h)$ ($l \rightarrow \infty$), which implies that $r_h^{k_l} \rightarrow 0$ in $L^2(\Omega)$ ($l \rightarrow \infty$). As this argumentation remains valid for each subsequence of $(r_h^k)_{k \in \mathbb{N}} \subseteq \mathcal{S}_D^{1,cr}(\mathcal{T}_h)$, the standard convergence principle yields that $r_h^k \rightarrow 0$ in $L^2(\Omega)$ ($k \rightarrow \infty$). In particular, there exists $k^* \in \mathbb{N}$ such that $\|r_h^{k^*}\|_{L^2(\Omega)} \leq \varepsilon_{stop}^h$. \square

5.2 Implementation details regarding the adaptive mesh refinement procedure

Before we present numerical experiments, we briefly outline the details of the implementations regarding the adaptive mesh refinement procedure. In general, we follow the *adaptive algorithm*, cf. [1, 23, 48]:

Algorithm 5.4 (AFEM). Let $\varepsilon_{\text{STOP}} > 0$, $\theta \in (0, 1]$, and \mathcal{T}_0 an initial triangulation of Ω , and choose $\varepsilon_0 \in \mathcal{L}^0(\mathcal{T}_0)$ such that $\varepsilon_0 > 0$ a.e. in Ω and $\|\varepsilon_0\|_{L^\infty(\Omega)} < 1$. Then, for every $i \in \mathbb{N} \cup \{0\}$:

(‘Solve’) Approximate the regularized, discrete primal solution $u_i^{cr} := u_{h_i, \varepsilon_i}^{cr} \in \mathcal{S}_D^{1, cr}(\mathcal{T}_i)$ minimizing (4.15). Post-process $u_i^{cr} \in \mathcal{S}_D^{1, cr}(\mathcal{T}_i)$ to obtain an approximation $\bar{u}_i^{cr} \in \mathcal{S}_D^{1, cr}(\mathcal{T}_i)$ with $\bar{u}_i^{cr} = 0$ on $\partial\Omega$ and a regularized, discrete dual solution $z_i^{rt} := z_{h_i, \varepsilon_i}^{rt} \in \mathcal{RT}_N^0(\mathcal{T}_i)$ maximizing (4.16). Then, define

$$\bar{z}_i^{rt} := \frac{z_i^{rt}}{\max\{1, \|z_i^{rt}\|_{L^\infty(\Omega; \mathbb{R}^d)}\}} \in \mathcal{RT}_N^0(\mathcal{T}_i). \quad (5.12)$$

(‘Estimate’) Compute the local refinement indicators $(\eta_{T, CR}^2(\bar{u}_i^{cr}, \bar{z}_i^{rt}))_{T \in \mathcal{T}_i}$, cf. Remark 4.2 (iv). If $\eta^2(\bar{u}_i^{cr}, \bar{z}_i^{rt}) \leq \varepsilon_{\text{STOP}}$, cf. Remark 4.2 (iii), then STOP; otherwise, continue with step (‘Mark’).

(‘Mark’) Choose a minimal (in terms of cardinality) subset $\mathcal{M}_i \subseteq \mathcal{T}_i$ such that

$$\sum_{T \in \mathcal{M}_i} \eta_{T, CR}^2(\bar{u}_i^{cr}, \bar{z}_i^{rt}) \geq \theta^2 \sum_{T \in \mathcal{T}_i} \eta_{T, CR}^2(\bar{u}_i^{cr}, \bar{z}_i^{rt}).$$

(‘Refine’) Perform a conforming refinement of \mathcal{T}_i to obtain \mathcal{T}_{i+1} such that each $T \in \mathcal{M}_i$ is refined in \mathcal{T}_{i+1} . Then, construct $\varepsilon_{i+1} \in \mathcal{L}^0(\mathcal{T}_{i+1})$ such that $\varepsilon_{i+1} > 0$ a.e. in Ω and $\|\varepsilon_{i+1}\|_{L^\infty(\Omega)} < c_i h_{i+1}^2$. Increase $i \mapsto i + 1$ and continue with step (‘Solve’).

Remark 5.5. (i) The regularized, discrete primal solution $u_i^{cr} \in \mathcal{S}_D^{1, cr}(\mathcal{T}_i)$ in step (‘Solve’) is computed using the semi-implicit discretized L^2 -gradient flow, cf. Algorithm 5.1, for fixed step-size $\tau = 1.0$, stopping criterion $\varepsilon_{\text{stop}}^{h_i} := \frac{h_i}{\sqrt{20}}$, and initial condition $u_i^0 = 0 \in \mathcal{S}_D^{1, cr}(\mathcal{T}_i)$. Appealing to Proposition 5.2 (ii), Algorithm 5.1 is unconditionally strongly stable, so that employing the fixed step-size $\tau = 1.0$ is a reasonable choice. The stopping criterion $\varepsilon_{\text{stop}}^{h_i} := \frac{h_i}{\sqrt{20}}$ ensures (cf. the argumentation below Algorithm 5.1) that the final iterate $u_{h_i}^{k^*} \in \mathcal{S}_D^{1, cr}(\mathcal{T}_i)$ is a sufficiently accurate approximation of the discrete primal solution, in the sense that its accuracy does not violate the best possible linear convergence rate, cf. Remark 5.6 (below).
(ii) As an approximation $\bar{u}_i^{cr} \in \mathcal{S}_D^{1, cr}(\mathcal{T}_i)$ with $\bar{u}_i^{cr} = 0$ on $\partial\Omega$, we employ

$$\bar{u}_i^{cr} := \begin{cases} u_i^{cr} & \text{if } u_i^{cr} = 0 \text{ on } \partial\Omega, \\ I_k^\partial u_i^{cr} & \text{else,} \end{cases} \quad (5.13)$$

where the operator $I_i^\partial: \mathcal{S}^{1, cr}(\mathcal{T}_i) \rightarrow \mathcal{S}_D^{1, cr}(\mathcal{T}_i)$ for every $v_{h_i} \in \mathcal{S}^{1, cr}(\mathcal{T}_i)$ is defined by

$$I_i^\partial v_i := \sum_{S \in \mathcal{S}_{h_i}; S \cap \partial\Omega = \emptyset} v_{h_i}(x_S) \varphi_S. \quad (5.14)$$

- (iii) Note that the particular choices in (ii) are only due to the imposed homogeneous Dirichlet boundary condition. In the case $\Gamma_D = \emptyset$, the choice $\bar{u}_i^{cr} := u_i^{cr} \in \mathcal{S}^{1, cr}(\mathcal{T}_i)$ is always admissible.
- (iv) If not otherwise specified, we employ the parameter $\theta = \frac{1}{2}$ in (‘Mark’).
- (v) To find the set $\mathcal{M}_i \subseteq \mathcal{T}_i$ in step (‘Mark’), we deploy the Dörfler marking strategy, cf. [30].
- (vi) The (minimal) conforming refinement of \mathcal{T}_i with respect to \mathcal{M}_i in step (‘Refine’) is obtained by deploying the red-green-blue-refinement algorithm, cf. [48].
- (vii) For the construction of the adaptively modified regularization parameter $\varepsilon_i \in \mathcal{L}^0(\mathcal{T}_i)$ in step (‘Refine’), we employ separately the following two cases:

$$\varepsilon_i := \begin{cases} \frac{\alpha}{d} |\Pi_{h_{i-1}} u_{i-1}^{cr} - g_{h_i}| h_i^2 + h_i^3 & \text{(local),} \\ h_i^2 & \text{(global).} \end{cases} \quad (5.15)$$

5.3 Example with Lipschitz continuous dual solution

We examine an example from [10]. In this example, we let $\Omega = (-1, 1)^d$, $\Gamma_D = \partial\Omega$, $d \in \{2, 3\}$, $r = \frac{1}{2}$, $\alpha = 10$, and $g = \chi_{B_r^d(0)} \in BV(\Omega) \cap L^\infty(\Omega)$. Then, the primal solution $u \in BV(\Omega) \cap L^\infty(\Omega)$ and a dual solution $z \in W^2(\operatorname{div}; \Omega) \cap L^\infty(\Omega; \mathbb{R}^d)$, for a.e. $x \in \Omega$ are defined by

$$u(x) := \left(1 - \frac{d}{\alpha r}\right) g(x), \quad z(x) := \begin{cases} -\frac{x}{r} & \text{if } |x| < r, \\ -\frac{rx}{|x|^d} & \text{if } |x| \geq r. \end{cases} \quad (5.16)$$

Note that $z \in W^{1,\infty}(\Omega; \mathbb{R}^d)$, so that, appealing to [25, 4], uniform mesh-refinement (i.e., $\theta = 1$ in Algorithm 5.4) is expected to yield the quasi-optimal convergence rate $\mathcal{O}(h^{\frac{1}{2}})$.

2D Case. The coarsest triangulation \mathcal{T}_0 of Figure 1 (initial triangulation of Algorithm 5.4) consists of 16 halved squares. More precisely, Figure 1 displays the triangulations \mathcal{T}_i , $i \in \{0, 15, 20, 25\}$, generated by Algorithm 5.4 using either the adaptively modified $\varepsilon_i \in \mathcal{L}^0(\mathcal{T}_i)$, cf. (local), or the global choice $\varepsilon_i := h_i^2$, cf. (global). For both choices, a refinement towards the circle $\partial B_r^2(0)$, i.e., the jump set J_u of the exact solution $u \in BV(\Omega) \cap L^\infty(\Omega)$, cf. (5.16), is reported. This behavior is also seen in Figure 2, where the regularized, discrete primal solution $u_{15}^{cr} \in \mathcal{S}_D^{1,cr}(\mathcal{T}_{15})$, the (local) L^2 -projection onto element-wise constant functions $\Pi_{h_{15}} u_{15}^{cr} \in \mathcal{L}^0(\mathcal{T}_{15})$, and the (local) L^2 -projections onto element-wise affine functions of the modulus of the regularized, discrete dual solution $z_{15}^{rt} \in \mathcal{RT}_N^0(\mathcal{T}_{15})$ and of the projected regularized, discrete dual solution $\bar{z}_{15}^{rt} \in \mathcal{RT}_N^0(\mathcal{T}_{15})$ are plotted. Figure 1, in addition, shows that using the adaptively modified $\varepsilon_i \in \mathcal{L}^0(\mathcal{T}_i)$, cf. (local), the refinement is more concentrated at the jump set J_u of the exact solution $u \in BV(\Omega) \cap L^\infty(\Omega)$, cf. (5.16). However, in Figure 3 it is seen that (local) does not result in an improved error decay, but an error decay comparable to (global). In addition, Figure 3 demonstrates that Algorithm 5.4 improves the experimental convergence rate of about $\mathcal{O}(h^{\frac{1}{2}})$ predicted by [25, 4] for uniform mesh-refinement to the quasi-optimal rate $\mathcal{O}(h)$, cf. Remark 5.6 (below). In addition, Figure 3 indicates the primal-dual error estimator is reliable and efficient with respect to the error quantity

$$\tilde{\rho}^2(\bar{u}_i^{cr}, \bar{z}_i^{rt}) := \frac{\alpha}{2} \|\bar{u}_i^{cr} - u\|_{L^2(\Omega)}^2 + \frac{1}{2\alpha} \|\operatorname{div} \bar{z}_i^{rt} - \operatorname{div} z\|_{L^2(\Omega)}^2, \quad i \in \mathbb{N}, \quad (5.17)$$

which, appealing to Remark 3.3 (iv), is a lower bound for sum of the optimal convexity measures.

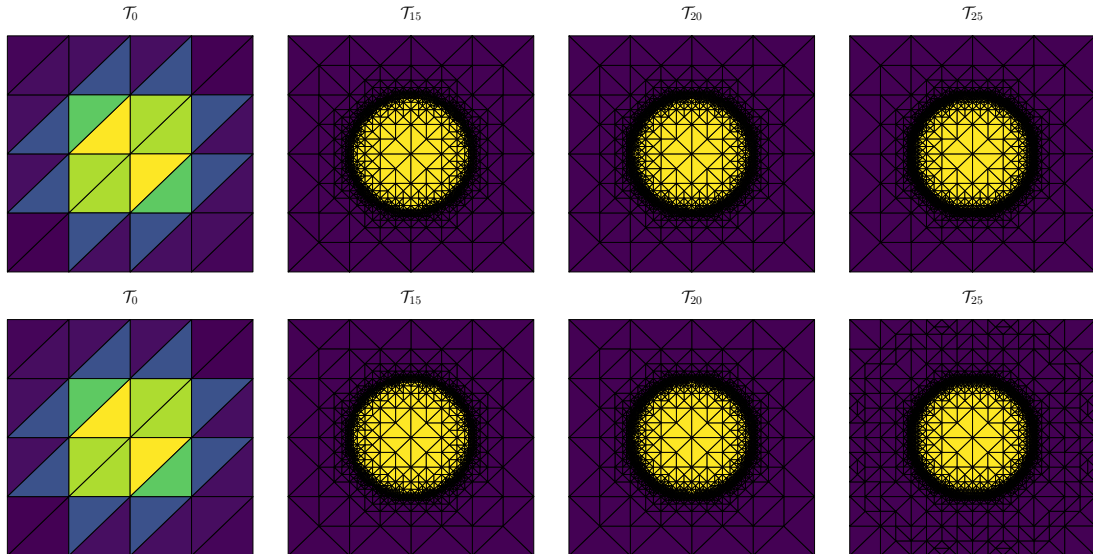


Figure 1: Initial triangulation \mathcal{T}_0 and adaptively refined meshes \mathcal{T}_i , $i \in \{0, 15, 20, 25\}$, generated by the adaptive Algorithm 5.4 (TOP: obtained using (local); BOTTOM: obtained using (global)).

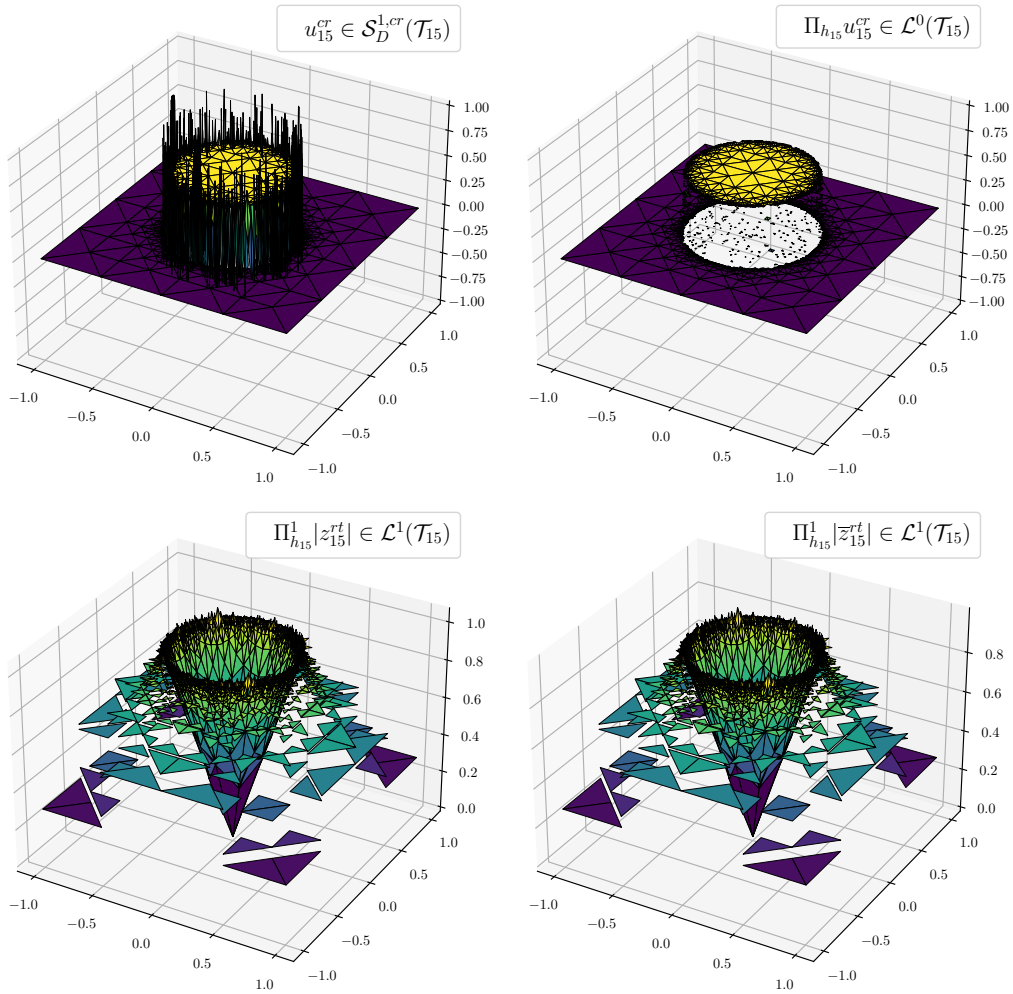
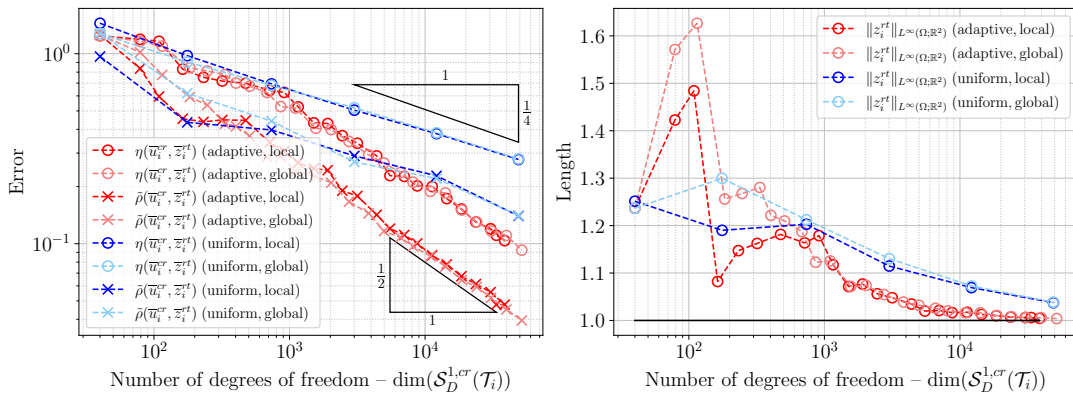


Figure 2: UPPER LEFT: Plot of $u_{15}^{cr} \in \mathcal{S}_D^{1,cr}(\mathcal{T}_{15})$, UPPER RIGHT: Plot of $\Pi_{h_{15}} u_{15}^{cr} \in \mathcal{L}^0(\mathcal{T}_{15})$; LOWER LEFT: Plot of $\Pi_{h_{15}}^1 |z_{15}^{rt}| \in \mathcal{L}^1(\mathcal{T}_{15})$; LOWER RIGHT: Plot of $\Pi_{h_{15}}^1 |\bar{z}_{15}^{rt}| \in \mathcal{L}^1(\mathcal{T}_{15})$; each obtained using (local).



3D Case. The initial triangulation \mathcal{T}_0 of Algorithm 5.4 consists of 27 cubes each divided into six tetrahedrons. Using either the adaptively modified $\varepsilon_i \in \mathcal{L}^0(\mathcal{T}_i)$, cf. (local), or the global choice $\varepsilon_i := h_i^2$, cf. (global), we report similar results to the 2D case: for both choices, a refinement towards the sphere $\partial B_r^3(0)$, i.e., the jump set J_u of the exact solution $u \in BV(\Omega) \cap L^\infty(\Omega)$, cf. (5.16), is reported, which can be seen in Figure 4, where the regularized, discrete primal solution $u_{10}^{cr} \in \mathcal{S}_D^{1,cr}(\mathcal{T}_{10})$ and the (local) L^2 -projection onto element-wise affine functions of the modulus of the regularized, discrete dual solution $z_{10}^{rt} \in \mathcal{RT}_N^0(\mathcal{T}_{10})$ are plotted. Figure 3 shows that the adaptive Algorithm 5.4 improves the experimental convergence rate of about $\mathcal{O}(h^{\frac{1}{2}})$ predicted by [25, 4] for uniform mesh-refinement to the quasi-optimal rate $\mathcal{O}(h)$, cf. Remark 5.6 (below).

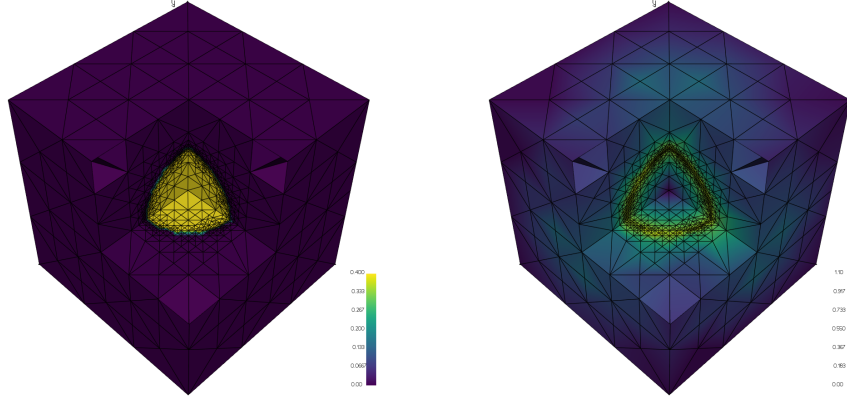


Figure 4: LEFT: Plot of $u_{10}^{cr} \in \mathcal{S}_D^{1,cr}(\mathcal{T}_{10})$; RIGHT: Plot of $\Pi_{h_{10}}^1 |z_{10}^{rt}| \in \mathcal{L}^1(\mathcal{T}_{10})$; each obtained using (local).

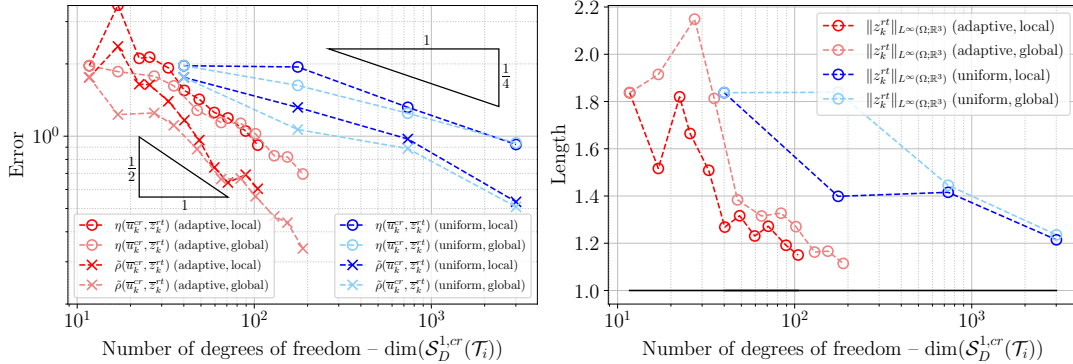


Figure 5: LEFT: Plots of $\eta(\bar{u}_i^{cr}, \bar{z}_i^{rt})$ and $\bar{\rho}(\bar{u}_i^{cr}, \bar{z}_i^{rt})$ using adaptive mesh refinement for $i = 0, \dots, 10$ and uniform mesh refinement for $i = 0, \dots, 3$; RIGHT: Plots of $\|z_i^{rt}\|_{L^\infty(\Omega; \mathbb{R}^3)}$ using adaptive mesh refinement for $i = 0, \dots, 10$ and uniform mesh refinement for $i = 0, \dots, 3$.

Remark 5.6 (A Comment on the optimality of linear convergence rates). *In one dimension, the L^2 -best-approximation error of the sign function on quasi-uniform partitions is of order $\mathcal{O}(h^{\frac{1}{2}})$, cf. [3, Example 10.5]. More generally, using that the intersection $BV(\Omega) \cap L^\infty(\Omega)$ is contained in fractional Sobolev spaces $W^{s,2}(\Omega)$ for all $s < 1/2$, cf. [47, Lemma 38.1], one cannot expect a higher convergence rate than $\mathcal{O}(h^{\frac{1}{2}})$ for generic, essentially bounded functions of bounded variation. For triangulations that are graded towards the jump sets of certain discontinuous functions with a quadratic grading strength, i.e., the local mesh-size satisfies $h_T \sim h^2$ for all elements $T \in \mathcal{T}_h$ at the discontinuity set, with the average mesh-size $h \sim \text{card}(\mathcal{N}_h)^{-1/d}$, a linear convergence rate $\mathcal{O}(h)$ has been established in [10]. Since our error estimates not only bound squared L^2 -errors but also control squares of L^p -norms of non-linear error quantities involving derivatives, cf. [10, Remark 5.4], a higher convergence rate than linear cannot be expected. In view of these aspects, the linear convergence rate $\mathcal{O}(h)$ for the devised adaptive strategy is quasi-optimal.*

5.4 Example without Lipschitz continuous dual solution

We examine an example from [10]. In this example, we let $\Omega = (-1.5, 1.5)^2$, $\Gamma_D = \partial\Omega$, $r = \frac{1}{2}$, $\alpha = 10$, and $g = \chi_{B_r^2(re_1)} - \chi_{B_r^2(-re_1)} \in BV(\Omega) \cap L^\infty(\Omega)$. Then, the primal solution $u \in BV(\Omega) \cap L^\infty(\Omega)$ and a dual solution $z \in W^2(\text{div}; \Omega) \cap L^\infty(\Omega; \mathbb{R}^2)$, for a.e. $x \in \Omega$ are defined by

$$u(x) := \left(1 - \frac{2}{\alpha r}\right) g(x), \quad z(x) := \begin{cases} \mp \frac{x \mp re_1}{r} & \text{if } |x \mp re_1| < r, \\ \mp \frac{r(x \mp re_1)}{|x \mp re_1|^2} & \text{if } |x \mp re_1| \geq r. \end{cases} \quad (5.18)$$

Note that $z \notin W^{1,\infty}(\Omega; \mathbb{R}^2)$, so that we cannot refer to [25, 4] in order to expect uniform mesh-refinement to yield the convergence rate $\mathcal{O}(h^{\frac{1}{2}})$. However, since $z|_{\Omega^\pm} \in W^{1,\infty}(\Omega^\pm; \mathbb{R}^2)$, where $\Omega^+ := \Omega \cap (\mathbb{R}_{>0} \times \mathbb{R})$ and $\Omega^- := \Omega \cap (\mathbb{R}_{<0} \times \mathbb{R})$, and since the coarsest triangulation \mathcal{T}_0 of Figure 6 and, hence, also all resulting refinements \mathcal{T}_i , $i \in \mathbb{N}$, of \mathcal{T}_0 resolve $J_z := \Omega \cap (\{0\} \times \mathbb{R})$, i.e., the jump set of $z \in W^2(\text{div}; \Omega) \cap L^\infty(\Omega; \mathbb{R}^2)$, in the sense that $J_z \subseteq \bigcup_{S \in \mathcal{S}_{h_i}} S$ for all $i \in \mathbb{N}$, referring to [6, Theorem 4.5], we can expect uniform mesh-refinement to yield the convergence rate $\mathcal{O}(h^{\frac{1}{2}})$.

The coarsest triangulation \mathcal{T}_0 of Figure 6 (initial triangulation of Algorithm 5.4) consists of 16 halved squares. More precisely, Figure 1 displays the triangulations \mathcal{T}_i , $i \in \{0, 15, 20, 25\}$, generated by Algorithm 5.4 using either the adaptively modified $\varepsilon_i \in \mathcal{L}^0(\mathcal{T}_i)$, cf. (local), or the global choice $\varepsilon_i := h_i^2$, cf. (global). For both choices, a refinement towards $\partial B_r^2(re_1) \cup \partial B_r^2(-re_1)$, i.e., the jump set J_u of the exact solution $u \in BV(\Omega) \cap L^\infty(\Omega)$, cf. (5.18), is reported. This behavior is also seen in Figure 7, where the regularized, discrete primal solution $u_{15}^{cr} \in \mathcal{S}_D^{1,cr}(\mathcal{T}_{15})$, the (local) L^2 -projection onto element-wise constant functions $\Pi_{h_{15}} u_{15}^{cr} \in \mathcal{L}^0(\mathcal{T}_{15})$, and the (local) L^2 -projections onto element-wise affine functions of the modulus of the regularized, discrete dual solution $z_{15}^{rt} \in \mathcal{RT}_N^0(\mathcal{T}_{15})$ and of the scaled regularized, discrete dual solution $\bar{z}_{15}^{rt} \in \mathcal{RT}_N^0(\mathcal{T}_{15})$ are plotted. Figure 6, in addition, shows that employing the adaptively modified regularization parameter, cf. (local), the refinement is more concentrated at the jump set J_u of the exact solution $u \in BV(\Omega) \cap L^\infty(\Omega)$, cf. (5.18). However, in Figure 8 it can be seen that (local) does not result in an improved error decay, but an error decay comparable to (global). In addition, Figure 8 demonstrates that Algorithm 5.4 improves the experimental convergence rate of about $\mathcal{O}(h^{\frac{1}{2}})$ predicted by [6, Theorem 4.5] for uniform mesh-refinement to the quasi-optimal rate $\mathcal{O}(h)$, cf. Remark 5.6. In addition, Figure 8 indicates the primal-dual error estimator is both reliable and efficient with respect to the error quantity (5.17).

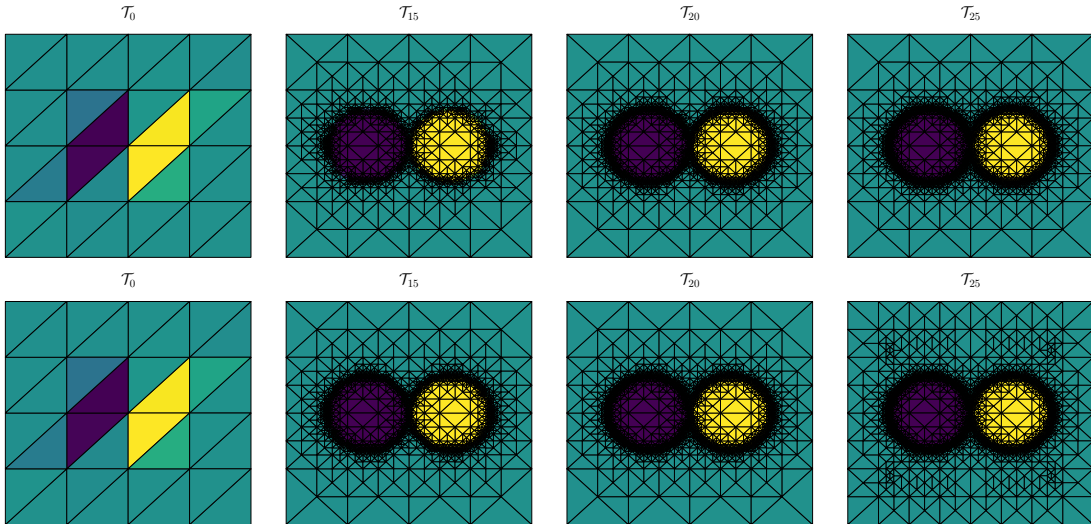


Figure 6: Initial triangulation \mathcal{T}_0 and adaptively refined meshes \mathcal{T}_i , $i \in \{0, 10, 20, 25\}$, generated by the adaptive Algorithm 5.4 (TOP: obtained using (local); BOTTOM: obtained using (global)).

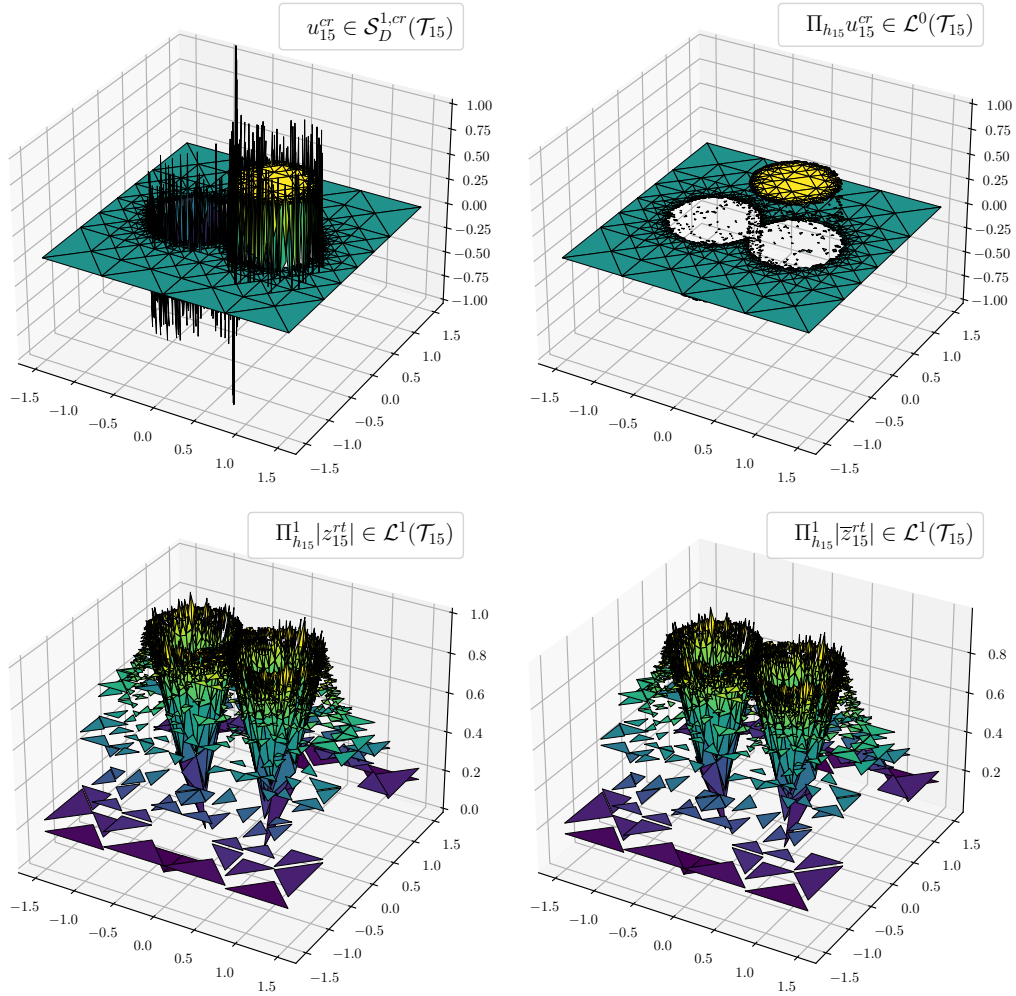


Figure 7: UPPER LEFT: Plot of $u_{15}^{cr} \in S_D^{1,cr}(\mathcal{T}_{15})$, UPPER RIGHT: Plot of $\Pi_{h_{15}} u_{15}^{cr} \in \mathcal{L}^0(\mathcal{T}_{15})$; LOWER LEFT: Plot of $\Pi_{h_{15}}^1 |z_{15}^{rt}| \in \mathcal{L}^1(\mathcal{T}_{15})$; LOWER RIGHT: Plot of $\Pi_{h_{15}}^1 |\bar{z}_{15}^{rt}| \in \mathcal{L}^1(\mathcal{T}_{15})$; each obtained using (local).

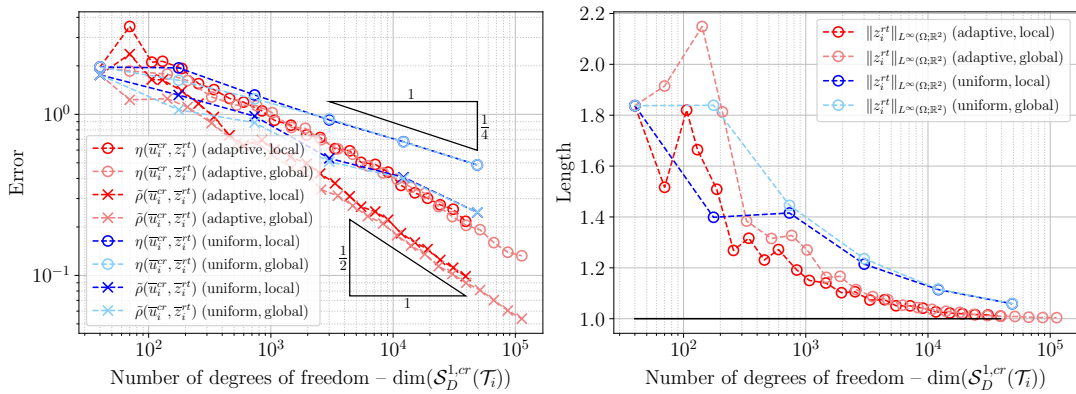


Figure 8: LEFT: Plots of $\eta(\bar{u}_i^{cr}, \bar{z}_i^{rt})$ and $\tilde{\rho}(\bar{u}_i^{cr}, \bar{z}_i^{rt})$ using adaptive mesh refinement for $i = 0, \dots, 25$ and uniform mesh refinement for $i = 0, \dots, 5$; RIGHT: Plots of $\|z_i^{rt}\|_{L^\infty(\Omega; \mathbb{R}^2)}$ using adaptive mesh refinement for $i = 0, \dots, 25$ and uniform mesh refinement for $i = 0, \dots, 5$.

5.5 Example with Lipschitz continuous primal solution and Lipschitz continuous dual solution

We examine an example from [5]. In this example, we let $\Omega = (-1.5, 1.5)^2$, $\Gamma_D = \partial\Omega$, $\alpha = 10$, $s(t) := \sqrt{3t}$ and $r(t) := \frac{1}{2}\sqrt{1-4t}$ for $t = 0.1$, and $g \in BV(\Omega) \cap L^\infty(\Omega)$ for a.e. $x \in \Omega$, be defined by

$$g(x) := \begin{cases} 1 + \frac{2-\alpha(s(t)^2+t)}{s(t)} & \text{if } |x| \leq s(t), \\ 1 + \frac{1-\alpha(|x|^2+t)}{|x|} & \text{if } s(t) < |x| \leq r(t), \\ 0 & \text{else.} \end{cases}$$

Then, the primal solution $u \in BV(\Omega) \cap L^\infty(\Omega)$ and a dual solution $z \in W^2(\text{div}; \Omega) \cap L^\infty(\Omega; \mathbb{R}^2)$ with $|z| \leq 1$ a.e. in Ω , for a.e. $x \in \Omega$ are defined by

$$u(x) := \begin{cases} 1 - \frac{s(t)^2+t}{s(t)} & \text{if } |x| \leq s(t), \\ 1 - \frac{|x|^2+t}{|x|} & \text{if } s(t) < |x| \leq r(t), \\ 0 & \text{else,} \end{cases} \quad z(x) := \begin{cases} -\frac{x}{s(t)} & \text{if } |x| \leq s(t), \\ -\frac{x}{|x|} & \text{if } s(t) < |x| \leq r(t), \\ -\frac{xr(t)}{|x|^2} & \text{else.} \end{cases} \quad (5.19)$$

Note that $z \in W^{1,\infty}(\Omega; \mathbb{R}^2)$, so that, appealing to [25, 4], uniform mesh-refinement is expected to yield the quasi-optimal convergence rate $\mathcal{O}(h^{\frac{1}{2}})$.

The coarsest triangulation \mathcal{T}_0 of Figure 9 (initial triangulation of Algorithm 5.4) consists of 16 halved squares. More precisely, Figure 9 displays the triangulations \mathcal{T}_i , $i \in \{0, 5, 10, 15\}$, generated by Algorithm 5.4 employing either $\varepsilon_i \in \mathcal{L}^0(\mathcal{T}_i)$, cf. (local), or $\varepsilon_i := h_i^2$, cf. (global). For both choices, a refinement mainly towards and on the set $\{|\nabla u| > 0\}$ is reported. This is also seen in Figure 10, where the regularized, discrete primal solution $u_{15}^{cr} \in \mathcal{S}_D^{1,cr}(\mathcal{T}_{10})$, the (local) L^2 -projection onto element-wise constant functions $\Pi_{h_{10}} u_{10}^{cr} \in \mathcal{L}^0(\mathcal{T}_{10})$, and the (local) L^2 -projections onto element-wise affine functions of the modulus of the regularized, discrete dual solution $z_{10}^{rt} \in \mathcal{RT}_N^0(\mathcal{T}_{10})$ and of the scaled regularized, discrete dual solution $\bar{z}_{10}^{rt} \in \mathcal{RT}_N^0(\mathcal{T}_{10})$ are plotted. Figure 9 shows that employing the adaptively modified regularization parameter, cf. (local), the refinement takes place at and on the set $\{|\nabla u| > 0\}$. However, in Figure 11, again, it can be seen that (local) does not result in an improved error decay, but an error decay comparable to (global). In addition, Figure 11 demonstrates that Algorithm 5.4 improves the experimental convergence rate of about $\mathcal{O}(h^{\frac{1}{2}})$ predicted by [25, 4] for uniform mesh-refinement to the quasi-optimal rate $\mathcal{O}(h)$, cf. Remark 5.6. In addition, Figure 11 indicates the primal-dual error estimator is both reliable and efficient with respect to the error quantity (5.17).

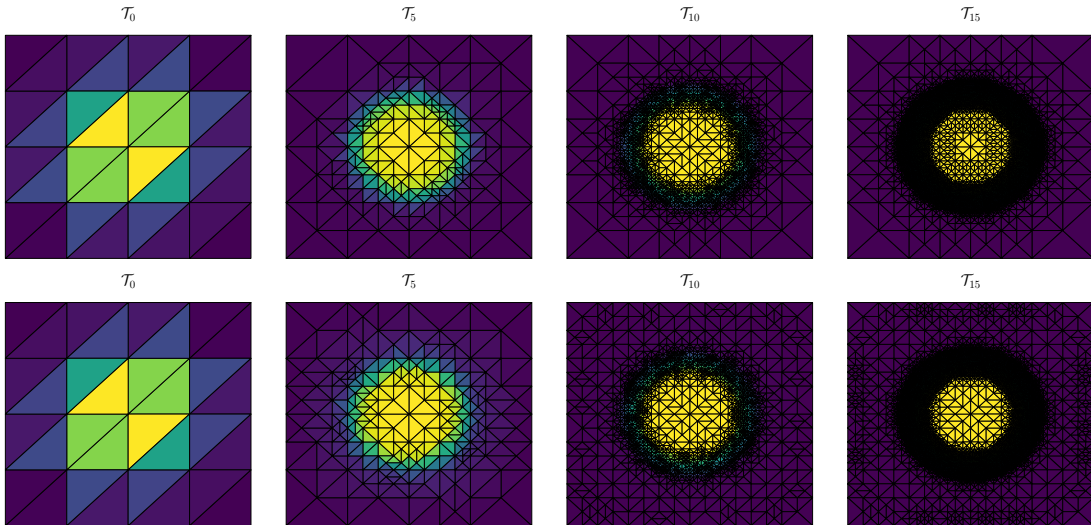


Figure 9: Initial triangulation \mathcal{T}_0 and adaptively refined meshes \mathcal{T}_i , $i \in \{0, 5, 10, 15\}$, generated by the adaptive Algorithm 5.4 (TOP: obtained using (local); BOTTOM: obtained using (global)).

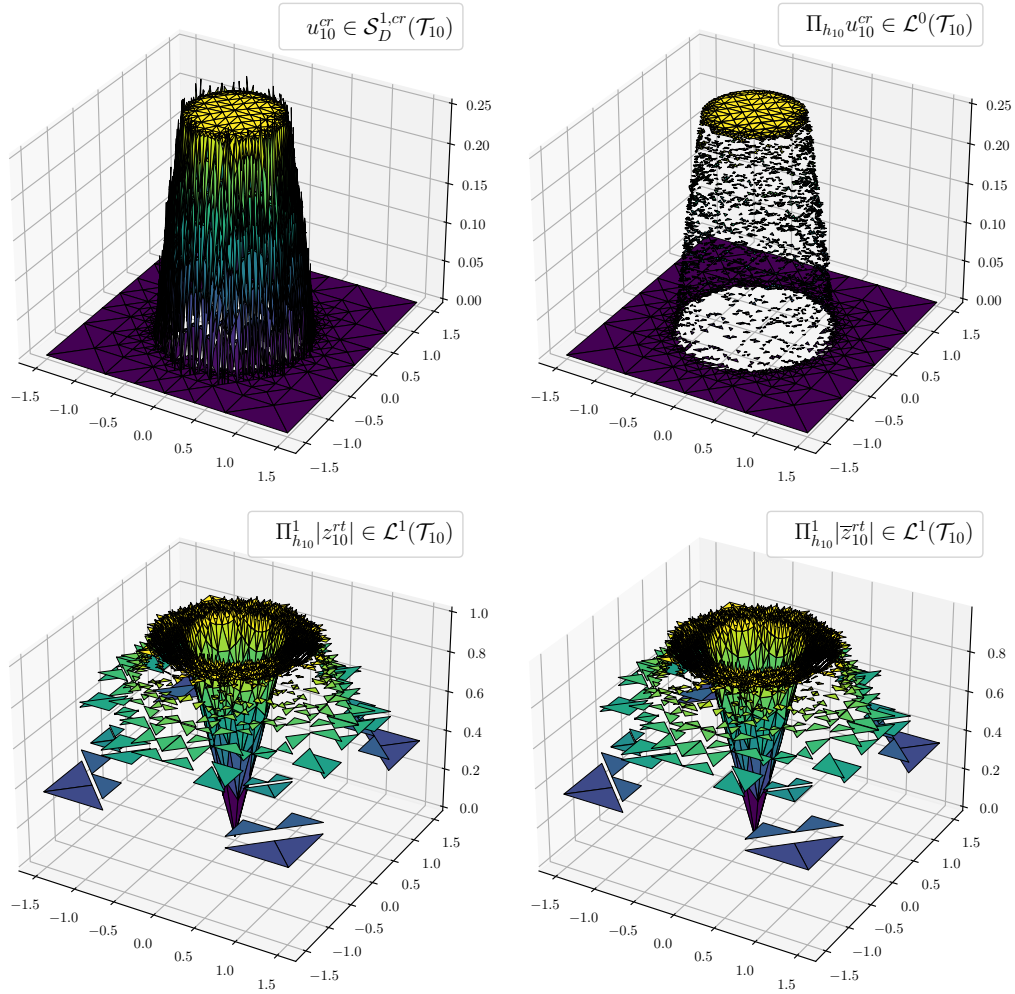


Figure 10: UPPER LEFT: Plot of $u_{10}^{cr} \in \mathcal{S}_D^{1,cr}(\mathcal{T}_{10})$; UPPER RIGHT: Plot of $\Pi_{h_{10}}^0 u_{10}^{cr} \in \mathcal{L}^0(\mathcal{T}_{10})$; LOWER LEFT: Plot of $\Pi_{h_{10}}^1 |z_{10}^{rt}| \in \mathcal{L}^1(\mathcal{T}_{10})$; LOWER RIGHT: Plot of $\Pi_{h_{10}}^1 |\bar{z}_{10}^{rt}| \in \mathcal{L}^1(\mathcal{T}_{10})$; each obtained using (local).

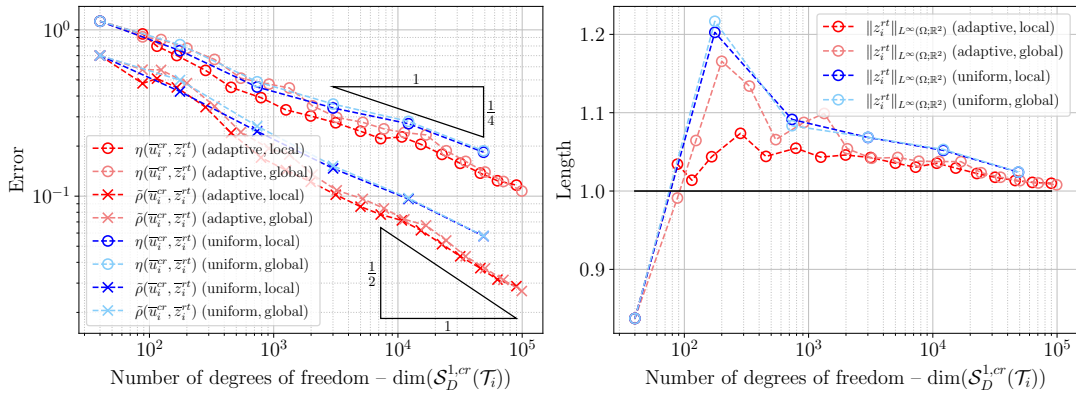


Figure 11: LEFT: Plots of $\eta(\bar{u}_i^{cr}, \bar{z}_i^{rt})$ and $\tilde{\rho}(\bar{u}_i^{cr}, \bar{z}_i^{rt})$ using adaptive mesh refinement for $i = 0, \dots, 20$ and uniform mesh refinement for $i = 0, \dots, 5$; RIGHT: Plots of $\|\bar{z}_i^{rt}\|_{L^\infty(\Omega; \mathbb{R}^2)}$ using adaptive mesh refinement for $i = 0, \dots, 20$ and uniform mesh refinement for $i = 0, \dots, 5$.

5.6 Example without Dirichlet boundary condition and without exact solution

We examine an example from [12, 8]. In this example, we let $\Omega = (-1, 1)^2$, $r = \frac{1}{2}$, $\Gamma_D = \emptyset$, $\alpha = 100$, and $g = \chi_{[-r, r]^2} \in BV(\Omega) \cap L^\infty(\Omega)$. Then, the primal solution and the dual solutions are not known. However, appealing to [25, Section 5.2], given the regularity of $g \in BV(\Omega) \cap L^\infty(\Omega)$, we can expect the convergence rate $\mathcal{O}(h^{\frac{1}{4}})$ using uniform mesh refinement.

The coarsest triangulation \mathcal{T}_0 of Figure 1 (initial triangulation of Algorithm 5.4) consists of 16 halved squares. More precisely, Figure 12 displays the triangulations \mathcal{T}_i , $i \in \{0, 15, 20, 25\}$, generated by Algorithm 5.4 using either the adaptively modified $\varepsilon_i \in \mathcal{L}^0(\mathcal{T}_i)$, cf. (local), or the global choice $\varepsilon_i := h_i^2$, cf. (global). For both choices, a refinement towards the square $\partial[-r, r]^2$, i.e., the jump set J_g of the data $g \in BV(\Omega) \cap L^\infty(\Omega)$ is reported. This behavior is also seen in Figure 13, where the regularized, discrete primal solution $u_{15}^{cr} \in \mathcal{S}_D^{1, cr}(\mathcal{T}_{15})$, the (local) L^2 -projection onto element-wise constant functions $\Pi_{h_{15}} u_{15}^{cr} \in \mathcal{L}^0(\mathcal{T}_{15})$, and the (local) L^2 -projections onto element-wise affine functions of the modulus of the regularized, discrete dual solution $z_{15}^{rt} \in \mathcal{RT}_N^0(\mathcal{T}_{15})$ and of the projected regularized, discrete dual solution $\bar{z}_{15}^{rt} \in \mathcal{RT}_N^0(\mathcal{T}_{15})$ are plotted. Figure 12, in addition, shows that using the adaptively modified $\varepsilon_i \in \mathcal{L}^0(\mathcal{T}_i)$, cf. (local), the refinement is, again, more concentrated at the jump set J_g of the data $g \in BV(\Omega) \cap L^\infty(\Omega)$. However, in Figure 3 it can be seen that (local) does not result in an improved error decay, but an error decay comparable to (global). In addition, Figure 14 demonstrates that Algorithm 5.4 improves the experimental convergence rate of about $\mathcal{O}(h^{\frac{1}{4}})$ predicted by [25, Section 5.2] for uniform mesh-refinement to the value $\mathcal{O}(h^{\frac{2}{5}})$. This, on the one hand, confirms the optimality of the a priori error estimates established in [25, Section 5.2] and, on the other hand, appealing to [25, 4], let us expect that there exists no Lipschitz continuous dual solution to the given data $g = \chi_{[-r, r]^2} \in BV(\Omega) \cap L^\infty(\Omega)$. The reported reduced error decay of $\mathcal{O}(h^{\frac{2}{5}})$ compared to [12], where an error decay of $\mathcal{O}(h^{\frac{1}{2}})$ is reported, might only be pre-asymptotic and due to slight accuracy losses resulting due to the global scaling step. This might be due to potential singularities of a dual solution located at the corners of the square $\partial[-r, r]^2$, as indicated in Figure 13. Therefore, it is possible that the error decay $\mathcal{O}(h^{\frac{1}{2}})$ in [12] may be reported after surpassing a potential pre-asymptotic regime.

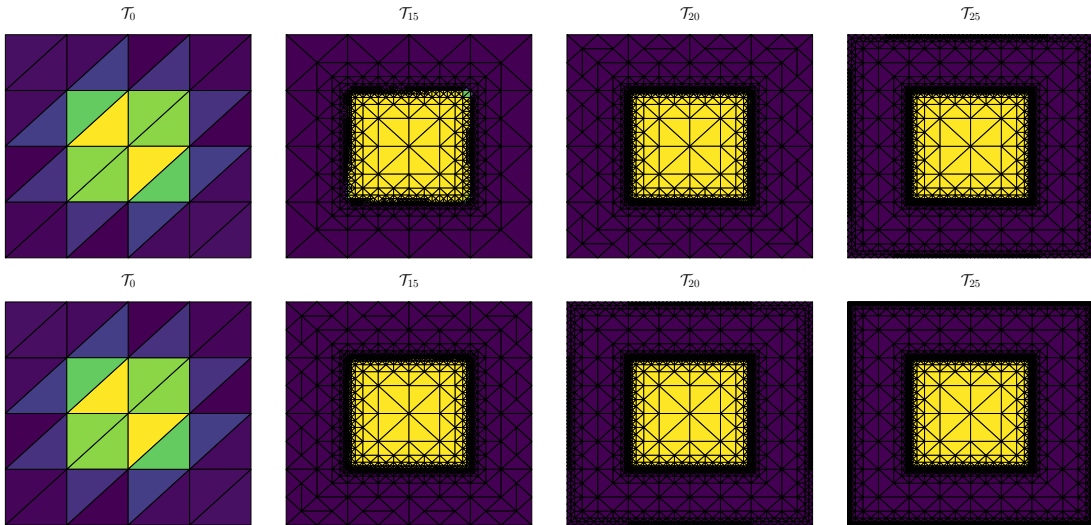


Figure 12: Initial triangulation \mathcal{T}_0 and adaptively refined meshes \mathcal{T}_i , $i \in \{0, 15, 20, 25\}$, generated by the adaptive Algorithm 5.4 (TOP: obtained using (local); BOTTOM: obtained using (global)).

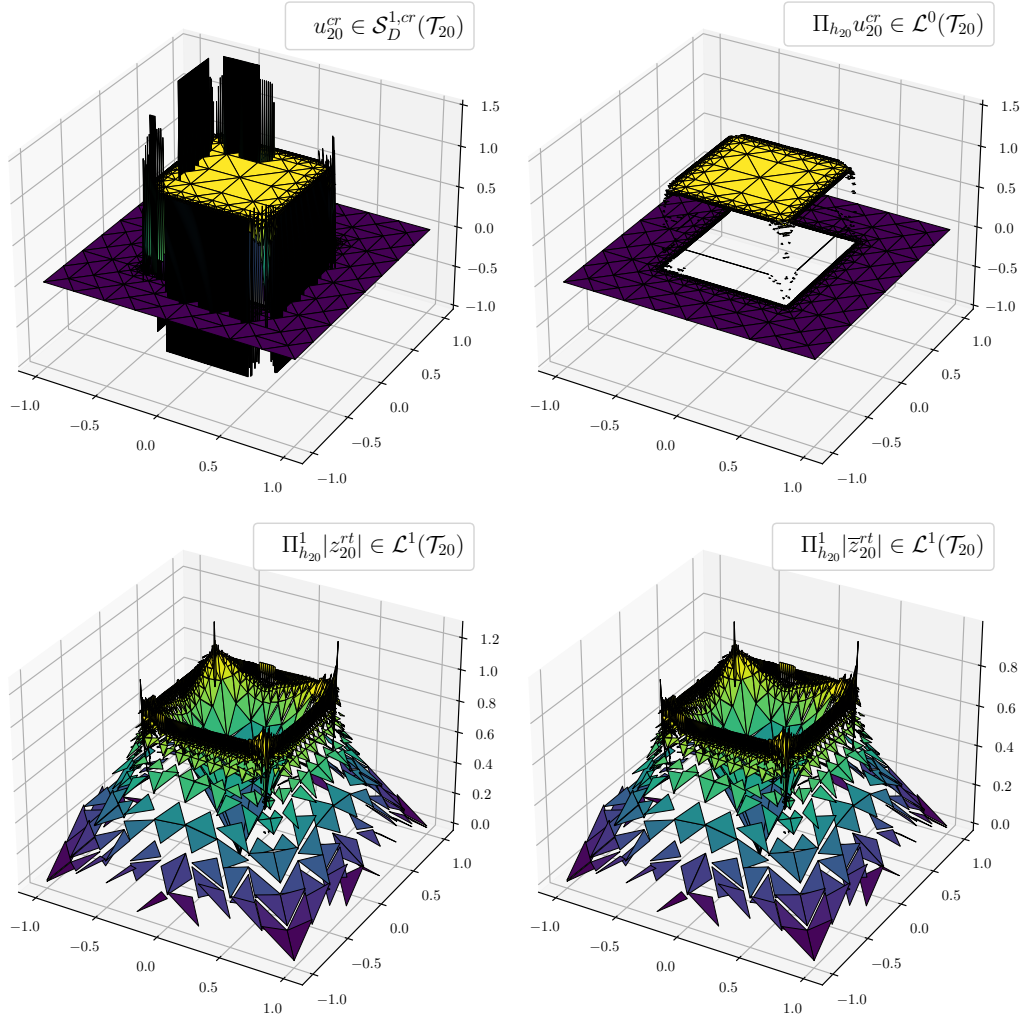


Figure 13: UPPER LEFT: Plot of $u_{20}^{cr} \in \mathcal{S}_D^{1,cr}(\mathcal{T}_{20})$; UPPER RIGHT: Plot of $\Pi_{h_{20}} u_{20}^{cr} \in \mathcal{L}^0(\mathcal{T}_{20})$; LOWER LEFT: Plot of $\Pi_{h_{20}}^1 |z_{20}^{rt}| \in \mathcal{L}^1(\mathcal{T}_{20})$; LOWER RIGHT: Plot of $\Pi_{h_{20}}^1 |\bar{z}_{20}^{rt}| \in \mathcal{L}^1(\mathcal{T}_{20})$; each obtained using (local).

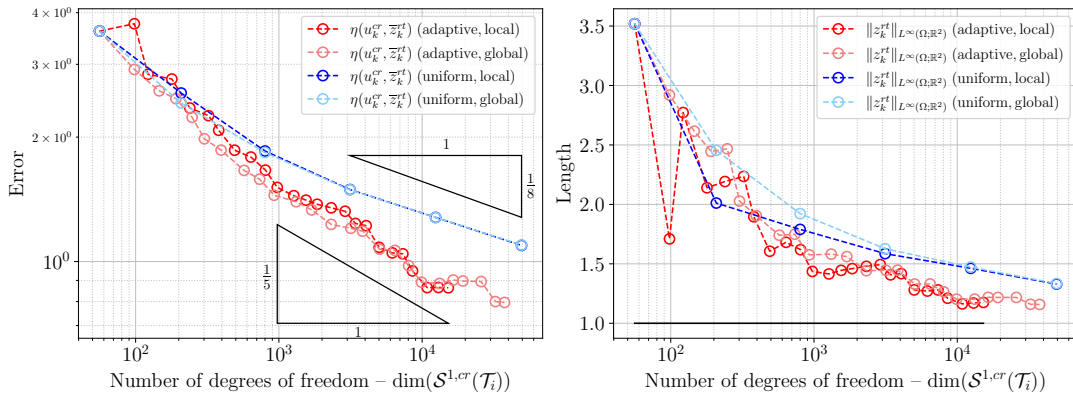


Figure 14: LEFT: Plots of $\eta(u_i^{cr}, \bar{z}_i^{rt})$ and $\tilde{\rho}(u_i^{cr}, \bar{z}_i^{rt})$ using adaptive mesh refinement for $i = 0, \dots, 25$ and uniform mesh refinement for $i = 0, \dots, 5$; RIGHT: Plots of $\|\bar{z}_i^{rt}\|_{L^\infty(\Omega; \mathbb{R}^2)}$ using adaptive mesh refinement for $i = 0, \dots, 25$ and uniform mesh refinement for $i = 0, \dots, 5$.

5.7 Numerical experiments with application to image processing

In order to benchmark the performance of the proposed numerical scheme (cf. Algorithm 5.1 and Algorithm 5.4) in a problem related to image processing, we examine a standard example from the field of image processing (cf. Section 5.7.1) and a new example (cf. Section 5.7.2).

5.7.1 The Cameraman image

We examine the cameraman image, which in a similar context has been considered in [12]. In this example, we let $\Omega := (0, 1)^2$, $\Gamma_D = \emptyset$, $\alpha = 1e+4$, and $g \in BV(\Omega) \cap L^\infty(\Omega)$ a piece-wise constant function taking its values in the interval $[0, 1]$, representing the cameraman image on a uniform triangulation with 66.049 nodes, cf. Figure 15. The adaptive algorithm (cf. Algorithm 5.4), employed as coarsening strategy, reduces the number of nodes within 30 iteration steps to 25.059 nodes which corresponds to 38.0% of the initial number of nodes, which results in a squared L^2 -error of $\|u_{30}^{cr} - g\|_{L^2(\Omega)}^2 \approx 2.211e-3$. The resulting coarsened image, represented by $u_{30}^{cr} \in \mathcal{S}^{1,cr}(\mathcal{T}_{30})$, is shown in Figure 15. The underlying grid \mathcal{T}_{30} shown in Figure 16 reveals the expected coarsening of the triangulation away from the edges.

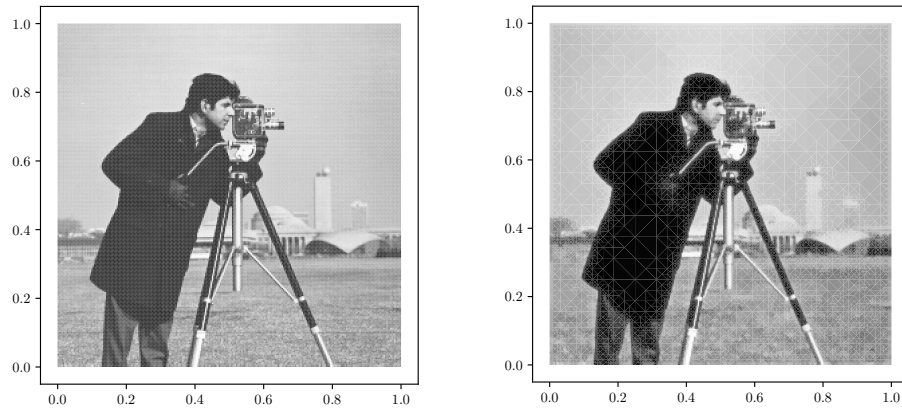


Figure 15: LEFT: Plot of the cameraman image $g \in BV(\Omega) \cap L^\infty(\Omega)$ on a grid with 66.049 nodes; RIGHT: Plot of coarsened image $u_{30}^{cr} \in \mathcal{S}^{1,cr}(\mathcal{T}_{30})$ on \mathcal{T}_{30} with 25.059 nodes, cf. Figure 16.

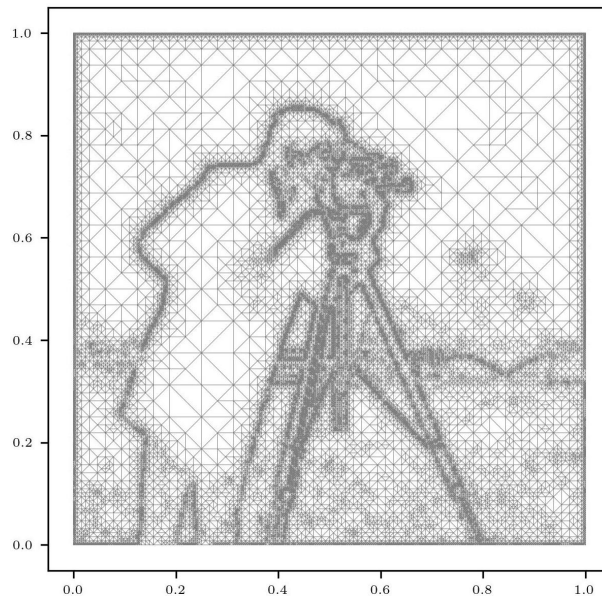


Figure 16: Triangulation \mathcal{T}_{30} in the coarsened image $u_{30}^{cr} \in \mathcal{S}^{1,cr}(\mathcal{T}_{30})$ on the right of Figure 15.

5.7.2 The Merle image

We examine an image of Merle, the male cat of the second author. In this example, we let $\Omega := (0, 1)^2$, $\Gamma_D = \emptyset$, $\alpha = 1e+4$, and $g \in BV(\Omega) \cap L^\infty(\Omega)$ a piece-wise constant function taking its values in the interval $[0, 1]$, representing the Merle image on a uniform triangulation with 140.625 nodes, cf. Figure 17. The adaptive algorithm (cf. Algorithm 5.4), employed as coarsening strategy, reduces the number of nodes within 30 iteration steps to 41.749 nodes which is 30.0% of the initial number of nodes, which results in a squared L^2 -error of $\|u_{30}^{cr} - g\|_{L^2(\Omega)}^2 \approx 2.162e-3$. The resulting coarsened image, represented by $u_{30}^{cr} \in \mathcal{S}^{1,cr}(\mathcal{T}_{30})$, is shown in Figure 17. The underlying grid \mathcal{T}_{30} shown in Figure 18 reveals the expected coarsening of the triangulation away from the edges.

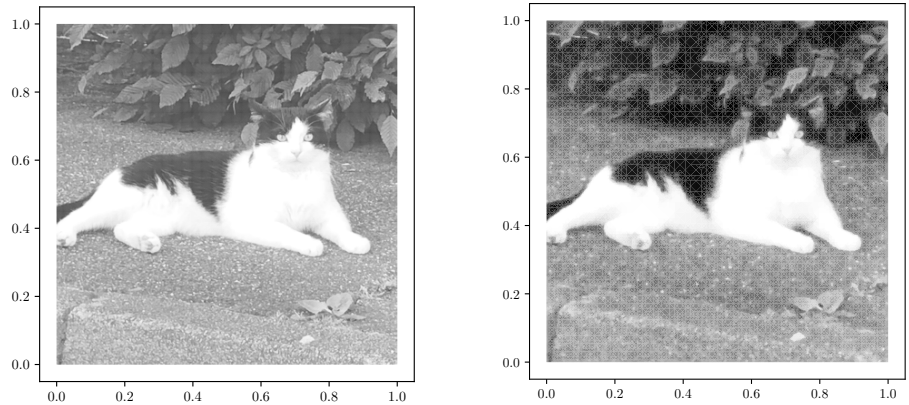


Figure 17: LEFT: Plot of the Merle image $g \in BV(\Omega) \cap L^\infty(\Omega)$ on a grid with 140.625 nodes; RIGHT: Plot of coarsened image $u_{30}^{cr} \in \mathcal{S}^{1,cr}(\mathcal{T}_{30})$ on \mathcal{T}_{30} with 41.749 nodes, cf. Figure 18.

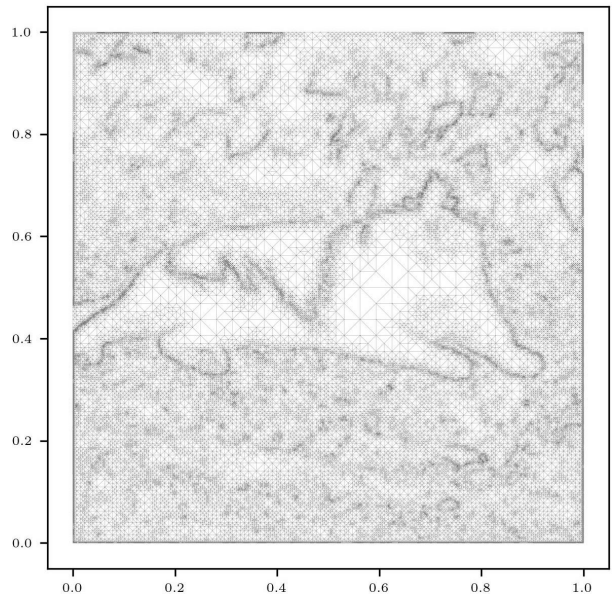


Figure 18: Triangulation \mathcal{T}_{30} in the coarsened image of $u_{30}^{cr} \in \mathcal{S}^{1,cr}(\mathcal{T}_{30})$ on the right of Figure 17.

REFERENCES

[1] M. AINSWORTH and J. T. ODEN, *A posteriori error estimation in finite element analysis*, *Pure and Applied Mathematics (New York)*, Wiley-Interscience [John Wiley & Sons], New York, 2000. doi:[10.1002/9781118032824](https://doi.org/10.1002/9781118032824).

- [2] S. BARTELS, Total variation minimization with finite elements: convergence and iterative solution, *SIAM J. Numer. Anal.* **50** no. 3 (2012), 1162–1180. doi:[10.1137/11083277X](https://doi.org/10.1137/11083277X).
- [3] S. BARTELS, *Numerical methods for nonlinear partial differential equations*, *Springer Series in Computational Mathematics* **47**, Springer, Cham, 2015. doi:[10.1007/978-3-319-13797-1](https://doi.org/10.1007/978-3-319-13797-1).
- [4] S. BARTELS, Nonconforming discretizations of convex minimization problems and precise relations to mixed methods, *Comput. Math. Appl.* **93** (2021), 214–229. doi:[10.1016/j.camwa.2021.04.014](https://doi.org/10.1016/j.camwa.2021.04.014).
- [5] S. BARTELS, L. DIENING, and R. H. NOCHETTO, Unconditional stability of semi-implicit discretizations of singular flows, *SIAM J. Numer. Anal.* **56** no. 3 (2018), 1896–1914. doi:[10.1137/17M1159166](https://doi.org/10.1137/17M1159166).
- [6] S. BARTELS and A. KALTENBACH, Error estimates for total-variation regularized minimization problems with singular dual solutions, *Numer. Math.* **152** no. 4 (2022), 881–906. doi:[10.1007/s00211-022-01324-w](https://doi.org/10.1007/s00211-022-01324-w).
- [7] S. BARTELS and A. KALTENBACH, Error analysis for a Crouzeix-Raviart approximation of the obstacle problem, 2023. doi:[10.48550/ARXIV.2302.01646](https://doi.org/10.48550/ARXIV.2302.01646).
- [8] S. BARTELS and M. MILICEVIC, Primal-dual gap estimators for *a posteriori* error analysis of nonsmooth minimization problems, *ESAIM Math. Model. Numer. Anal.* **54** no. 5 (2020), 1635–1660. doi:[10.1051/m2an/2019074](https://doi.org/10.1051/m2an/2019074).
- [9] S. BARTELS, R. H. NOCHETTO, and A. J. SALGADO, A total variation diminishing interpolation operator and applications, *Math. Comp.* **84** no. 296 (2015), 2569–2587. doi:[10.1090/mcom/2942](https://doi.org/10.1090/mcom/2942).
- [10] S. BARTELS, R. TOVEY, and F. WASSMER, Singular solutions, graded meshes, and adaptivity for total-variation regularized minimization problems, *ESAIM Math. Model. Numer. Anal.* **56** no. 6 (2022), 1871–1888. doi:[10.1051/m2an/2022056](https://doi.org/10.1051/m2an/2022056).
- [11] S. BARTELS and Z. WANG, Orthogonality relations of Crouzeix-Raviart and Raviart-Thomas finite element spaces, *Numer. Math.* **148** no. 1 (2021), 127–139. doi:[10.1007/s00211-021-01199-3](https://doi.org/10.1007/s00211-021-01199-3).
- [12] S. BARTELS, Error control and adaptivity for a variational model problem defined on functions of bounded variation, *Math. Comp.* **84** no. 293 (2015), 1217–1240. doi:[10.1090/S0025-5718-2014-02893-7](https://doi.org/10.1090/S0025-5718-2014-02893-7).
- [13] S. BARTELS and C. CARSTENSEN, A convergent adaptive finite element method for an optimal design problem, *Numer. Math.* **108** no. 3 (2008), 359–385. doi:[10.1007/s00211-007-0122-x](https://doi.org/10.1007/s00211-007-0122-x).
- [14] L. BAUMGÄRTNER, R. BERGMANN, R. HERZOG, S. SCHMIDT, and J. VIDAL-NÚÑEZ, Total generalized variation for piecewise constant functions on triangular meshes with applications in imaging, *SIAM Journal on Imaging Sciences* **16** no. 1 (2023), 313–339. doi:[10.1137/22M1505281](https://doi.org/10.1137/22M1505281).
- [15] H. H. BAUSCHKE and P. L. COMBETTES, Convex analysis and monotone operator theory in hilbert spaces, in *CMS Books in Mathematics*, 2011.
- [16] L. BAÑAS and A. WILKE, *A posteriori* estimates for the stochastic total variation flow, *SIAM J. Numer. Anal.* **60** no. 5 (2022), 2657–2680. doi:[10.1137/21M1447982](https://doi.org/10.1137/21M1447982).
- [17] F. BERTRAND and D. BOFFI, The Prager-Synge theorem in reconstruction based *a posteriori* error estimation, in *75 years of mathematics of computation*, *Contemp. Math.* **754**, Amer. Math. Soc., [Providence], RI, [2020] ©2020, pp. 45–67. doi:[10.1090/conm/754/15152](https://doi.org/10.1090/conm/754/15152).
- [18] D. BRAESS, *Finite Elemente. Theorie, schnelle Löser und Anwendungen in der Elastizitätstheorie*, 5th revised ed. ed., *Springer-Lehrb. Mastercl.*, Berlin: Springer Spektrum, 2013 (German). doi:[10.1007/978-3-642-34797-9](https://doi.org/10.1007/978-3-642-34797-9).
- [19] D. BRAESS, *A posteriori* error estimate and a comparison theorem for the nonconforming P_1 element, *Calcolo* **46** no. 2 (2009), 149–155. MR [2520373](https://doi.org/10.1007/s10092-009-0003-z). doi:[10.1007/s10092-009-0003-z](https://doi.org/10.1007/s10092-009-0003-z).
- [20] A. BRAIDES, *Approximation of free-discontinuity problems*, *Lecture Notes in Mathematics* **1694**, Springer-Verlag, Berlin, 1998. doi:[10.1007/BFb0097344](https://doi.org/10.1007/BFb0097344).
- [21] L. BRÉGMAN, The relaxation method of finding the common point of convex sets and its application to the solution of problems in convex programming, *USSR Computational Mathematics and Mathematical Physics* **7** no. 3 (1967), 200–217. doi:[https://doi.org/10.1016/0041-5553\(67\)90040-7](https://doi.org/10.1016/0041-5553(67)90040-7).
- [22] C. CARSTENSEN and D. J. LIU, Nonconforming FEMs for an optimal design problem, *SIAM J. Numer. Anal.* **53** no. 2 (2015), 874–894. doi:[10.1137/130927103](https://doi.org/10.1137/130927103).
- [23] J. CASCON, C. KREUZER, R. NOCHETTO, and K. SIEBERT, Quasi-optimal convergence rate for an adaptive finite element method, *SIAM J. Numer. Anal.* **46** no. 5 (2008), 2524–2550. doi:[10.1137/07069047X](https://doi.org/10.1137/07069047X).
- [24] V. CASELLES, A. CHAMOLLE, S. MOLL, and M. NOVAGA, A characterization of convex calibrable sets in \mathbb{R}^N with respect to anisotropic norms, *Ann. Inst. H. Poincaré Anal. Non Linéaire* **25** no. 4 (2008), 803–832. doi:[10.1016/j.anihpc.2008.04.003](https://doi.org/10.1016/j.anihpc.2008.04.003).

- [25] A. CHAMBOLLE and T. POCK, Crouzeix-Raviart approximation of the total variation on simplicial meshes, *J. Math. Imaging Vision* **62** no. 6-7 (2020), 872–899. doi:[10.1007/s10851-019-00939-3](https://doi.org/10.1007/s10851-019-00939-3).
- [26] M. CROUZEIX and P.-A. RAVIART, Conforming and nonconforming finite element methods for solving the stationary Stokes equations. I, *Rev. Française Automat. Informat. Recherche Opérationnelle Sér. Rouge* **7** no. R-3 (1973), 33–75.
- [27] B. DACOROGNA, *Direct methods in the calculus of variations*, second ed., *Applied Mathematical Sciences* **78**, Springer, New York, 2008.
- [28] L. DIENING and C. KREUZER, Linear convergence of an adaptive finite element method for the p -Laplacian equation, *SIAM J. Numer. Anal.* **46** no. 2 (2008), 614–638. doi:[10.1137/070681508](https://doi.org/10.1137/070681508).
- [29] L. DIENING and M. RŮŽIČKA, Interpolation operators in Orlicz-Sobolev spaces, *Numer. Math.* **107** no. 1 (2007), 107–129. doi:[10.1007/s00211-007-0079-9](https://doi.org/10.1007/s00211-007-0079-9).
- [30] W. DÖRFLER, A convergent adaptive algorithm for Poisson’s equation, *SIAM J. Numer. Anal.* **33** no. 3 (1996), 1106–1124. doi:[10.1137/0733054](https://doi.org/10.1137/0733054).
- [31] I. EKELAND and R. TÉMAM, *Convex analysis and variational problems*, english ed., *Classics in Applied Mathematics* **28**, Society for Industrial and Applied Mathematics (SIAM), Philadelphia, PA, 1999, Translated from the French. doi:[10.1137/1.9781611971088](https://doi.org/10.1137/1.9781611971088).
- [32] A. ERN and J. L. GUERMOND, *Finite Elements I: Approximation and Interpolation*, *Texts in Applied Mathematics* no. 1, Springer International Publishing, 2021. doi:[10.1007/978-3-030-56341-7](https://doi.org/10.1007/978-3-030-56341-7).
- [33] F. FIERRO and A. VEESER, A posteriori error estimators for regularized total variation of characteristic functions, *SIAM J. Numer. Anal.* **41** no. 6 (2003), 2032–2055. doi:[10.1137/S0036142902408283](https://doi.org/10.1137/S0036142902408283).
- [34] M. HINTERMÜLLER and K. KUNISCH, Total bounded variation regularization as a bilaterally constrained optimization problem, *SIAM J. Appl. Math.* **64** no. 4 (2004), 1311–1333. doi:[10.1137/S0036139903422784](https://doi.org/10.1137/S0036139903422784).
- [35] J. D. HUNTER, Matplotlib: A 2d graphics environment, *Computing in Science & Engineering* **9** no. 3 (2007), 90–95. doi:[10.1109/MCSE.2007.55](https://doi.org/10.1109/MCSE.2007.55).
- [36] A. LOGG and G. N. WELLS, DOLFIN: automated finite element computing, *ACM Trans. Math. Software* **37** no. 2 (2010), Art. 20, 28. doi:[10.1145/1731022.1731030](https://doi.org/10.1145/1731022.1731030).
- [37] L. D. MARINI, An inexpensive method for the evaluation of the solution of the lowest order Raviart-Thomas mixed method, *SIAM J. Numer. Anal.* **22** no. 3 (1985), 493–496. doi:[10.1137/0722029](https://doi.org/10.1137/0722029).
- [38] M. E. A. MUSY, [marcomusy/vedo: 2023.4.4](https://arxiv.org/abs/2023.4.4), March 2023. doi:[10.5281/zenodo.7734756](https://doi.org/10.5281/zenodo.7734756).
- [39] R. H. NOCHETTO, G. SAVARÉ, and C. VERDI, A posteriori error estimates for variable time-step discretizations of nonlinear evolution equations, *Communications on Pure and Applied Mathematics* **53** no. 5 (2000), 525–589. doi:[https://doi.org/10.1002/\(SICI\)1097-0312\(200005\)53:5<525::AID-CPA1>3.0.CO;2-M](https://doi.org/10.1002/(SICI)1097-0312(200005)53:5<525::AID-CPA1>3.0.CO;2-M).
- [40] S. OSHER, M. BURGER, D. GOLDFARB, J. XU, and W. YIN, An iterative regularization method for total variation-based image restoration, *Multiscale Modeling & Simulation* **4** no. 2 (2005), 460–489. doi:[10.1137/040605412](https://doi.org/10.1137/040605412).
- [41] W. PRAGER and J. L. SYNGE, Approximations in elasticity based on the concept of function space, *Quart. Appl. Math.* **5** (1947), 241–269. doi:[10.1090/qam/25902](https://doi.org/10.1090/qam/25902).
- [42] P.-A. RAVIART and J. M. THOMAS, A mixed finite element method for 2nd order elliptic problems, in *Mathematical aspects of finite element methods (Proc. Conf., Consiglio Naz. delle Ricerche (C.N.R.), Rome, 1975)*, 1977, pp. 292–315. Lecture Notes in Math., Vol. 606.
- [43] S. REPIN and J. VALDMAN, Error identities for variational problems with obstacles, *ZAMM Z. Angew. Math. Mech.* **98** no. 4 (2018), 635–658. doi:[10.1002/zamm.201700105](https://doi.org/10.1002/zamm.201700105).
- [44] S. I. REPIN, A posteriori error estimates for approximate solutions to variational problems with strongly convex functionals, *J. Math. Sci. (New York)* **97** no. 4 (1999), 4311–4328, Problems of mathematical physics and function theory. doi:[10.1007/BF02365047](https://doi.org/10.1007/BF02365047).
- [45] L. I. RUDIN, S. OSHER, and E. FATEMI, Nonlinear total variation based noise removal algorithms, *Phys. D* **60** no. 1-4 (1992), 259–268, Experimental mathematics: computational issues in nonlinear science (Los Alamos, NM, 1991). doi:[10.1016/0167-2789\(92\)90242-F](https://doi.org/10.1016/0167-2789(92)90242-F).
- [46] M. RŮŽIČKA and L. DIENING, Non-Newtonian fluids and function spaces, in *Nonlinear Analysis, Function Spaces and Applications, Proceedings of NAFSA 2006 Prague*, **8**, 2007, pp. 95–144.
- [47] L. TARTAR, *An introduction to Sobolev spaces and interpolation spaces*, *Lecture Notes of the Unione Matematica Italiana* **3**, Springer, Berlin; UMI, Bologna, 2007.
- [48] R. VERFÜRTH, *A Posteriori Error Estimation Techniques for Finite Element Methods*, Oxford University Press, 04 2013. doi:[10.1093/acprof:oso/9780199679423.001.0001](https://doi.org/10.1093/acprof:oso/9780199679423.001.0001).
- [49] E. ZEIDLER, *Nonlinear functional analysis and its applications. III*, Springer-Verlag, New York, 1985, Variational methods and optimization, Translated from the German by Leo F. Boron. doi:[10.1007/978-1-4612-5020-3](https://doi.org/10.1007/978-1-4612-5020-3).